THE ENDOCANNABINOID SYSTEM AND ENDOTHELIAL FUNCTION IN COLIFORM MASTITIS

By

Carsten Carl Friedrich Walker

A DISSERTATION

Submitted to
Michigan State University
in partial fulfillment of the requirements
for the degree of

Comparative Medicine and Integrative Biology-Doctor of Philosophy

2022

ABSTRACT

Dysfunctional inflammation is a major cause of severe diseases in dairy cows, such as coliform mastitis, leading to diminished milk production, negatively impacting cow well-being, and possibly resulting in death, even with medical intervention. Endocannabinoids (**EC**) are potent lipid-based mediators, that modulate inflammation in humans and rodents to via stimulation of shared and dedicated cannabinoid receptors-1 and -2 (**CB1/2**). Closely related to the cyclooxygenase derived oxylipids targeted by non-steroidal anti-inflammatory drugs (**NSAID**) in dairy cattle, endocannabinoids have gotten very little attention regarding involvement in dairy inflammation. To address this gap, we determined EC and oxylipid concentrations in plasma of dairy cows suffering from naturally occurring acute coliform mastitis. We showed that concentrations of one of the most thoroughly studied EC, arachidonoylethanolamide (**AEA**), increased after medical intervention with an NSAID, only among those cows that died of the infection. We were also able to show that among those cows that died of the infection, the NSAID flunixin meglumine was not able to reduce isoprostane (**IsoP**) production, the gold-standard biomarker of oxidative stress. Elevated AEA was demonstrated in several human and rodent inflammatory models in response to NSAID treatment and associated with analgesic effects of the drug. However, AEA also induces ROS production and time dependent pro-inflammatory signaling in immune cells. Thus, we set out to establish the presence of the EC system (**ECS**) in bovine aortic endothelial cells and the effect of elevated AEA during endotoxin challenge on endothelial barrier and cell function. We found that ECS related genes are expressed in bovine aortic endothelial cells and expression is affected by endotoxin challenge. We also determined that addition of AEA further reduced endothelial barrier integrity of endothelial cells pre-treated with endotoxin, via CB1 mediated mitochondrial dysfunction, oxidative stress, and activation of

apoptotic signaling. We showed for the first time that EC concentrations are affected by coliform mastitis and that increased plasma AEA concentrations following NSAID treatment may contribute to the death of the animal. Our work suggests that even though AEA may possess anti-inflammatory and analgesic effects in other cell types, increased concentrations of the EC have detrimental effects on endothelial cells pre-treated with endotoxin. The focus of future studies should be determining the timing dependent effects of increased AEA, as studies with concurrent endotoxin and AEA treatment show anti-inflammatory effects of the EC. Additionally, the usage of ECS targeted drugs in combination or without NSAIDs should be investigated, as we showed that antagonism of CB1 resulted in improved endothelial function during endotoxin challenge.

This dissertation is dedicated to Dr. Lorraine Sordillo, who provided the opportunity and mentorship to achieve this goal. I also dedicate it to past and present mentors, who have and continue to shape my education and values. Finally, I would like to thank my friends and especially my family, who have tirelessly supported me throughout last four years. Thank you, I am profoundly grateful.

ACKNOWLEDGEMENTS

I would like to thank the following entities for supporting this work: Agriculture and Food Research Initiative (AFRI) Competitive Grants Program (2014-68004-21972; 2017-67015-26676; and 2017-38420-26759) from the USDA National Institute of Food and Agriculture, and the Meadow Brook Laboratory Endowment, Michigan State University. I give many thanks to my guidance committee members: Lorraine Sordillo, G. Andres Contreras, Ángel Abuelo, Kin Sing Stephen Lee, and Barry Bradford. I would also like to thank the Meadow Brook lab manager Jeff Gandy for the exceptional assistance and training, as well as my remarkable colleagues in the Meadow Brook and associated laboratories. Finally, I thank Dr. Tony Schillmiller of the Michigan State University Mass Spectrometry and Metabolomics Core (East Lansing, MI) for his training in liquid chromatography.

TABLE OF CONTENTS

INTRODUCTION 1

CHAPTER 1: The Bovine Endocannabinoid System: Potential Target to Improve Immune and Inflammatory Responses in Dairy Cattle 4
1.1: INTRODUCTION 4
1.2: BIOSYNTHESIS AND DEGRADATION 5
1.3: RECEPTORS 11
1.4: INFLAMMATION 21
1.5: THERAPEUTIC POTENTIAL 32
1.6: CONCLUSIONS AND FUTURE DIRECTIONS 35

CHAPTER 2: Flunixin Meglumine Reduces Milk Isoprostane Concentrations in Holstein Dairy Cattle Suffering from Acute Coliform Mastitis 36
2.1: INTRODUCTION 36
2.2: MATERIALS AND METHODS 39
2.3: RESULTS 44
2.4: DISCUSSION 50
2.5: CONCLUSIONS 55

CHAPTER 3: The Effect of Cyclooxygenase Inhibition on Endocannabinoid and Oxylipid Profiles during Naturally Occurring Acute Coliform Mastitis in Holstein Dairy Cows 57
3.1: INTRODUCTION 57
3.2: MATERIALS AND METHODS 60
3.3: RESULTS 64
3.4: DISCUSSION 81
3.5: CONCLUSIONS 88

CHAPTER 4: Anandamide Alters Barrier Integrity of Bovine Vascular Endothelial Cells during Endotoxin Challenge 90
4.1: INTRODUCTION 90
4.2: MATERIALS AND METHODS 92
4.3: RESULTS 101
4.4: DISCUSSION 113
4.5: CONCLUSIONS 117

CONCLUSIONS 119

REFERENCES 121

APPENDIX A: SUPPLEMENTAL MATERIALS 149

INTRODUCTION

With over $2 billion in annual losses, mastitis is the costliest disease affecting adult dairy cattle in North America (Rollin et al., 2015; NAHMS, 2014). Coliform mastitis often is associated with dysfunctional inflammation, leading to systemic involvement, and possible death, even with medical intervention (Rollin et al., 2015; NAHMS, 2014; Erskine et al., 1988; Nakajima et al., 1997; Ohtsuka et al., 2001; Oliveria et al., 2013). Proper clearance of the coliform bacteria requires an effective immune response facilitated by rapid initiation of the inflammatory response to eliminate the source of the infection followed by a timely resolution of inflammation to restore immune homeostasis. However, a dysfunctional inflammatory response also can lead to further tissue damage and systemic involvement (Sordillo, 2018; Porcherie et al., 2012). Therefore, proper local and systemic inflammatory signaling is crucial to prevent a dysfunctional inflammatory response. Vascular endothelial cells are uniquely positioned between the systemic circulation and the underlying tissues. As such, endothelial cells play an essential role in orchestrating the onset and resolution of inflammation through the production of soluble mediators, regulation of vascular tone, and passage of immune cells (Sordillo, 2018; Porcherie et al., 2012; Sordillo et al., 1995; Hoeben et al., 2000; De Schepper et al., 2008; Aitken et al., 2011; Aitken et al., 2011; Ryman et al., 2016; Mavangira et al., 2020).

Targeted breakdown of the endothelial barrier is part of the pathogenesis of acute coliform infections and dysfunction followed by loss of barrier integrity results in excess inflammation and tissue damage (Sordillo, 2018; Aitken et al., 2011; Ryman et al., 2015). Endothelial cells are a major producer of lipid-based mediators during inflammatory events caused by exposure to coliform endotoxin, lipopolysaccharide (LPS). Lipid-based mediators can act on immune mediating cells directly (Ryman et al., 2015; Ryman et al., 2016; Mavangira et al., 2020) and

through interactions with complement mechanisms (Ryman et al., 2015; Cheng et al., 2007; Hinson et al., 1996). However, a class of lipid-based mediators that was ignored previously in bovine are the lipid-based retrograde neurotransmitters known as endocannabinoids (EC). In humans and rodents, EC modulate inflammation through a dedicated EC system comprised of cannabinoid receptors (CB) and their ligands, fatty acid ethanolamides and glycerols (Turcotte et al., 2015; Witkamp, 2016). Additionally, several EC are capable to binding to non-CB receptors, such as transient receptor potential vanilloid – 1 (TRVP1) and the G-protein receptor – 55 (Gp55) (Pertwee et al., 2010). Activity of arachidonoylethanolamide (AEA) and 2-arachidonoyl-glycerol (2-AG) and their respective receptors in immune mediating cells and subsequent effects on inflammation are extensively reviewed in Chapter 1.

Currently published data on the bovine EC system does not include information on systemic concentrations in response to acute coliform mastitis. To address this information gap, we carried out an *in-vivo* longitudinal descriptive study of naturally occurring acute coliform mastitis, treated with the non-steroidal anti-inflammatory drug (NSAID) flunixin meglumine (FM). In chapter 2 we demonstrate the fluctuations of inflammatory and oxidative stress markers associated with acute coliform mastitis, while chapter 3 describes EC and oxylipid concentrations in plasma over the time course of the infection. Most notable are the variations in EC concentrations between animals that survived the infection and those that did not and the associated lack of reduction of oxidative stress markers among those cows that died. Not only is this study the first of its kind, but it also demonstrates that bovine systemic plasma EC concentrations fluctuate over the course of the infection and that some EC could be used as markers of inflammation and possibly extent of inflammatory activation.

Even though, the EC system was found in several bovine tissues (Bonsale et al., 2018; Zachut et al., 2018; Kuhla et al., 2019), the effects of the EC system on immune mediating cells, such as vascular endothelial cells are unknown. While research in humans and rodents shows extensive effects of the EC system on inflammatory regulation (Turcotte et al., 2015; Witkamp, 2016), cellular metabolism (Tsuboi et al., 2018), and proliferation (Hofman et al., 2014; Hutch and Hegg, 2016). Of particular interest to endothelial cell function is AEA, due to reports of inflammatory modulation (Turcotte et al., 2015; Chiurchiu et al., 2016; Ligresti et al., 2014), production of reactive oxygen species (ROS) production (Lipina and Hundal, 2016; Liu et al., 2020), and effect on vascular tone (Baranowska-Kuczko et al., 2014; Stanley et al., 2016). To elucidate the effects of AEA on bovine vascular endothelial cells, the presence of the EC system must be demonstrated.

Due to the breakdown of the vascular endothelium during acute coliform mastitis, the barrier integrity of the cells is crucial. To establish the effect of AEA on the endothelial barrier integrity the electric cell-substrate impedance sensing (ECIS) system was used. Combined with commercially available assays for viability, ROS, cytotoxicity, and more, we were able to elucidate the activity of AEA on bovine vascular endothelial cells during LPS challenge. Findings from human and rodent research indicates that cannabinoid receptor 1 (CB1) activation by AEA induces ROS production that may be detrimental. Using pharmacological agents to inhibit endothelial CB1 and downstream actions, we report reduced ROS production and subsequent oxidative and mitochondrial stress markers, as well as improved barrier integrity and reduced activation of apoptotic pathways.

CHAPTER 1: The Bovine Endocannabinoid System: Potential Target to Improve Immune and Inflammatory Responses in Dairy Cattle

1.1: INTRODUCTION

Modern dairy cattle can suffer from dysfunctional inflammatory responses to pathogens from around three weeks before calving, well into peak and even late lactation. The highest incidence of infectious diseases in North America occurs during this period (LeBlanc, 2006; Ingvartsen and Moyes, 2013). With a properly regulated inflammatory response, dairy cows can eliminate pathogens quickly and effectively, without excessive damage to healthy tissues (Sordillo, 2018). The endocannabinoid system (**ECS**) is well known to modulate fear, memory, and pain, but is also involved in metabolism and inflammation (Rahaman and Ganguly, 2021; Osafo et al., 2021). The ECS is made up of fatty acid-based mediators, the endocannabinoids (**EC**); their respective enzymes responsible for synthesis and degradation; and a network of dedicated and shared receptors. Dedicated receptors, cannabinoid-receptor-1 and -2 (**CB1** and **CB2**, respectively), are most densely expressed in the central nervous system (**CNS**), but are also present in adipocytes, hepatocytes, as well as endothelial and immune cells (Giacobbe et al., 2021). Ability to stimulate non-CB receptors, such as transient receptor potential vanilloid-1 (**TRPV1**) and peroxisome proliferator-activated receptors (**PPAR**), enables the ECS to modulate a wide range of physiological functions with great sensitivity to concentration and location (Ye et al., 2019). Indeed, EC can exert pro- or anti-inflammatory effects depending on several factors, including concentration, and downstream signaling (Cabral et al., 2015).

Extensive research into the ECS is underway in human medicine, particularly regarding inflammation and cancer biology. However, the ECS of dairy cows has not been studied in the context of inflammation and immune function until very recently. Eicosanoids, non-EC fatty acid-

based inflammatory mediators such as prostaglandins and thromboxanes, are studied in dairy cattle with the goal to improve inflammatory regulation during high-risk periods (Sordillo, 2018). Studies on the bovine ECS have focused on the reproductive and central nervous systems (Osycka-Salut et al., 2020; Kuhla et al., 2020), with new data emerging on metabolic effects (Zachut et al., 2018; Myers et al., 2021). The purpose of this review is to summarize current findings on the ECS of dairy cattle, including extrapolations from human findings, and data from comparative physiology studies in other species, to provide areas of future research. This review will focus on the effects of the two most thoroughly studied EC, arachidonoylethanolamide (alternatively, anandamide; **AEA**) and 2-arachidonoyl-glycerol (**2-AG**), along with their effect on dairy reproduction, inflammation, and immune system. We will also discuss therapeutic potential.

1.2: BIOSYNTHESIS AND DEGRADATION

Endocannabinoids are enzymatically synthesized from fatty acids stored within cellular lipid bilayers, in response to the proper stimuli. Initially only thought to be synthesized on demand by nearly all cells, it is now clear that AEA and 2-AG can be stored within adiposomes of cells (Maccarrone, 2017). Pro-inflammatory signaling such as activation of pattern recognition receptors (**PRRs**), elevated tumor necrosis factor alpha (**TNFα**), as well as tissue injury are known to stimulate EC synthesis and release from storage. Relative concentrations of each EC are dependent on specific stimuli, location, timing, and downstream effects, contributing to the sensitivity of the physiological effects of the ECS.

Arachidonoylethanolamide

Arachidonoylethanolamide synthesis is initiated via ligation of a previously membrane-bound phosphatidylethanolamine (**PE**) and arachidonic acid (**AA**) by Ca^{2+} dependent or independent N-acyltransferase (**NAT** and **iNAT**, respectively), resulting in the intermediate *N*-arachidonoyl-

phosphatidylethanolamine (**NAPE**) (Figure 1.1). Following the formation of NAPE, four pathways of AEA synthesis have been documented, the predominant of which is catalyzed by a Ca^{2+} dependent *N*-arachidonylphosphatidylethanolamine-specific phospholipase D (**NAPE-PLD**). Hydrolysis of NAPE via NAPE-PLD yields AEA and a phosphatidic acid (Biringer, 2021).

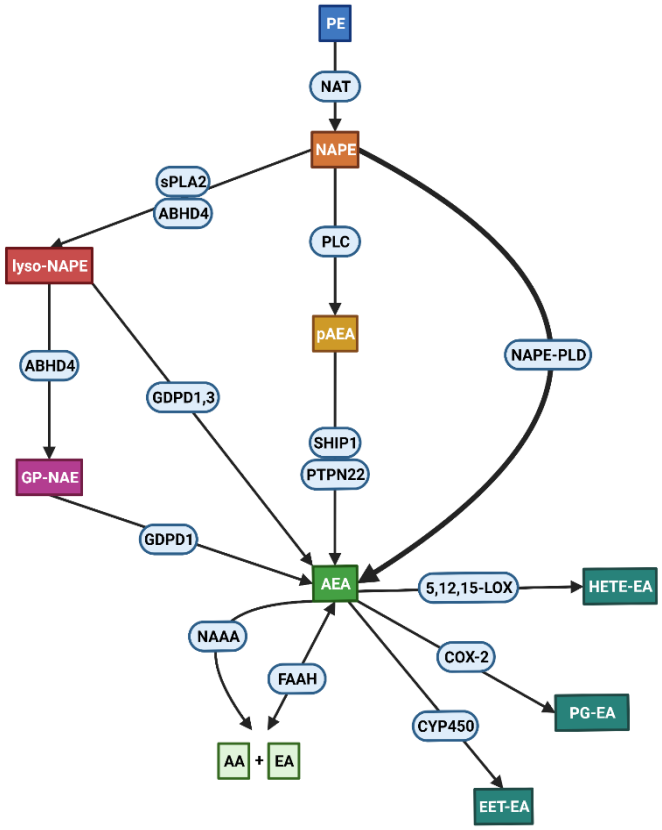

Figure 1.1: Synthesis, degradation, and metabolism of arachidonoylethanolamide (AEA).

Secondary and tertiary pathways of AEA synthesis are mediated by calcium sensitive phospholipases. Phospholipase C (**PLC**) hydrolyzes NAPE to phospho-AEA (**pAEA**) and the byproduct 1,2-diacylglycerol (**1,2-DAG**). Subsequent dephosphorylation of pAEA by phosphatidylinositol 3,4,5-trisphosphate 5-phosphatase 1 (**SHIP1**) and the tyrosine phosphatase non-receptor type 22 (**PTPN22**) results in synthesis of AEA. Whereas secreted phospholipase A_2

(**sPLA$_2$**) hydrolyzes NAPE to glycerophospho-*N*-acylethanolamine (**GP-NAE**), which is further hydrolyzed by the lysophospholipase D glycerophosphodiester phosphodiesterase domain containing 1 (**GDPD1**), resulting in AEA synthesis. Lastly, synthesis of AEA via hydrolase domain-containing protein-4 (**ABHD4**) and lysophospholipase D isoforms 1 and 3 (**GDPD1,3**) is upregulated during low AEA concentrations and inhibition of NAPE-PLD (Liu et al., 2008; Simon and Cravatt, 2006).

Degradation of AEA may occur via enzymatic hydrolysis or oxidation (Figure 1.1). The enzymes fatty acid amide hydrolase (**FAAH**) and n-acylethanolamine acid amidase (**NAAA**) can cleave the ethanolamine (C_2H_7NO) group from the AA core of AEA, resulting in free AA to be metabolized into inflammatory mediators. However, FAAH may also synthesize AEA from free AA and ethanolamine (Figure 1.1), whereas NAAA is only capable of hydrolysis and has only ~50% of the affinity for AEA that FAAH does (Basavarajappa, 2007). Furthermore, AEA itself can also be metabolized through the cyclooxygenase-2 (**COX-2**) (Rouzer and Marnett, 2011), 5-,12- and 15-lipoxygenase (**5-/12-/15-LOX**) (Van der Stelt et al., 2000), and several cytochrome P450 (**CYP450**) pathways (Urquhart et al., 2015), yielding ethanolamide-bound mediators such as prostaglandin-ethanolamides (**PG-EA**), hydroxyeicosatetraenoic acid-ethanolamides (**HETE-EA**), and epoxyicosatrienoyl-ethanolamides (**EET-EA**), respectively. The most extensively studied metabolite of AEA in humans and other species is $PGF_{2\alpha}$-EA, due to its identical pharmacological profile of the antiglaucoma drug bimatoprost (Rouzer and Marnett, 2011; Turcotte et al., 2015). The highly sensitive and redundant nature of AEA synthesis, along with the plethora degradation and metabolic pathways, allows for precise timing and localization of AEA mediated effects on immune cell and inflammatory function.

In bovine, recent studies on the metabolic involvement of the ECS revealed elevated plasma AEA concentrations during metabolic stress associated with parturition and lactation (Kuhla et al., 2020). Additionally, elevated concentrations of AEA in adipose tissue during lactation supports metabolic involvement of the ECS in dairy cows (Zachut et al., 2018). Furthermore, the degree of body weight loss is associated with AEA concentrations, possibly pointing towards underlying inflammatory conditions due to metabolic dysregulation, as is seen in murine and humans (Rakotoarivelo et al., 2021). Nonetheless, the majority of AEA research to date is focused on the reproductive system. In the bovine oviduct, AEA concentrations fluctuate during the oestrus cycle (Gervasi et al., 2013), and bull sperm is capacitated by AEA interaction with TRPV1 (Osycka-Salut et al., 2020). However, indicators for inflammatory involvement of the bovine ECS were also elucidated in the reproductive system. During endometritis, AEA was elevated in plasma and proposed as a biomarker of endometrial inflammation (Bonsale et al., 2018). Furthermore, uterine mRNA expression of AEA synthesizing enzymes was increased compared to healthy animals, and degradation enzyme mRNA expression was decreased, indicating that elevated AEA concentrations are due to regulation of specific pathways.

2-arachidonoyl-glycerol

Synthesis of 2-AG may also occur via multiple pathways (Figure 1.2). Although all 2-AG synthesis pathways start with 2-arachidonoyl containing phospholipids, the main substrate are inositol phospholipids, namely 2-arachidonoyl-phosphatidylinositol 4,5-bisphosphate (**PIP2**). Hydrolysis of PIP2 by PLC results in the formation of diacylglycerol (**DAG**) containing 2-arachidonoyl. In adipose tissue and hepatocytes, DAG is also synthesized from triacylglycerol (**TAG**) precursors via hormone sensitive lipase (**HSL**) and adipose triglyceride lipase (**ATGL**) (Morak et al., 2012). Deacetylation of DAG by diacylglycerol lipase (**DAGL**) results in 2-AG

formation and is considered the main pathway of 2-AG synthesis (Tsuboi et al., 2018). Within the CNS of humans, DAGLα is the pre-dominantly expressed enzyme (Jain et al., 2013), whereas in murine macrophages and dendritic cells, only DAGLβ is expressed and active (Hsu et al., 2012), indicating of key functional differences of the ECS within the CNS and periphery/immune cells. Additionally, PIP2 can be hydrolyzed by PIP2-specific phosphatase (**PIP2P**), resulting in phosphatidyl inositol (**PI**). The phosphatidic acid-preferring phospholipase A1 (**DDHD1**) catalyzes hydrolysis of PI to 2-arachidonoyl-lysophosphatidylinositol (**2-ALPI**), which is further hydrolyzed by lyso-PLC, yielding 2-AG. Lastly, 2-AG synthesis may initiate from 2-arachoidonoyl - lysophosphatidic acid (**2-ALPA**) via dephosphorylation by 2-arachidonoyl LPA-specific phosphatase (**2-LPAP**) (Hiroyama and Takenawa, 1998).

Thought to be the major pathway of 2-AG degradation, hydrolysis to AA and glycerol ($C_3H_8O_3$) is catalyzed by numerous enzymes (Figure 1.2). Monoacylglycerol lipase (**MAGL**) is the principal enzyme facilitating 2-AG hydrolysis to AA and glycerol in the CNS (Blankman et al., 2007) and adipose tissue of murine (Tornqvist and Belfrage, 1976). Minor hydrolysis enzymes within the CNS and adipose tissue are α/β-hydrolase domain-containing protein-6 and -12 (**ABHD6** and **ABHD12**, respectively). Lastly, hydrolysis of 2-AG to AA and glycerol is also catalyzed by FAAH, which can hydrolyze 2-AG at rates comparable to AEA (Goparaju et al., 1999). Although MAGL remains the major enzyme in the CNS (Blankman et al., 2007; Goparaju et al., 1999), murine microglial cells do not express MAGL and hydrolysis is attributed to FAAH and ABHD6 (Marrs et al., 2010). However, AA and glycerol are not the only products of 2-AG hydrolysis, with MAG acyltransferase (**MAGT**) and MAG kinase (**MAGK**), yielding DAG and 2-ALPA, respectively (Coleman and Haynes, 1986). Oxidization of 2-AG through the COX, LOX and CYP pathways, yields bioactive lipid mediators, such as prostaglandin-glycerols (**PG-G**) and

hydroxyeicosatetraenoic acid-glycerols (**HETE-G**), that are emerging as novel inflammatory mediators (Rouzer and Marnett, 2011; Turcotte et al., 2015). Synthesis of 2-AG under a variety of conditions combined with the ability to be metabolized into active mediators, highlights the importance and sensitivity of the ECS.

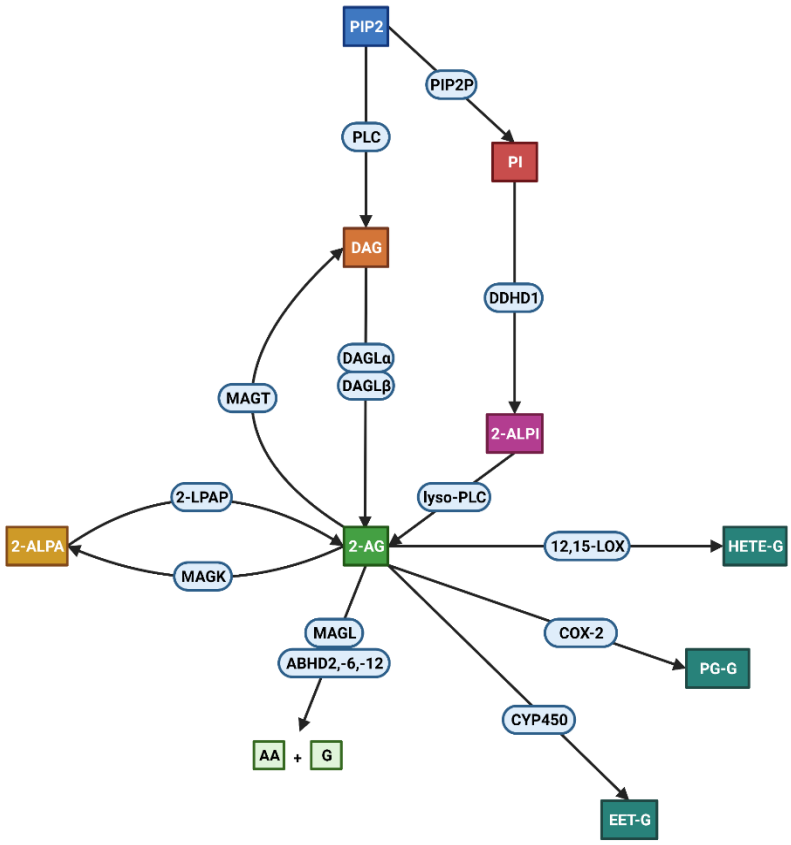

Figure 1.2: Synthesis, degradation, and metabolism of 2-AG.

Record of 2-AG concentrations during inflammatory conditions in dairy cows is unfortunately not available. However, mRNA expression of the 2-AG degradation enzyme MAGL did not differ between Holstein cows and their healthy controls (Bonsale et al 2018). Nonetheless, elevated 2-AG during inflammatory conditions reported in other species, may results in greater metabolism of 2-AG through COX-2 and elevated synthesis of 2-AG derived active lipid

mediators. The importance of lipid mediators in inflammation of dairy cows is well documented (Contreras and Sordillo, 2011; Mavangira and Sordillo, 2018), and COX, LOX and CYP are expressed in variety of dairy cow tissue, such as vascular endothelial cells, adipose, renal, and mammary tissues (Contreras et al., 2017; Kuhn et al., 2020). Combined with recently recorded fluctuations in EC concentrations during inflammatory events in dairy cattle (Kuhla et al., 2020), products of AEA and 2-AG oxidation may be of great value to further the understanding of the complex network of lipid based inflammatory mediators.

1.3: RECEPTORS

Cannabinoid receptors-1 and -2 are Gα-protein coupled receptors (GPRs) that, depending on cell type and manner of activation, possess wide range of activity, such as modulation of Ca^{2+} currents, cellular metabolism, and cell survivability (Matsuda et al., 1990; Munro et al., 1993). Relative expression of CB2 among immune cells is 10-100 times higher than that of CB1 (Han et al., 2009), whereas CB1 is greatly expressed in the CNS (Galiegue et al., 1995). Anandamide displays a higher binding affinity for CB1 than CB2, while 2-AG preferentially binds to CB2 over CB1. However, 2-AG has a higher binding affinity for both CB1 and -2 than AEA (Sugiura and Waku, 2000) and is found in greater concentrations within the CNS and circulation (Stella et al., 1997). Even with advancements in our understanding of CB activity, there are still several unknown factors that contribute to the overall ECS bioactivity. Beyond the CB receptors, AEA and 2-AG are capable of interaction with non-CB receptors, such as TRPV1, ion channels, PPARα/γ, and GPRs -18, -55, and -119 (**GPR18**, **GPR55**, and **GPR119**, respectively) (Ye et al., 2019). Furthermore, the metabolism of AEA and 2-AG through the COX, LOX, and CYP pathways yields active lipid mediators that are capable of binding to key inflammatory receptors such as prostaglandin-F (**FP**) and -E (**EP**) receptors, highlighting the complexity of bioactivity of

the ECS regarding modulation of physiological mechanisms (Buisseret et al., 2019). Lastly, signaling of CB and non-CB receptors can also occur from within the cell, as several ECS related GPRs have been identified in endosomes and the trans-Golgi network (Godbole et al., 2017; Irannejad et al., 2017), the nuclear membrane (Boivin et al., 2008), endoplasmic reticulum (Andersson et al., 2003), and mitochondrial membrane (Suofu et al., 2017).

CB1

Initially cloned in 1990, CB1 is the most abundant GPR in the CNS (Matsuda et al., 1990). In human and murine models of the central and peripheral nervous system, CB1 effects are mediated via $G_{i/o}$, G_S, $G_{q/11}$, $G_{12/13}$, and β-arrestin (Figure 1.3) (Lauckner et al., 2005; Flores-Otero et al., 2014). In neural, vascular, and immune cells, activation of Gα and GS proteins leads to enhanced activity of adenylyl cyclase (**AC**), which increases cyclic adenosine monophosphate (**cAMP**) concentrations. Conversely, $G\alpha_{i/o}$ activation results in inhibition of AC and decreased concentrations of cAMP (Leo and Abood, 2021), which is the predominant mechanism under physiological conditions, stimulating innate immune functions of monocytes, macrophages, and neutrophils, such as increased production of cytokine, chemokine, and lipid mediators, as well as phagocytosis and intracellular killing of pathogens (Serezani et al., 2008).

Inhibition of AC activity modulates activation of several mitogen-activated protein kinase (**MAPK**) pathways involved in innate immune functions, cell survivability, and proliferation. Essential MAPK pathways in immune cells are extracellular signaling regulated protein kinase-1 and -2 (**Erk1/2**) (Bouaboula et al., 1995), c-Jun N-terminal kinase (**JNK**) (Rueda et al., 2000), and p38 MAPK (Derkinderen et al., 2001). In macrophages and neutrophils, JNK and p38 MAPK is required for reactive oxygen species (**ROS**) production (El-Benna et al., 2009), whereas the

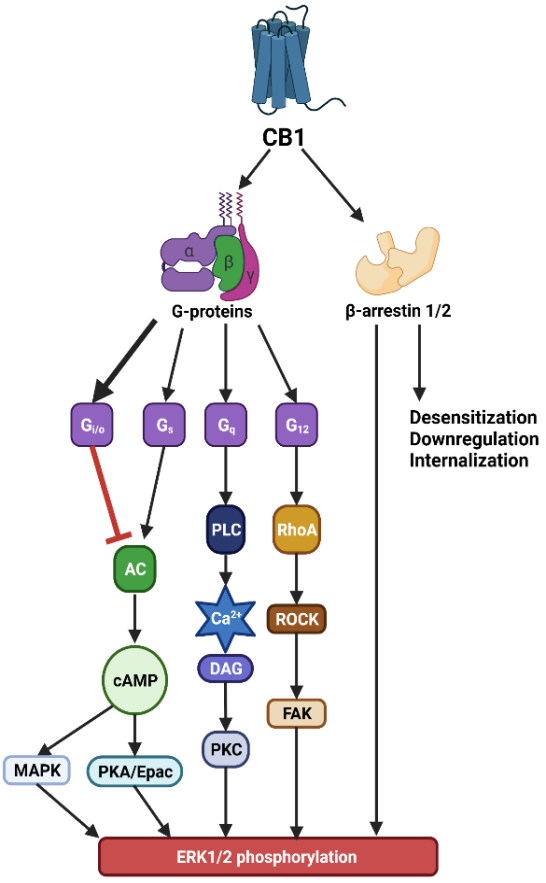

Figure 1.3: Schematic representation of cannabinoid receptor – 1 (CB-1) downstream pathways following agonism/antagonism. AC: adenylyl cyclase; cAMP: cyclic adenosine monophosphate; ERK1/2 pathway is essential to cell proliferation and growth via modulation of the mammalian target of rapamycin (**mTOR**) activation (Roux and Blenis, 2004). CB1: cannabinoid receptor-1; Epac: exchange protein activated by cAMP; ERK1/2: extracellular signaling regulated protein kinase-1 and -2; FAK: nuclear focal adhesion kinase; MAPK: mitogen-activated protein kinase; PKA: protein kinase A; PKC: protein kinase C; PLC: phospholipase-C; RhoA: Ras homolog family member A; ROCK: Rho-associated protein kinase.

activation of protein kinase A (**PKA**) by cAMP results in modulation of electrical currents via ion transporters, namely potassium ($\mathbf{K^+}$) channels. Decreased concentration of cAMP due to AC inhibition by CB1 agonism, inhibits PKA phosphorylation of K^+ channels, altering polarization of immune cells. During CB1 agonism is a key mechanism contributing to the rapid and transient increase of cytosolic calcium ($\mathbf{Ca^{2+}}$), as hyperpolarization is not sustained without efflux of K^+ in macrophages, t-cells, and dendritic cells (Feske et al., 2015). However, elevated cytosolic Ca^{2+} is not due to CB1 mediated Ca^{2+} influx via ion channels, as CB1 agonism activates outward propelling Ca^{2+} channels (Eldeeb et al., 2016), and stimulates Ca^{2+} release from the endoplasmic reticulum (**ER**). Indeed, CB1 agonism is shown to inhibit inward propelling Ca^{2+} channels in humans (Chemin et al., 2001). Additionally, binding of cAMP to exchange protein activated by cAMP (**Epoc**) allows for further modulation of intracellular signals affecting metabolism, gene expression, cell cycle, and differentiation. Furthermore, signaling via $G_{12/13}$ is poorly understood as research is limited to hippocampal neurons, but data suggests that $G_{12/13}$ signaling is involved in neurite growth and cell contractility (Roland et al., 2014). Activation of the various downstream mechanisms is dependent on substrate and allosteric modulator binding (Ye et al., 2019), which is represented in the concentration, time, and location dependent effects of CB1 agonism and antagonism. Lastly, intracellular CB1 receptors located on the ER and lysosomes are responsible for Ca^{2+} release from storage. However, extracellular administration of AEA did not result in intracellular CB1 agonism, highlighting the importance of AEA induced intracellular AEA synthesis and release (Brailoiu et al., 2011). Additionally, internalization of activated CB1 occurs via β-arrestin-2, whereas β-arrestin-1 is involved in the ERK1/2 pathway (Ahn et al., 2013), highlighting the importance of conformational changes of CB1 due to allosteric modulation.

In dairy cows, the CB1 receptor is becoming a key target for cellular metabolism and energy homeostasis, particularly the effect of CB1 agonism/antagonism in adipocytes is of great interest (Myers et al., 2021). Other than adipose tissue, CB1 mRNA expression within the CNS of dairy cows is increased during metabolic stress during early lactation (Kuhla et al., 2020). Which may not only be indicative of an altered metabolic state but may also act on the immune response via the hypothalamic-pituitary-adrenal (**HPA**) axis (Chrousos, 1995). Unfortunately, the gene expression of CB1 was not recorded during endometritis in Holstein dairy cows, which is the only inflammatory study of the bovine ECS to date (Bonsale et al., 2018).

CB2

First cloned in 1993 (Munro et al., 1993), CB2 was initially believed to be restricted to immune cells (Cabral et al., 2008). However, it was later shown that CB2 is expressed in the CNS and periphery at low levels and up regulated in response to inflammatory stimuli or tissue injury (Galiegue et al., 1995; Pacher and Mechoulam, 2011). In human blood immune cells, CB2 protein expression is greater in natural killer (**NK**) cells, B lymphocytes, and monocytes, compared to CD4+ and CD8+ T lymphocytes or neutrophils (Graham et al., 2010).

Effects of CB2 agonism/antagonism vary greatly depending on cell type, concentration, receptor dimerization, and allosteric modulation (Saroz et al., 2019). Even though mechanistic evaluation of CB2 is not as detailed as CB1, similarly, to CB1, CB2 agonism leads to inhibition of AC via $G\alpha_{i/o}$-proteins and decreased cAMP, whereas CB2 signaling through $G\alpha_s$ stimulates AC and increased cAMP (Saroz et al., 2019). Release of intracellular Ca^{2+} via PLC was shown to involve $G\alpha_q$ in human embryonic kidney cells (Malysz et al., 2009), and signaling through β-arrestin-2 leads to internalization of CB2, while β-arrestin-1 is involved in translocation of CB2 to the ER and Ca^{2+} release (Nogueras-Ortiz et al. 2017). Lastly, models utilizing CB2 knockout mice

demonstrated elevated expression of adhesion proteins and pro-inflammatory mediators (Steffens and Pacher, 2012), supporting CB2 as a key inflammatory regulator and expression of CB2 in immune cells such as macrophages is dependent on state of activation/ timing.

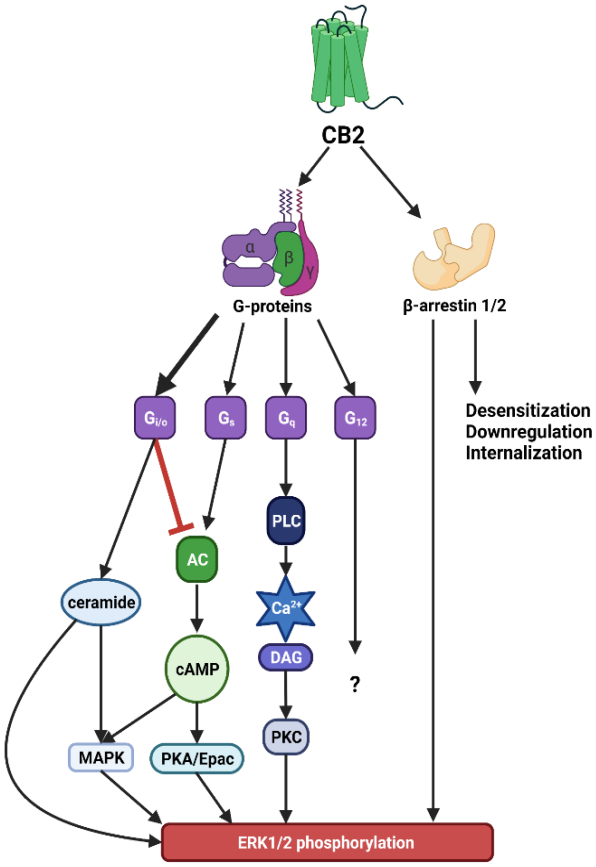

Figure 1.4: Schematic representation of cannabinoid receptor – 2 (CB2) downstream pathways following agonism/antagonism. See text for details. AC: adenylyl cyclase; cAMP: cyclic adenosine monophosphate; CB1: cannabinoid receptor-1; Epac: exchange protein activated by cAMP; ERK1/2: extracellular signaling regulated protein kinase-1 and -2; MAPK: mitogen-activated protein kinase; PKA: protein kinase A; PKC: protein kinase C; PLC: phospholipase-C.

During periods of metabolic stress associated with lactation in dairy cows, CB2 mRNA expression is upregulated within the CNS (Kuhla et al., 2020). In calf pulmonary endothelial cells, CB2 not CB1 agonism by AEA initiated PLC and inositol 1,4,5-trisphosphate (**IP3**) production, leading to increased intracellular Ca^{2+}, which originated from the ER (Zoratti et al., 2003). However, no immune challenge of the calf pulmonary endothelial cells was carried, restricting the information to confirming mechanisms of action under physiological conditions. Nonetheless, in uterine tissue of Holstein dairy cows suffering from endometritis, CB2 mRNA expression is increased compared to healthy animals (Bonsale et al., 2018).

TRPV1

Likely the most thoroughly studied non-CB receptor involved in EC signaling is TRPV1. Highly expressed in neural tissue and to lesser degree in immune cells, gastrointestinal (**GI**) epithelial cells, as well as vascular and renal endothelial cells, TRPV1 is a non-selective ion channel. Agonism of TRPV1 leads to Ca^{2+} influx into the cell, activating protein kinase C (**PKC**), which can phosphorylate and inhibit CB1 function (Garcia et al., 1998). Calcium influx via TRPV1 also activates calcium/calmodulin-dependent protein kinase 2 (**CaMKKβ**), stimulating adenosine monophosphate activated protein kinase (**AMPK**), crucial for mitochondrial health (Herzig and Shaw, 2017). Not only does extracellular AEA bind to TRPV1, but intracellular AEA can also activate TRPV1, resulting in Ca^{2+} entering the cell via the ion channel. Indeed, a dose of 100 nM intracellular AEA was sufficient to elicit TRVP1 mediated elevated cytosolic Ca^{2+} in human embryonic kidney cells and rat dorsal ganglion (van der Stelt et al., 2005).

Several recorded effects of AEA and 2-AG have been attributed to CB and non-CB receptor stimulation. For example, activation of MAPK by AEA in human vascular endothelial cells was only partially inhibited by CB1 antagonism and knockout (Liu et al., 2000). Additionally,

EC may interact with non-CB receptors in a novel manner, compared to the receptor's classic agonist (Muller and Reggio, 2020; Li et al., 2021). In fact, the analgesic effects attributed to AEA are thought to mainly be mediated through TRPV1 (Akopian et al., 2009; Di Marzo et al., 2002). The ability to affect intracellular Ca^{2+}, alter CB receptor function, and partially mediate several EC related effects on a wide range of cell types, makes TRPV1 a crucial component of the ECS and a potential target for therapeutics.

PPARs

Greatly expressed in the vasculature of humans and murine, PPARα, -β/δ, and -γ are ligand -activated transcription factors that stimulate gene expression by binding to the promoter region of the target gene (Zoete et al., 2007). Both AEA and 2-AG are substrates for PPARs (O'Sullivan, 2016). Activity of PPARγ stimulation by AEA is dependent on nitric oxide (**NO**) production and superoxide dismutase (**SOD**) activity (O'Sullivan et al., 2009), and, along with PPARβ/δ, were shown to be crucial in vascular endothelial cell health (d'Uscio et al., 2014) and myocardial metabolism (Li et al., 2009). Whereas PPARα is involved in vascular remodeling, tone, overall blood pressure regulation, and oxidative stress (**OS**) (Guellich et al., 2013; Duan et al., 2009). Agonism of PPARs results in anti-inflammatory effects through inhibition of nuclear factor kappa-light-chain-enhancer of activated B cells (**NF-kB**) (Manning et al., 1995), interleukin-6 (**IL-6**) production, and attenuating COX-2 expression (Usuda and Kanda, 2014). Additionally, agonism of PPARγ by COX-2 metabolites of AEA has been proposed in murine splenic cells, resulting in inhibition of IL-2 secretion (Rockwell and Kaminski, 2004). Intracellular EC concentrations therefore play a key role in gene expression, placing emphasis on transport and synthesis regulation. In macrophages, PPARγ modulates polarization, maturation, and metabolism. However, PPARγ knock out macrophages challenged with LPS displayed elevated concentrations

of pro-inflammatory cytokines such as IL12, IL1β, and TNFα (Heming et al., 2018). Additionally, in murine dendritic cells, agonism of PPARγ reduces maturation and activation and substantially inhibited dendritic cell ability to prime naïve CD4+ T-cells (Klotz et al., 2007).

GPR18

Initially discovered in 1997 (Gantz et al., 1997), GPR18 was deorphanized in 2006 (Kohno et al., 2006). It is activated by AEA, and the plant based exo-cannabinoid abnormal cannabidiol (**AbnCBD**) (Pertwee, 2006). In murine and humans, GPR18 is ubiquitously expressed in the CNS, cardiovascular system, GI tract, adipose tissue, skeletal muscle, pancreas, kidney, spleen, liver, and leukocytes (Takenouchi et al., 2012). Agonism of GPR18 results in decreased cAMP concentrations due to inhibition of AC via $G\alpha_{i/o}$ (Kohno et al., 2006). Additionally, G_q coupling in GPR18-transfected human T-cells (Kohno et al., 2006) was observed in response to treatment with N-arachidonoyl glycine (**NAGly**), an AEA derivative. The breadth of GPR18 signal transduction pathways is similar to that of the CB receptors and effects mirror that of CB1, showcasing the redundancy of the ECS.

GPR55

Isolated and cloned in 1999 (Sawzdargo et al., 1999), GPR55, a rhodopsin-like, purinergic GPR, is expressed in central and peripheral nervous tissue, adipose tissue, endometrium, small intestine, immune cells, and blood vessels (Chiurchiu et al., 2015). Inflammatory involvement of GPR55 has been demonstrated and among immune cells, GPR55 is greatly expressed in monocytes, NK cells, and microglia of the CNS (Chiurchiu et al., 201). Indeed, $GPR55^{-/-}$ knockout mice of a colitis model had decreased pro-inflammatory cytokine concentrations compared to the control (Stancic et al., 2015). Similar to the CB receptors, GPR55 agonism and antagonism exhibit opposite effects in neural and peripheral tissues. Agonism of GPR55 in neural tissue of mice

increased anti-inflammatory cytokines IL-4 and IL-10 (Staton et al 2008). Contrasting to CB receptor activation however, GPR55 agonism only leads to G_q and $G\alpha_{12/13}$ protein coupling (Lauckner et al., 2008). Coupling of G_q proteins, leads directly to the activation of PLC and stimulation of inward-propelling Ca^{2+} channels (Lauckner et al., 2008). Whereas, coupling of $G\alpha_{12/13}$ proteins, leads to activation of the ras homolog gene family member A (**RhoA**) and Rho-associated protein kinase (**ROCK**). Activation of ROCK in turn leads to elevated MAPK, activation of PLC, activating inward-propelling Ca^{2+} channels. Therefore, GPR55 agonism dependent increase in intracellular Ca^{2+} is mechanistically different than that of the CB receptors. Additionally, GPR55 can form heteromers with CB1 and -2, resulting in novel signaling pathways. Activation of the GPR55 and CB2 heteromer is ligand concentration dependent, and agonism of both GPR55 and CB2, inhibits CB2 signaling. Whereas antagonism of CB2 inhibits GPR55 agonism, and CB2 agonism is inhibited by GPR55 antagonism (Moreno et al., 2014). Heteromers and interactions of this kind have been documented in human neutrophils and human embryonic kidney (**HEK293**) cells (Moreno et al., 2014).

GPR119

Predominantly expressed in the GI tract and pancreas in humans, GPR119 regulates energy balance and has gained attention as a potential target to treat type-2 diabetes (Ye et al., 2019). A non-AA based EC, oleoylethanolamide (**OEA**), and 2-AG are agonists of GPR119, resulting in elevated intracellular cAMP concentrations via $G\alpha_S$ coupling. Agonism of GPR119 stimulates secretion of glucagon-like peptide-1 (**GLP-1**) in the intestinal tract and glucose-dependent release of insulin in pancreatic islet β-cells (Furman et al., 2004). Activation of GPR119 leads to elevated cAMP and release of GLP-1 is PKA dependent (Lauffer et al., 2009). Additionally, elevated cAMP can activate MAPK, which is also PKA mediated. The role GPR119 plays in inflammation and

immune cells is highlighted through the effect on cholesterol efflux from human macrophage derived foam cells (Hu et al., 2014). However, further elucidation of GPR1119 signaling has proven difficult, as allosteric modulation of the receptor is also possible.

1.4: INFLAMMATION

Inflammation is a key contributor to an effective immune response. As part of the innate immune system, inflammation is facilitated by a wide range of cells, such as monocytes, neutrophils, macrophages, and vascular endothelial cells. Regulation of inflammatory responses depends on a delicate balance of cytokines, oxylipids or eicosanoids, and other mediators such as reactive oxygen species (**ROS**). Of great interest are the COX-2 metabolites of AEA and 2-AG, as COX-2 expression is significantly increased during inflammatory events. Considering differential effects dependent on concentration, location, timing, and downstream signaling cascades of EC themselves and the bioactivity of EC metabolites, the entirety of inflammatory involvement of the ECS is only starting to be understood.

However, effects of ECS stimulation are associated with neuroprotective effects during inflammatory events, reduced ROS production and improved antioxidant capacities. Whereas ECS stimulation of peripheral tissues, particularly immune mediating cells, results in increased ROS production and pro-inflammatory effects. Nonetheless, anti-inflammatory effects of AEA were already demonstrated to include the inhibition of early-stage inflammatory chemoattractant cytokines secretion, such as IL-6, IL-8, and monocyte chemoattractant protein-1 (**MCP-1**), as well as eliminating LPS -triggered activation of the NF-kB pathway in human periodontal tissues (Nakajima et al., 2006). In dairy cows the endometrial mRNA expression of NAPE-PLD and CB2 significantly increased during endometritis compared to healthy animals, and the expression of catabolic enzymes FAAH and NAAA were significantly decreased (Bonsale et al., 2018),

indicating an upregulation of AEA during inflammatory conditions (Dirandeh and Ghaffari, 2018). Conversely to the pre-dominantly anti-inflammatory properties of AEA, 2-AG exerts both pro- and anti-inflammatory effects on immune cells. Results of 2-AG treatment not only vary depending on the species and cell type, but there are also contradictory findings within cell types (Kaplan et al., 2005)

Lastly, effects of active metabolites of AEA and 2-AG on inflammation are scarce, and predominantly focused on the product of AEA metabolism through COX-2, $PGF_{2\alpha}$-EA, as it closely resembles the antiglaucoma drug bimatoprost in structure (Woodward et al., 2003). Additionally, $PGF_{2\alpha}$-EA is perhaps the only EC metabolite that has been studied in bovine, specifically in relation to the reproductive system (Wiltbank et al., 1995). However, recent studies in murine highlight the effect of 2-AG metabolites on immune mediating cells and potential anti-inflammatory effects (Alhouayek et al., 2018). To fully understand the complexity of inflammatory regulation by the ECS, ROS production during acute and chronic inflammation is of particular interest.

Reactive Oxygen Species and Oxidative Stress

Essential to, and products of inflammation are free radicals, or ROS (Yang et al., 2013). Produced by neutrophils for purposes of chemotaxis (Hattori et al., 2010), cell lysis after phagocytosis of the pathogen via lipid-peroxidation (Cordeiro, 2014), and apoptotic signaling (Redza-Dutordoir and Averill-Bates, 2016), ROS are important signaling molecules, and drive monocyte-to-macrophage differentiation (Tan et al., 2016). Inability to neutralize ROS produced may lead to further upregulation of the inflammatory through activation of MAPK or NF-kB (Redza-Dutordoir and Averill-Bates, 2016). Runaway ROS production, overwhelming the organism's antioxidant potential (**AOP**), may result in macromolecule damage, known as

oxidative stress (**OS**) (Yoshida, 2013). In murine and humans, endocannabinoids modulate ROS production under acute and chronic inflammatory conditions. However, effects vary greatly depending on cell type and concentrations.

Specifically, CB1 activation by μM concentrations of AEA result in MAPK activation, ROS production, and cell death of several non-neuronal cell types (Rajesh et al., 2010). Indeed, anandamide concentrations greater than 5 μM induced swelling in isolated rat liver mitochondria, elevated ROS production, OS, and apoptosis (Catanzaro et al., 2009). In murine cardiomyocytes, μM concentrations of AEA induced MAPK activation, ROS production leading to OS, and cell death (Mukhopadhyay et al., 2010). In human primary hepatic stellate cells, but not hepatocytes, 2-AG increased mitochondrial permeability and ROS production, and cell death was independent of CB activation and instead dependent on AOP, as depletion of glutathione (**GSH**) resulted in apoptosis (Siegmund et al., 2007). Conversely, in neural tissue, AEA agonism of CB1 is associated with reduced ROS production, reduction of OS, and protective effects during chronic inflammatory conditions (Muller et al., 2019). The dual nature of the ECS within neural and immune mediating cells highlights the difficulty of systemic therapeutics and nutritional supplementation.

Macrophages and Monocytes

Formed in bone marrow, monocytes are recruited to inflammatory sites via cytokines, chemokines, and other messengers. Dependent on specific stimuli, monocytes differentiate into macrophages or dendritic cells during inflammation and injury (Kratofil et al., 2016). Monocytes express CB1 and CB2, and CB1 mediated effects are associated with monocyte migration and increased pro-inflammatory cytokine production (Mai et al., 2015). Indeed, monocytes induced to differentiate to macrophages had greatly increased expression of CB1 and altered the ratio of

CB1:CB2 from 1:17 to 1:3 (Han et al., 2009). Possible key mechanism of monocyte differentiation is CB1 activation, as CB1 expression increases with CB1 agonism in murine monocytes (Mai et al., 2015). Conversely, nM AEA treatment of monocytes is associated with decreased production of IL-4, IL-6, and IL-8, the mechanism of which is yet to be elucidated (Berdyshev et al., 1997). Whereas reduction of TNFα production in monocytes associated with AEA treatment is shown to depend on the COX-2 metabolite PGE_2-EA (Brown et al., 2013). Lastly, GPR55 mediated increased pro-inflammatory cytokine production in human monocytes (Chiurchiu et al., 2015), highlights the redundant nature of the ECS.

Table 1.1: Effects of AEA and 2-AG on immune cells and associated pathways.

Cell Type	AEA	Pathway	2-AG	Pathway
Monocyte	↓ IL-6, IL-8, IL-4, IFNγ	-	↑ NO production	CB1
	↓ TNFα	COX-2		
	↑ Mobility	-		
Macrophage	↓ IL-6, IL-12, IL-13, NO	-	↑ NO production	COX-2, CB2
	↓ Cytotoxicity	-	↑ Number of phagocytotic cells	CB2
	↑ IL-10	-	↑ IL-6, MCP1	-
	↑ ROS production	GPR18	↑ Adhesion molecules, chemokines, migration	CB2
			↓ MIP1	COX-2
			↑ Ca^{2+} influx, 2-AG chemotaxis	-
T-cell	↓ pro-inflammatory cytokines	CB2	↓ IL-2	PPARγ/COX-2/CB2
	↓ TH1/TH17 response	CB1	↓ IL-2 dependent proliferation	CB2
	↓ CD8+ T-cell migration	CB2	↓ CD3+/CD8+ induced proliferation	-
NK cell	↓ TNFα, cytotoxicity	GPR55	↑ Mobility/migration	CB2
Neutrophil	↑ Respiratory burst	CB2	↓ Degranulation, ROS release	GPR55
	↓ Migration	GPR55	↑ Migration	GPR55
	↓ TNFα, neutrophil recruitment	-	↓ TNFα, neutrophil recruitment	-
	↓ Degranulation, ROS production	GPR55	↑ LTB4, Ca^{2+} mobilization	-
	↑ Chemotaxis	CB1		
Dendritic cell	↑ Apoptosis	CB1/2	↑ Chemotractant/migration towards 2-AG	-
	↓ TNFα, IL-6, IL-12, IFNγ	CB2		
	↓ TH1/17 response	CB2		

As key components of the innate immune system, macrophages reside in tissues, acting as lookouts or first responders to infection by pathogens, and tissue injury, but are also actively recruited to sites of inflammation. Excessive recruitment of monocytes/macrophages to inflammation sites can be detrimental and is associated with many acute and chronic inflammatory conditions (Oishi and Manabe, 2018). Macrophage expression of CB1 does not fluctuate after differentiation from monocytes and remains expressed to a lesser degree than CB2. Treatment of human macrophages with LPS, ROS, or AEA increased ROS production, and enhanced phagocytosis (Mai et al., 2015). Yet, rapid degradation of AEA by FAAH in resting, primed, and responsive cells, limits AEA agonism of CB1. Nonetheless, CB1 mediated effects of AEA are thought to play a key role in regulating and possibly prolonging the pro-inflammatory action of activated macrophages, as elevated concentrations of AEA and decreased expression of FAAH and NAAA were recorded in murine macrophages after treatment with LPS and ROS (Liu et al., 2003). Conversely, AEA also exerts anti-inflammatory effects on macrophages, such as decreased NO, IL-12, IL-13, and increased IL-10 production (Correa et al., 2011). However, similar to monocytes, effects of AEA are also mediated through non-CB receptors and active metabolites. For example, MAPK dependent elevated ROS production associated with AEA treatment is GPR18 mediated (Takenouchi et al., 2012). Additionally, the non-CB receptor GPR119 exerts anti-inflammatory effects on foam cells, yet neither AEA nor 2-AG can stimulate GPR119 without inhibition of their respective degradation enzymes (Hu et al., 2014). Unlike CB1 expression, CB2 expression by macrophages is highly variable. While not being expressed in resting or fully activated macrophages, CB2 is greatly expressed in primed or responsive cells (Cabral et al., 2015). The time dependent expression indicates CB2 as a key receptor in macrophage inflammatory action. Although 2-AG synthesis by macrophages remained unchanged in response

to LPS treatment (Liu et al., 2003), CB2 agonism by 2-AG increased NO release (Chang et al., 2001), expression of adhesion molecules (Kishimoto et al., 2003), chemokine production, and ultimately migration (Kishimoto et al., 2004). Additionally, in murine macrophages, PGD_2-G, a COX-2 metabolite of 2-AG, reduced mRNA expression of macrophage inflammatory protein-1α (Alhouayek et al., 2018). Conversely, PGE_2-G activates murine macrophages at picomolar concentrations (Nirodi et al., 2004).

Differential expression of receptors and enzymes involved in ECS signaling at various stages of monocyte/macrophage activation strengthens the ECS as a highly sensitive target for inflammatory modulation. Excessive ROS production of macrophages in infected tissues is one of the main underlying factors for dysfunctional inflammation and localized OS in dairy cattle (Sordillo, 2018). Particularly during acute mastitis infections, a dysregulated ECS may contribute to excessive macrophage recruitment and the inability to resolve inflammation in a timely manner.

T-cell and NK cells

Major components of the adaptive immune system, T-cells, or T-lymphocytes, directly cause cell death through lysis of infected cell membranes. Additionally, T-cells can activate other immune cells, and produce inflammatory cytokines (Kumar et al., 2018). Whereas NK cells are considered effector lymphocytes and are part of the innate immune system. Major functions of NK cells are to detect and limit the spread of cancer and microbial infections (Vivier et al., 2008). In humans, CB2 activation by AEA decreases pro-inflammatory cytokine production in CD4+ and CD8+ T cells (Cencioni et al., 2010). Anandamide also reduces the Th-17 cell-mediated response in a rodent hypersensitivity model, by initiating production of IL-10 and induction of micro RNAs (**miRNAs**) primarily targeting pro-inflammatory mediators and silencing them (Jackson et al., 2014). In human keratinocytes, AEA inhibits the production of TH1/TH17-polarizing cytokines

via CB1 and the mTOR pathway (Chiurchiu et al., 2016). In T-cells of humans, 2-AG inhibits IL-2 release through PPARγ and COX-2 (Rockwell et al., 2006). Inhibition of IL-2 by 2-AG is also mediated through CB2 and results in decreased IL-2 dependent proliferation of human T-cells and 2-AG increased migration of human natural killer (NK) cells via CB2 (Kishimoto et al., 2005) and agonism of the non-CB receptor GPR55 in human NK cells challenged with LPS, increased TNFα production and cell cytotoxicity (Chiurchiu et al., 2015).

Results obtained from histological staining of hypothalamic samples from dairy cows between 11 and 66 days postpartum, show an increased NAPE-PLD and decreased FAAH expression (Kuhla et al., 2020). Changes in EC concentrations and receptor expression, or EC tone, in the CNS of postpartum dairy cows, can significantly alter metabolism and immune-mediated inflammation through action on the HPA axis (Chrousos, 1995), potentially acting through a Th17 mediated response (Hill and Tasker, 2012). Additionally, targeting the ECS in cases of bovine leukemia may be of interest, as the proviral load is controlled by T-cells (Florins et al., 2009).

Neutrophils

Originating in bone marrow, neutrophils are part of the innate immune system and patrol the organism in search for signs of infection. Within the circulating blood stream, neutrophils monitor for specific intracellular adhesion molecules (**ICAMs**) expressed by endothelial cells during inflammation, to infiltrate underlying, infected tissue (Borregaard, 2010). Possessing a range of toxic antimicrobial weapons, neutrophils store these substances in a specialized organelle, the granule, to safely move through the circulation and tissue without causing unnecessary damage. Recognition of pathogens leads to elimination of via antimicrobial peptides, oxidative burst via ROS release, or phagocytosis (Amulic et al., 2012). Neutrophil recruitment and TNFα concentrations are suppressed by both AEA and 2-AG during LPS induced lung inflammation in

mice (Berdyshev et al., 1998). Activation of CB2 via a stable AEA analog, methanandamide, induces respiratory burst in human neutrophils, whereas AEA does not, due to rapid hydrolysis by FAAH. Anandamide also suppresses neutrophil migration, degranulation, and ROS production via the GPR55 receptor discovered to be highly expressed in neutrophils. Conversely, 2-AG activates human neutrophils via release of myeloperoxidase, biosynthesis of leukotriene B4, kinase activation, and calcium mobilization (Chouinard et al., 2011). Activation of GPR55 by 2-AG increased human neutrophil migration towards 2-AG while simultaneously inhibiting their degranulation and ROS release (Balenga et al., 2011).

Excessive neutrophil migration and tissue infiltration is associated with excessive ROS production, OS, and tissue damage during infectious diseases in bovine, such as acute mastitis (Sordillo, 2018) and respiratory disease (Bassel and Caswell, 2018). Elevated AEA concentrations, due to changes in synthesis and degradation enzyme mRNA expression, in Holstein dairy cows suffering from endometritis may facilitate inflammatory resolution via suppression of neutrophil migration and degranulation. Conversely, although not recorded in endometritis cases of Holstein cows, elevated 2-AG during inflammatory conditions may act as a facilitator of neutrophil recruitment and onset of the inflammatory response.

Dendritic Cells

Dendritic cells are immune cells which act as a bridge between the innate and adaptive immune systems. Residing in tissue, dendritic cells are considered antigen presenting cells (**APC**) and recruit adaptive immune cells dependent on specific antigen proteins presented on their cell surface. Dendritic cells are also the only APC capable of stimulating naïve T-cells, making them crucial in the adaptive immune response (Balan et al., 2019). In murine dendritic cells, AEA induces CB1/2 dependent apoptosis (Do et al., 2004), differentiation to CD80/86, and production

of IL-12 and IL-23 (Ribeiro et al., 2010). Whereas 2-AG induces chemotaxis and TH1 mediated responses in murine dendritic cells (Maestroni, 2004). Conversely, in human dendritic cells, CB2 activation via AEA inhibits production of TNFα, IL-6, IL-12, and IFNα, as well as TH1/TH17 mediated responses (Chiurchiu et al., 2013). In human immature and mature dendritic cells 2-AG acts as a chemoattractant (Maestroni, 2004), and mature human dendritic cells have elevated 2-AG concentrations (Matias et al., 2002).

Dendritic cells of bovine play a key role in recruitment of T-cells during viral infections such as bovine leukemia. Modulation of chemoattractant release, cell survival, and differentiation via the ECS may allow for improved dendritic cell function and T-cell responses, possibly lowering the proviral load of bovine leukemia and reducing transmission rate (Miyauchi et al., 2021).

Vasculature

Of great importance to local and systemic inflammatory regulation is the vasculature. Endothelial cells are crucial mediators of inflammation, not only forming the barrier between circulating blood and the underlying infected tissue, but also facilitating leukocyte infiltration and inflammatory cytokine production, as well as vascular tone. Targeted breakdown of the vascular endothelium is in fact part of the pathology of coliform mastitis in dairy cows (Sordillo, 2018, Ryman et al., 2015). Furthermore, endothelial cells are integral producers of fatty acid-based mediators such as prostaglandins and thromboxanes, as well as EC (Biringer, 2021).

The vaso-modulatory properties of the ECS have been heavily studied in humans and rodents, with varying results. In isolated rat aortic rings, activation of TRPV1 in endothelial cells by a 1 minute, 100 nM AEA exposure, results in an acute release of nitric oxide, lasting for 2-3 minutes, but does not lead to vasodilation (Poblete et al., 2005). Similar effects were seen in human arteries (Stanley

et al., 2016). In human primary coronary artery endothelial cells, AEA induced a concentration- and time-dependent activation of MAPK, cell death and ROS generation (Rajesh et al., 2010). Interestingly, in the same cell type, 2-AG causes brief and transient relaxation at doses below 0.1 μM and constriction above 3 μM. Denudation did not change the vascular effects of 2-AG, indicating no endothelial cell-mediated mechanism for 2-AG mediated effects. Additionally, selective inhibition of CB1/2 did not alter effects and thromboxane B2 (**TXB2**) (a potent vasoconstrictor PG product of AA metabolism via COX2) was increased, indicating the lack of ECS involvement in 2-AG-mediated effects (Stanke-Labesque et al., 2004, Stanley and O'Sullivan, 2014). These findings suggest that low concentrations of AEA and 2-AG activate CB1/2 as well as TRVP1 to induce acute and transient effects within endothelial cells, potentially leading to vasorelaxation. Whereas increased concentrations, greater than 3 μM, induce vasoconstriction via COX metabolite of AA-mediated pathways. However, it is also suggested that low concentrations of the ECs can bind to receptors on the cell surface and excessive EC are transported into the cell, where they either bind to intracellular receptors, are stored within adiposomes, or are metabolized into AA and byproducts (ethanolamide or glycerol). In human vascular endothelial cells (**ECV304**) 10 μM of AEA activated p42/44 MAPK and reached peak levels after only 5 minutes, immediately followed by a rapid decline in activity (Liu et al., 2000). In calf pulmonary endothelial cells, AEA initiated intracellular calcium signaling through activation of CB2, not CB1, triggering signaling via PLC and IP3 (Zoratti et al., 2003). Essential in EC synthesis from phospholipids, PLC modulation by AEA emphasizes the delicate signaling and feedback loops involved in EC regulation. Agonism of GPR18 by AEA in human and murine pulmonary arteries results to vasodilation/relaxation of the smooth muscles (Herradon et al., 2007). Additionally, agonism of GPR55 by AbnCBD is not involved in the vasodilator effects observed (Johns et al., 2007), perhaps

indicating ligands specific activation patterns of GPR55, as observed with CB1. Lastly, only a select few EC metabolites have been studied for their effects on vasculature, and existing data predominantly focuses on renal tissue. Nonetheless, metabolites of 2-AG via CYP pathways into 11,12-, and 14,15-EET-G promotes the vasodilatation of rat mesenteric arteria smooth muscle, independent of endothelial cell presence (Awumey et al., 2008). Synthesis of AEA and 2-AG derived metabolites by endothelial cells may therefore be imperative for smooth muscle function, vascular health, and affect other tissue types, as metabolites are also released into circulation.

1.5: THERAPEUTIC POTENTIAL

Utilizing the ECS as an indicator of metabolic state has already been proposed in dairy cattle (Zachut et al., 2018; Myers et al., 2021), as it is indicative of metabolic dysregulation in humans suffering from type-2 diabetes and obesity (Di Marzo et al., 2008). Additionally, EC concentration changes may also be useful to determine inflammatory state of dairy cattle. However, the expression of EC synthesis and catabolic enzymes may not be a clear indicator of EC concentrations or inflammatory state, as has been demonstrated in humans, rodents, and even the bovine reproductive system.

Beyond a potential inflammatory marker for dairy cattle, the ECS provides several promising drug targets to alter the inflammatory state of the animal. Inhibition of FAAH by URB597, resulting in elevated AEA concentrations, reduces ROS production in chronic inflammatory conditions in mice (McDougall et al., 2017) and improves nonsteroidal anti-inflammatory drug (**NSAID**) efficacy while reducing negative side effects associated with long term administration of NSAIDs in humans, such as GI ulcers or bleeding (Gyires and Zadori, 2016). However, inhibition of FAAH by URB597 in non-inflammatory conditions increases ROS production and cell death (Biernacki et al., 2018). Improved NSAID efficacy, analgesic effects,

and reduced ROS production associated with the addition of a FAAH inhibitor may be beneficial for the dairy industry, as the current NSAID treatment for acute infections does not confer an improved survival rate (Nakajima et al., 1997; Walker et al., 2021). Additionally, inhibition of NAAA in human CD68+ macrophages challenged with LPS, reduces expression of inducible nitric oxide synthase (**iNOS**) and TNFα (Riberio et al., 2015). Inhibition of the catabolic enzymes FAAH and NAAA may therefore be a suitable target for therapeutics to improve dysregulated inflammatory responses in dairy cattle. Furthermore, the inhibition of 2-AG metabolism through COX-2 is postulated to reduce inflammation during LPS challenges, even though PGD_2-G reduces pro-inflammatory mediator production in human and murine macrophages (Alhouayek et al., 2018).

Perhaps a therapeutic target that is less suspectable to dynamic changes are the ECS receptors. Particularly the antagonism of CB1 has proven to reduce inflammatory mediator and ROS production. In human umbilical vein endothelial cells (**HUVAC**), the inverse CB1 agonist SR141716A (rimonabant) decreases TNFα induced IL-6 production, therefore having anti-inflammatory effects in endothelial cells (Huang et al., 2010). Rimonabant also reduces AEA induced ROS production in murine cardiomyocytes (Mukhopadhyay et al., 2010) and human primary coronary artery endothelial cells (Rajesh et al., 2010). However, rimonabant is associated with detrimental effects within the CNS and has therefore been banned as a drug by the FDA (Sam et al., 2011). Nonetheless, targeting CB1 may be a promising avenue of inflammatory modulation in dairy cattle, particularly due to the high degree of functional modulation of CB1. In recent studies on CB1 functionality targeting the allosteric sites of the receptor discovered in 2005 (Price et al., 2005), allosteric modulation of CB1 exhibits distinct pharmacological characteristics from orthosteric agonists and antagonists. Beyond CB receptors, rimonabant may act as an agonist of

GPR55 or antagonist for TRPV1, further adding to the complexity of the drug's effects (Henstridge et al., 2010). Concerning the antagonism of CB2, the antagonist SR144528 results in decreased 2-AG induced migration of human and murine B-cells, dendritic cells, and eosinophils (Maestroni, 2004; Tanikawa et al., 2007). Depending on timing of therapeutic administration, CB2 antagonism may therefore ameliorate dysfunctional inflammatory responses. However, anti-inflammatory effects of AEA are also mediated through CB2 (Correa et al., 2011; Chiurchiu et al., 2013), once again highlighting the complexity and difficulties of immune and inflammatory modulation by the ECS.

However, there are numerous questions that need to be addressed before any pharmacological or nutritional intervention strategies can be implemented. A select few studies have reported on the effect of feeding ruminants exo-cannabinoids from plant sources (Artegoitia et al., 2016; Kleinhenz et al., 2022), however, data is not consistent and extremely sparse. The findings on ECS effects on the metabolic state of dairy cows are currently outpacing the work done on inflammatory status, as a maladjusted metabolic state is an underlying cause of dysfunctional inflammation in dairy cows (Contreras and Sordillo, 2011). However, administration or supplementation of ECS targeted drugs and exo-canabinoids is met with hesitation by consumers, due to concern for contamination of animal products. Nonetheless, we demonstrated the potential of targeting the bovine ECS and the benefits for dairy cows associated with therapeutic and nutritional intervention strategies. Current and future research on the inflammatory involvement of the bovine ECS in dairy cows must start with systemic concentrations of EC, expression of ECS associated genes in bovine immune mediating cells and inflamed/ infected tissue, as well as the effects of different diets on the ECS. Once baseline values of EC in circulation, and genes associated with the ECS are established, pathway specific studies can be undertaken.

Pharmacological agents that may not be suitable for humans and rodents, may be of benefit to bovine, such as rimonabant. However, even with a large body of evidence for rimonabant's anti-inflammatory properties, the effects on the bovine CNS must be elucidated prior. The extent to which the ECS is present within mammals makes it a lucrative target for pharmaceutical intervention for several medical conditions, inflammatory or not, but it is also its single biggest drawback. As such, the ECS is a novel system in dairy cows, and it will take extensive research and collaboration to elucidate its full effect on inflammatory regulation.

1.6: CONCLUSIONS AND FUTURE DIRECTIONS

Although scientific advances provide insights into fatty acid-based inflammatory mediators, effects of NSAIDs, and improved nutritional and management strategies, dysfunctional inflammation remains a problem for dairy cows during the periparturient period and well into peak and late lactation. Based on the effects of the ECS on inflammatory cytokines, ROS production, and immune cells demonstrated in humans and other species, there may be real therapeutic potential for the dairy industry. With proper modulation of ECS signaling, it may be possible to: 1) increase feed intake and decrease lipolysis; 2) improve inflammatory resolution in response to a pathogen; 3) improve efficacy of NSAID treatments; 4) reduce ROS production and incidence rate of OS; 5) and serve as a natural analgesic. Improved metabolic and inflammatory states will increase animal welfare and decrease cost associated with dysfunctional inflammatory events.

CHAPTER 2: Flunixin Meglumine Reduces Milk Isoprostane Concentrations in Holstein Dairy Cattle Suffering from Acute Coliform Mastitis

2.1: INTRODUCTION

Mastitis is the costliest infectious disease in the US dairy industry, with over $2 billion in annual deficits due to loss of milk production and potential death of the animal (Rollin et al., 2015; NAHMS, 2014). Particularly problematic in dairy cows are coliform mastitis cases that are the result of Escherichia coli (E. coli) (NAHMS, 2014; Erskine et al., 1988; Nakajima et al., 1997; Ohtsuka et al., 2013; Oliveira et al., 2013). Targeted breakdown of the mammary epithelium during coliform mastitis results in decline of milk quality and production (Sordillo et al., 1995; Hoeben et al., 2000; De Schepper et al., 2008; Aitken et al., 2011; Aitken et al., 2011; Ryman et al., 2015; Sordillo, 2018; Mavangira et al., 2020). Some animals mount an effective inflammatory response to clear the pathogen without clinical signs and quickly restore the quality and quantity of milk. However, acute coliform infections can cause dysfunctional inflammation and excessive tissue damage, leading to significant and sometimes permanent cessation of milk production from affected mammary glands. Acute cases of coliform mastitis with systemic involvement may also cause death of infected animals (Rollin et al., 2015; NAHMS, 2014; Erskine et al., 1988; Nakajima et al., 1997; Ohtsuka et al., 2013; Oliveira et al., 2013).

An effective immune response is highly dependent on properly regulated inflammation, with rapid onset and timely resolution (Aitken et al., 2011; Ryman et al., 2015). Stimulation of the Toll-like receptor 4 (TLR4) by the endotoxin lipopolysaccharide (LPS) results in the synthesis of proinflammatory mediators such as tumor necrosis factor alpha (TNFα), interleukin-6 (IL-6), and neutrophil adhesion molecules (Bodiga et al., 2010; Tanaka et al., 2014; Porcherie et al., 2012; Kumar et al., 2011; Goldammer et al., 2004; Liang et al., 2004). Crucially, TLR4 activation by

LPS induces the classical pro-inflammatory enzyme cyclooxygenase-2 (COX-2), increasing the production of fatty acid-derived pro-inflammatory lipid mediators called eicosanoids that include prostaglandins, leukotrienes, and thromboxanes (De Schepper et al., 2008; Ryman et al., 2015; Sordillo, 2018; Liang et al., 2004). Moreover, induction of COX-2 is amplified by TNFα, creating a feedback loop (Hoeben et al., 2000; Aitken et al., 2011; Liang et al., 2004), resulting in elevated eicosanoid concentrations that induce IL-6 production by macrophages and neutrophils (Liang et al., 2004; Lloyd et al., 2007; Hinson et al., 1996). During inflammation, mediators not only act on localized mammary tissues, but also can have systemic effects, leading to increased mobilization of adipose tissue and increased circulating non-esterified fatty acids (NEFAs) (Oliveira et al., 2013; Sordillo, 2018; Contreras and Sordillo, 2011; Sordillo and Mavangira, 2014; Mavangira et al., 2016; Kuhn et al., 2018; Han et al., 2020). Prolonged elevated NEFAs results in systemically increased production of cytokines, adhesion molecules, eicosanoids through increased expression of COX-2 and free radicals, such as reactive oxygen species (ROS) (Hussey et al., 2013; Contreras et al., 2012; Zhang et al., 2018).

Even though ROS are essential to cell signaling and phagocytotic removal of bacteria by neutrophils, lack of adequate antioxidant potential (AOP) to neutralize ROS can be detrimental (Schieber and Chandel, 2014; Sordillo and Aitken, 2009; Lykkesfeldt and Svendsen, 2007). Excessive ROS causes oxidative stress (OS), which can further increase inflammation, as well as the likelihood of redox signaling-induced cell death (Aitken et al., 2011; Sordillo, 2018; Contreras and Sordillo, 2011; Sordillo and Mavangira, 2014; Mavangira et al., 2016; Kuhn et al., 2018; Schieber and Chandel, 2014; Sordillo and Aitken, 2009; Lykkesfeldt and Svendsen, 2007; Hernanz et al., 2013; Mittal et al., 2014). During OS, ROS damage cellular lipids, proteins, and DNA, the products of which are used as biomarkers to quantify OS. Lipids are particularly susceptible to

ROS damage during OS and products of non-enzymatic peroxidation of arachidonic acid (AA) called isoprostanes (IsoP) are commonly measured to quantify the extent of OS in dairy cattle and humans (Sordillo and Aitken, 2009; Hernanz et al., 2013; Mittal et al., 2014; Milne et al., 2015; Milne et al., 2007; Celi, 2010). In dairy cattle, plasma IsoP concentrations are elevated during naturally occurring coliform mastitis and correlate with systemic oxidant status (Mavangira et al., 2016). Additionally, milk IsoP concentrations are correlated with inflammation and represent lipid peroxidation events of the mammary gland rather than systemic oxidant status (Mavangira et al., 2016; Kuhn et al., 2018). Not only does OS result in tissue damage, but it also further induces the inflammatory response, increasing the likelihood of disease progression with systemic involvement (Aitken et al., 2011; Ryman et al., 2015; Sordillo, 2018; Sordillo and Mavangira, 2014; Mavangira et al., 2016; Schieber and Chandel, 2014; Sordillo and Aitken, 2009; Lykkesfeldt and Svendsen, 2007; Hernanz et al., 2013; Mittal et al., 2014; Milne et al., 2015).

A key feature of acute coliform mastitis is excessive eicosanoid synthesis that leads to many systemic symptoms such as pyrexia, nociceptive, and inflammatory pain (Aitken et al., 2011; Ryman et al., 2015; Sordillo, 2018; Mavangira and Sordillo, 2020; Bodiga et al., 2010, Liang et al., 2004; Sordillo and Mavangira, 2014; Contreras et al., 2012). Focused research on eicosanoid biosynthesis and activity has led to FDA approval for the administration of the non-steroidal anti-inflammatory drug (NSAID) flunixin meglumine (FM) to animals suffering from endotoxemia associated with acute coliform mastitis (US FDA, 1998). Competitive inhibition of the COX-2 enzyme by FM reduces eicosanoid concentrations observed in naturally occurring and experimentally induced systemic coliform mastitis, resulting in reduced rectal temperature and analgesic effects (Rollin et al., 2015, NAHMS, 2014; Myers et al., 2009; Yeiser et al., 2012; Stock and Coetzee, 2015). However, efficacy of FM treatment has not been optimized, as approximately

half of all dairy cows suffering from acute coliform mastitis succumb to the infection (Nakajima et al., 1997; Ohtsuka et al., 2001). Increased interest in the underlying mechanism of the conflicting reports on efficacy of FM treatment has been focused on classic markers of inflammation pre- and post-FM treatment. For example, previous studies found that ex vivo COX-2 mRNA expression in whole blood of dairy cows is not altered eight hours post-FM treatment, whereas TNFα mRNA expression was significantly reduced (Donalisio et al., 2012, Sintes et al., 2020). Although OS plays a central role in the pathogenesis of coliform mastitis, there is no information available on how oxidant status is affected in animals treated with FM for endotoxemia associated with acute coliform mastitis.

The effect of FM on the oxidant status and markers of oxidative stress may hold answers to the underlying mechanisms resulting in the seemingly equivocal survival of animals suffering from naturally occurring acute coliform mastitis. Therefore, the goal of this study was to establish a time-course of blood and milk biomarkers of inflammation, oxidant status, and OS for animals suffering from naturally occurring systemic coliform mastitis treated with FM. We hypothesize that FM treatment will reduce the OSi and IsoP concentrations in dairy cows suffering from endotoxemia associated with acute coliform mastitis.

2.2: MATERIALS AND METHODS

Animal Selection and Study Design

All animals in this study were Holstein dairy cattle housed at a commercial dairy in mid-Michigan. A total of 16 animals, 8 with acute coliform mastitis and 8 matched healthy control animals, were used in this study. Animals were enrolled in this study when suffering from acute coliform mastitis with systemic involvement and on-farm protocol dictated that veterinary care, including intravenous treatment with the NSAID flunixin meglumine, was necessary. Cows had

to have positive E. coli milk cultures (>100 colony forming units) and at least 2 signs of systemic clinical disease. Signs of acute coliform mastitis included increased core body temperature (>39.2 C), tachycardia (heart rate > 80 beats/minute), tachypnea (respiratory rate > 30 breaths/minute), episcleral injection, local signs of mammary gland inflammation including discoloration, swelling, heat and pain on palpation, and typical serum-like watery milk as determined by the herd veterinarian. Initial blood and milk samples were collected immediately before treatment with a single intravenous dose of flunixin meglumine (2.2 mg/kg IV), ceftiofur sodium (2.2 mg/kg SC), and oral electrolyte fluids according to standard farm treatment protocols (pre-FM treatment); 8 h post-treatment (post-FM treatment); and again, immediately before the animal succumbed to the infection or recovered and was returned to the milking herd or sold (Resolution). One animal succumbed to the infection within 4 h of the post-FM treatment sample and no third sample collection was possible. A total of 8 individually matched control (MC) animals were chosen based on the enrolled systemic coliform animals and matched for days in milk (DIM), lactation number (LAC), and phenotype (number of milking quarters). Mean days in milk (DIM) for systemically infected animals was 101.63 (50.3) and the mean lactation number was 3.125 (0.687). Animals enrolled in the MC group did not receive FM and had negative bacterial milk cultures, no overt clinical signs, and a somatic cell count of <200,000 cells/mL.

Blood and Milk Sample Collection

Blood samples were collected with Vacutainer tubes containing serum separator and EDTA. Pre-treatment samples of systemic coliform infected animals were collected from the jugular vein, all subsequent blood samples from the same animal were collected from the coccygeal vein. Blood samples from healthy matched control animals were taken from the coccygeal vein and occurred within 14 days of initial pre-treatment sample from the paired

systemically infected animal. Blood collection at each sampling point consisted of two 10 mL EDTA tubes and two 15 mL serum separator tubes. After transport on ice, EDTA tubes were treated with 4 µL/mL of antioxidant/reducing agent (ARA) before centrifugation at 1449g for 15 min at 4 C. Serum separator tubes were kept at room temp until properly coagulated, before being placed on ice and centrifuged at 1449g for 15 min at 4 C. After processing, 1 mL of serum and plasma was aliquoted into 1.5/2 mL microcentrifuge tubes and snap frozen in liquid nitrogen before being stored at -80 C. Milk samples were obtained at the same time as blood samples were taken and placed on ice. Milk samples were obtained aseptically from all active quarters of the animals, including the infected quarter(s), and pooled. Volume of pooled samples was at least 10 mL. Two 1 mL aliquots of each pooled milk sample were flash frozen without the addition of ARA, the remainder of the pooled sample was treated with 4 µL/mL ARA and then aliquoted and snap frozen in liquid nitrogen before being stored at -80 C.

Blood and Milk Biomarker Analysis

Blood biomarkers haptoglobin and NEFAs were analyzed in serum using commercially available kits for the small-scale biochemistry analyzer (CataChemWell-T; Catachem Inc.). Serum ROS was carried out using the Oxyselect in vitro kits (Cell BioLabs Inc., San Diego, CA, USA), as previously outlined in Putman et al., 2018. Briefly, 96-well microtiter plates (Black Isoplate-96, PerkinElmer,Waltham, MA) were read using the Biotek H1 plate reader (Biotek, Winooski, VT, USA). Dichlorofluorescent dye fluorescence was determined at 480 nm of excitation and 530 nm of emission. A standard curve (0–10,000 nM) was created to ensure fluorescence at various concentrations. Background fluorescence was eliminated by subtracting blank values from sample values. Units were measured as relative fluorescence units (RFU) per microliter. Serum AOP was carried out as previously described by Re et al., 1999. Briefly, the AOP of a sample was determined

by the ability to reduce 2,20-azinobis-3-ethylbenzothiazoline-6-sulfonic acid (ABTS) (Sigma-Aldrich, St. Louis, MO, USA) and standardized to the reduction capacity of trolox (synthetic vitamin E analog). Serum amyloid a (SAA) was analyzed using commercially available kits from Tridelta Development Ltd. (Maynooth, Ireland). ELISAs were performed for TNFα and IL-6, using standard bovine ELISA kits from Thermo Fischer Scientific (Waltham, MA, USA). All assays were read out using the Biotek H1 plate reader.

Reagents

Acetonitrile, methanol, and formic acid of liquid chromatography–MS grade were purchased from SigmaAldrich (St. Louis, MO). Deuterated and non-deuterated isoprostane standards were purchased from Cayman Chemical (Ann Arbor, MI, USA). Butylated hydroxy toluene (BHT) was purchased from Acros (Waltham, MA, USA), 156 EDTA and triphenylphosphine were purchased from SigmaAldrich, and indomethacin was purchased from Cayman Chemical.

Solid-Phase Extraction (SPE) of Blood and Milk

Blood and milk samples were extracted and analyzed using methods published previously by Mavangira et al., 2016. Briefly, milk (4 mL) and plasma (2 mL) samples were mixed with an antioxidant-reducing agent mixture (4 L of antioxidant-reducing agent/1 mL of sample) to prevent degradation of preformed oxylipids and prevent ex-vivo lipid peroxidation as described previously the antioxidant-reducing agent mixture consisted of 50% methanol, 25% ethanol, and 25% water with 0.9 mM of BHT, 0.54 mM EDTA, 3.2 mM TPP, and 5.6 mM indomethacin.

Plasma extractions were done using an Oasis plasma protocol on an Extrahera robot by Biotage (Charlotte, NC, USA). The samples, including formic acid, ARA, and Internal Standard were loaded into Oasis HLB 12 cc 500 mg LP extraction columns (Waters, Milford, MA, USA)

and eluted using a 90:10 acetonitrile (ACN) and methanol (MeOH). Once the samples were eluted, they were evaporated using a Savant SpeedVac, resuspended in 150 L of 2:1 MeOH and ddH2O, filtered through an Amicon Ultrafree-MC filter (Sigma-Aldrich, St. Louis, MO, USA) and transferred to a chromatography vial with insert and stored at - 20 C until LC/MS/MS analysis.

Milk solid-phase extractions with hydrolysis were done on samples treated with ARA using methods previously described in Mavangira et al., 2015 with modifications. Briefly, 1 mL of whole milk treated with ARA was thawed on ice and treated with an additional 20 L of ARA before addition if 710 L of 6 M potassium hydroxide (KOH). After 45 min of incubation at 45 C the samples were cooled to room temp and 3 mL of acetonitrile with 1% formic acid was added and vortexed. Supernatant was removed after centrifugation at 1976g for 10 min at 4 C and added to 40 mL of HPLC-grade water. At this time, the internal standard was added and SPE using the Oasis HLB 12 cc 500 mg LP extraction columns as described in Mavangira et al., 2015.

LC/MS/MS Analysis

Details of LC/MS/MS analysis are described in Mavangira et al., 2016. In short, the quantification of metabolites was accomplished on a Waters Xevo-TQ-S tandem quadrupole mass spectrometer using multiple reaction monitoring (MRM). Chromatography separation was performed with an Ascentis Express C18 HPLC column (10 cm 2.1 mm; 2.7 m particles, Sigma-Aldrich, St. Louis, MO, USA) at 50 C, with the autosampler at 10 C. Mobile phase A was water containing 0.1% formic acid, and mobile phase B was acetonitrile. Flow rate was fixed at 0.3 mL/ min. Liquid chromatography separation took 15 min per sample. MRM parameters including cone voltage, collision voltage, precursor ion, product ion, and dwell time were optimized based on Waters QuanOptimize software by flow injection of pure standard for each individual compound. Total IsoP concentrations were obtained by addition of IsoP detected in each sample type.

Statistical Analysis

All statistics were calculated using SAS9.4. For pairwise comparison. The Wilcoxon Rank-Sum score was used and means with standard error of the mean (SEM) was reported. Multiple comparisons of timepoints over the course of the infection were done using a two-way ANOVA, with uneven timepoints, repeated measures, and Tukey–Kramer adjustment. Non-normally distributed data were either log10 or square root transformed and back transformed for graphical representation. Multiple comparisons were sliced by time and treatment, for the discrete analysis.

2.3: RESULTS

Survival Rate

Of the eight animals with acute coliform mastitis that were enrolled in this study, four animals survived. Therefore, an inclusive and discrete analysis of the infection outcome groups were performed.

Blood

Eight hours after treatment with FM, no overall change in any of the inflammatory biomarkers analyzed in this study was observed among animals with systemic coliform mastitis. Similarly, there was no change in inflammatory marker concentrations 8 h post-FM treatment, when analyzed by infection outcome. Interestingly, pre-FM treatment concentrations of haptoglobin, IL-6, and NEFAs were significantly different between infection outcome groups (Figure 2.1). Pre-treatment concentrations of IL-6 and NEFAs were elevated ($p = 0.0005$ and $p = 0.0334$, respectively), whereas haptoglobin concentrations were decreased among those animals that survived the infection, compared to those that did not ($p = 0.0181$). Haptoglobin remained significantly decreased 8 h post-FM treatment among the animals that survived compared to those that did not ($p = 0.0057$) and IL-6 remained elevated ($p = 0.0019$). Even though no change from

pre- to post-FM treatment was observed, NEFA concentrations were no longer significantly elevated among animals that died at 8 h post-FM treatment when compared to those that survived (Figure 2.1).

Analysis of the overall blood oxidant status revealed a decrease in OSi from pre- to post-FM treatment ($p = 0.0134$) which is most likely driven by an overall increase in AOP post-FM treatment ($p = 0.0194$) (Table 2.1a). However, when analyzed by infection outcome, no change in AOP from pre- to post-FM treatment was observed in either outcome group. Interestingly, the OSi of the animals that survived was decreased 8 h post-FM treatment ($p = 0.0094$), whereas the OSi of those that died remained unchanged (Table 2.1b).

Only the IsoPs 5-iso-iPF2-VI and 8,12-iso-iPF2-VI were detected in blood and neither had significant changes in concentrations, overall and by infection outcome, from pre- to post-FM treatment. Total blood IsoP concentrations were also not affected by 8 h of FM treatment. However, pre-FM treatment total IsoP concentrations were significantly elevated among animals that died compared to those that survived ($p = 0.0358$) but were no longer different 8 h post-FM treatment.

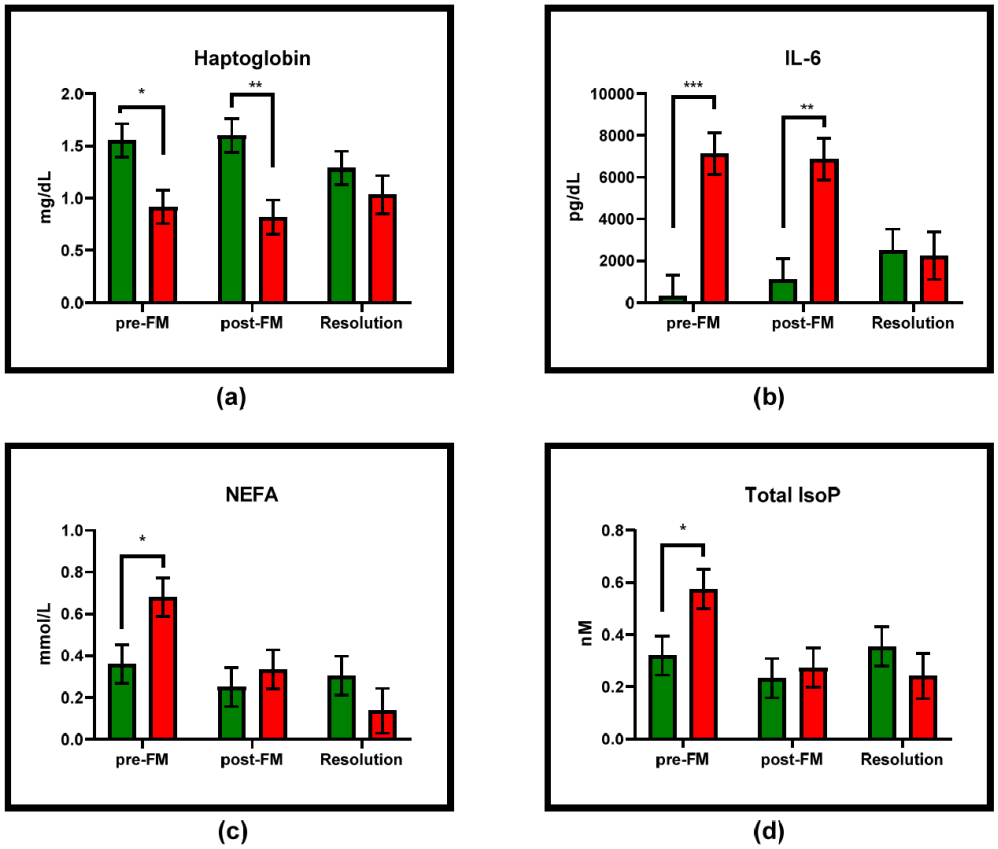

Figure 2.1. Concentrations (mean ±SEM) of blood biomarkers that differed between the infection outcome groups (green bars = survived; red bars = died) at any of the sampling timepoints: (**a**) haptoglobin was elevated among cows that survived pre and post-FM treatment, but was not different between outcome groups at resolution; (**b**) IL-6 was elevated pre- and post-FM treatment among cows that died, but was not different between outcome groups at resolution; (**c**) NEFAs were elevated pre-FM treatment among cows that died, but not post-FM treatment or at resolution; (**d**) total IsoP pre-FM treatment were elevated among cows that died, but not post-FM treatment or at resolution. * $p < 0.05$, ** $p < 0.01$, and *** $p < 0.001$.

Table 2.1. Blood biomarkers of oxidant status over the course of systemic coliform mastitis with FM treatment in Holstein cows.

a) All animals	**Concentrations**								
	Pre-FM Treatment (*N* = 8)			**Post-FM Treatment (*N* = 8)**			**Resolution (*N* = 7)**		
Biomarker	Mean		SEM	Mean		SEM	Mean		SEM
ROS (RFU/µL)	2.358^{ab}	±	0.227	1.859^{a}	±	0.227	2.914^{b}	±	0.239
AOP (TE/µL)	4.415^{a}	±	0.170	5.043^{b}	±	0.170	4.270^{a}	±	0.181
OSi (ROS/AOP)	0.538^{a}	±	0.056	0.373^{b}	±	0.056	0.716^{c}	±	0.059

$^{a–d}$ Means within a row with different superscripts are different ($p<0.05$).

b) Survival only	**Concentrations**								
	Pre-FM Treatment (*N* = 4)			**Post-FM Treatment (*N* = 4)**			**Resolution (*N* = 4)**		
Biomarker	Mean		SEM	Mean		SEM	Mean		SEM
ROS (RFU/µL)	2.528^{a}	±	0.310	1.880^{a}	±	0.310	2.535^{a}	±	0.310
AOP (TE/µL)	4.532^{ab}	±	0.224	5.335^{a}	±	0.224	4.505^{b}	±	0.224
OSi (ROS/AOP)	0.562^{a}	±	0.073	0.348^{b}	±	0.073	0.602^{a}	±	0.073

$^{a–d}$ Means within a row with different superscripts are different ($p < 0.05$).

Milk

Flunixin meglumine treatment decreased overall ROS concentrations in milk from pre to 8 h post-FM treatment ($p = 0.0054$), increased AOP ($p = 0.0051$), and lowered the overall OSi ($p = 0.0131$) (Table 2.2). However, FM treatment only decreased ROS concentration among those animals that died ($p = 0.0045$) and increased AOP only among those that survived ($p < 0.0001$), resulting in a decreased OSi among those animals that died ($p = 0.0003$), but not those that survived. Most strikingly, elevated AOP among animals that survived compared to those that died persisted throughout all three sample times (Figure 2.2), whereas OSi of the animals that survived is only decreased pre-FM treatment ($p = 0.0135$) but not 8 h post-FM treatment when compared

to animals that died. At no timepoint are ROS concentrations different among infection outcome groups.

Table 2.2. Milk biomarkers of oxidant status over the course of systemic coliform mastitis with FM treatment in Holstein cows.

a) All animals	**Concentrations**								
	Pre-FM Treatment (*N* = 8)			**Post-FM Treatment (*N* = 8)**			**Resolution (*N* = 7)**		
Biomarker	Mean		SEM	Mean		SEM	Mean		SEM
ROS (RFU/µL)	15221.000[a]	±	2985.490	7695.380[b]	±	2985.490	11000.00[ab]	±	3066.370
AOP (TE/µL)	6.363[a]	±	0.900	8.563[b]	±	0.900	6.918[a]	±	0.922
OSi (ROS/AOP)	3750.410[a]	±	1031.890	1467.460[b]	±	1031.890	3031.870[ab]	±	1059.940

[a–d] Means within a row with different superscripts are different ($p < 0.05$).

b) Survival only	**Concentrations**								
	Pre-FM Treatment (*N* = 4)			**Post-FM Treatment (*N* = 4)**			**Resolution (*N* = 4)**		
Biomarker	Mean		SEM	Mean		SEM	Mean		SEM
ROS (RFU/µL)	11757.000[a]	±	4339.200	7317.380[a]	±	4339.200	9031.750[a]	±	4339.200
AOP (TE/µL)	7.750[a]	±	0.578	11.550[b]	±	0.578	9.325[a]	±	0.578
OSi (ROS/AOP)	1556.820[a]	±	1056.530	646.830[a]	±	1056.530	984.500[a]	±	1056.530

[a–d] Means within a row with different superscripts are different ($p < 0.05$).

c) Death only	**Concentrations**								
	Pre-FM Treatment (*N* = 4)			**Post-FM Treatment (*N* = 4)**			**Resolution (*N* = 3)**		
Biomarker	Mean		SEM	Mean		SEM	Mean		SEM
ROS (RFU/µL)	18685.000[a]	±	4339.200	8073.380[b]	±	4339.200	13548.000[ab]	±	4566.120
AOP (TE/µL)	4.975[a]	±	0.578	5.575[a]	±	0.578	4.537[a]	±	0.636
OSi (ROS/AOP)	5944.010[a]	±	1056.530	2288.080[b]	±	1056.530	5542.340[a]	±	1111.05

[a–d] Means within a row with different superscripts are different ($p < 0.05$).

Table 2.3. Milk biomarkers of oxidative stress over the course of systemic coliform mastitis with FM treatment in Holstein cows.

a) All animals	**Concentrations**								
	Pre-FM Treatment (*N* = 8)			**Post-FM Treatment (*N* = 8)**			**Resolution (*N* = 7)**		
Biomarker (nM)	Mean		SEM	Mean		SEM	Mean		SEM
5-iso-iPF2α-VI	9.300[a]	±	1.3163	3.550[b]	±	1.3163	3.993[b]	±	1.3867
8,12-iso-iPF2α-VI	22.388[a]	±	3.1743	7.225[b]	±	3.1743	7.458[b]	±	3.3755
8-iso-15®-PGF2α	2.100[a]	±	0.364	1.600[a]	±	0.364	1.119[a]	±	0.3878
8-iso-15-keto-PGE2	3.500[a]	±	0.6616	1.538[a]	±	0.6616	2.206[a]	±	0.7058
Total IsoP	37.288[a]	±	4.769	13.913[b]	±	4.769	14.733[b]	±	5.0478

[a–d] Means within a row with different superscripts are different ($p < 0.05$)

b) Survival only	**Concentrations**								
	Pre-FM Treatment (*N* = 4)			**Post-FM Treatment (*N* = 4)**			**Resolution (*N* = 4)**		
Biomarker (nM)	Mean		SEM	Mean		SEM	Mean		SEM
5-iso-iPF2α-VI	10.775[a]	±	1.9483	3.400[b]	±	1.9483	4.525[ab]	±	1.9483
8,12-iso-iPF2α-VI	26.350[a]	±	4.6684	7.250[b]	±	4.6684	8.125[b]	±	4.6684
8-iso-15®-PGF2α	2.050[a]	±	0.5489	1.625[a]	±	0.5489	1.400[a]	±	0.5489
8-iso-15-keto-PGE2	3.300[a]	±	0.996	1.575[a]	±	0.996	1.725[a]	±	0.996
Total IsoP	42.475[a]	±	7.0826	13.850[b]	±	7.0826	15.775[b]	±	7.0826

[a–d] Means within a row with different superscripts are different ($p < 0.05$).

In milk, 8-iso-15(R)-PGF2 and 8-iso15-keto-PGE2, as well as 5-iso-iPF2-VI and 8,12-iso-iPF2-VI, were detected and contributed to the total IsoP values. Eight-hour treatment with FM decreased overall 5-iso-iPF2-VI and 8,12-iso-iPF2-VI concentrations ($p = 0.0024$ and $p = 0.0039$, respectively), as well as the total IsoP concentration ($p = 0.0017$) from pre- to post-treatment (Table 2.3). Strikingly, the discrete analysis of infection outcome groups revealed that none of the IsoP detected, nor the total IsoP concentration, changed pre- to post-FM treatment in animals that died of the infection. Whereas 5-iso-iPF2-VI, 8,12-iso-iPF2-VI, and total IsoP were decreased after at 8 h post-FM treatment ($p = 0.0064$, $p = 0.0131$, and $p = 0.0084$, respectively). However, at no sample time were any of the individual IsoP, or the total IsoP, different from one another.

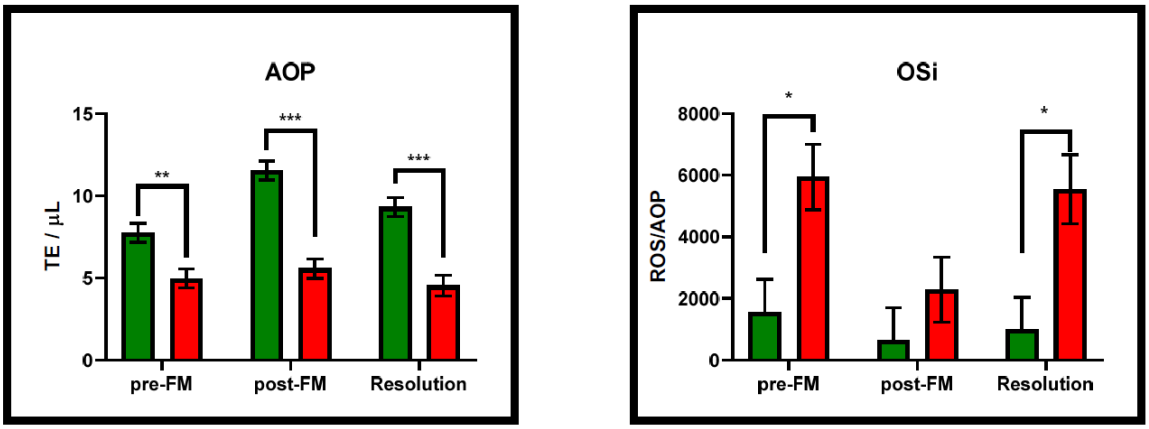

Figure 2.2. Concentrations (mean SEM) of milk biomarkers that differed between the infection outcome groups (green bars = survived; red bars = died) at any of the sampling timepoints: (a) AOP was elevated among cows that survived at all three timepoints; (b) the OSi was elevated pre-FM treatment and at resolution among cows that died, but not post-FM treatment. * $p < 0.05$, ** $p < 0.01$, and *** $p < 0.001$.

2.4: DISCUSSION

Traditional Inflammatory Markers

Cytokines and acute-phase proteins such as TNF, IL-6, and haptoglobin have been used as inflammatory markers during acute coliform mastitis. Elevated TNFα and IL-6 have been associated with the severity of systemic and local inflammation (Nakajima et al., 1997; Ohtsuka et al., 2001; Oliveira et al., 2013; Sordillo et al., 1995; Hoeben et al., 2000, Aitken et al., 2011, Aitken et al., 2011; Sordillo, 2018; Fernandes et al., 2019; Sordillo and Peel, 1992), and a reduction in TNFα by FM treatment has been demonstrated in vitro and ex vivo (Myers et al., 2009; Donalisio et al., 2012; Sintes et al., 2020). However, these classical inflammatory biomarkers may not be accurate particularly when assessed under field conditions with naturally occurring coliform

mastitis. The lack of disparity in TNFα concentrations with FM treatment or between infection outcome groups recorded in our study may be due to the timing of sampling, as the duration of the elevated TNFα concentrations differ greatly among varying experimental designs of induced mastitis (Hoeben et al., 2000; Donalisio et al., 2012, Sintes et al., 2020; Pezeshki et al., 2011; Fernandes et al., 2019; Sordillo and Peel, 1992). Additionally, elevated IL-6 concentrations among animals that died in this study are in contrast to earlier reports of elevated IL-6 among animals that survived naturally occurring coliform mastitis (Nakajima et al., 1997) and the lack of difference in IL-6 concentrations observed among mild and acute infections (Ohtsuka et al., 2001). Haptoglobin concentrations increase with naturally occurring coliform mastitis (NAHMS, 2014; Mavangira et al., 2016; Sordillo and Peel, 1992), but there was no link between disease severity and haptoglobin concentrations following intramammary challenge with E. coli (Pezeshki et al., 2011). Prior to this study, no data exist comparing haptoglobin concentrations among animals that survived and died of coliform mastitis. Less serum haptoglobin concentrations among cows that died in this study may be indicative of a prolonged exposure to endotoxin, as repeated experimental LPS infusion (every 24 h) resulted in peak haptoglobin concentrations at 48 h with a reduction within 72 h (Fernandes et al., 2019). However, haptoglobin concentrations were shown to be increased during naturally occurring acute infections with systemic involvement compared to mild cases, reaching peak concentrations 3 days after establishment of systemic involvement and initial sampling (Ohtsuka et al., 2001). Ultimately, the limited in vivo studies of naturally occurring coliform mastitis that record TNFα, IL-6, and/or haptoglobin provide conflicting results. Attempts to describe classical inflammatory biomarkers with induced coliform mastitis also are conflicting, which may be due to variation in experimental design and the timing of infection with respect to appearance of clinical symptoms. Due to the dynamic nature of the cytokine and acute-phase

protein cascades, the use of classical inflammatory markers such as TNFα, IL-6, and haptoglobin may be less effective under field conditions. Elevated NEFA concentrations have been linked to severity of inflammation during coliform mastitis (Mavangira et al., 2016; Mavangira et al., 2015). Elevated pre-FM treatment circulating NEFAs among cows that died in this study, when compared to those that survived, may be indicative of an exacerbated inflammatory response since circulating NEFAs and COX-2 enzyme can be increased via upregulation of Toll-like receptor (TLR) signaling (Lloyd et al., 2007; Hussey et al., 2013; Zhang et al., 2018). Increased production of pro-inflammatory eicosanoids through the COX pathway can then lead to further adipose mobilization and NEFA release, creating a positive feedback cycle (Contreras and Sordillo, 2011; Contreras et al., 2012). Additionally, relevant is that elevated NEFAs can increase mitochondrial ROS production (Mittal et al., 2014; Garaude et al., 2016) and contribute to the elevated milk ROS seen in this study. Serum NEFA concentrations among the cows that died were no longer elevated compared to the cows that survived post-FM treatment, which can be attributed to a reduction in pro-inflammatory eicosanoids or direct action of FM on adipocytes (Zentella de Pina, et al., 2007).

Additionally, NEFAs are a source of polyunsaturated fatty acids (PUFAs) that serve as substrates for enhanced arachidonic acid (AA) metabolism through the COX pathway, consisting of the inducible COX-2 and constitutively expressed COX-1 enzymes (Smith and Malkowski, 2019). Metabolism of AA results not only in pro-inflammatory eicosanoids, but also ROS mediators able to damage cellular macromolecules directly and modulate ROS signaling pathways (Schieber and Chandel, 2014; Mavangira and Sordillo, 2018; Van't Erve et al., 2015). Particularly during E. coli mastitis, TLR4 activation by LPS and subsequent production of specific eicosanoids responsible for endothelial barrier impairment was documented (Aitken et al., 2011; Ryman et al., 2015; Sordillo, 2018; Bodiga et al., 2010; Celi, 2010). Lastly, availability of PUFA substrate was

shown to greatly influence lipid mediator production through COX-2 in dairy cattle suffering from coliform mastitis, most likely through the interaction of the allosteric and catalytic subunits of the COX isomers (Mavangira et al., 2015, Smith and Malkowski, 2019; Zou et al., 2012; Doug et al., 2013; Dong et al., 2016) and shunting of substrates to other enzymatic and non-enzymatic metabolic pathways of fatty acids (Mavangira et al., 2015).

Oxidant Status and Isoprostanes

This study documented for the first time that IsoP are potentially superior biomarkers over classically used cytokines or acute-phase proteins in establishing the extent of inflammation and efficacy of NSAID treatment in dairy cattle suffering from acute coliform mastitis. As products of ROS-mediated lipid peroxidation, IsoP may present ideal endpoint biomarkers of excessive inflammation. Moderate amounts of ROS are crucial signaling molecules of cellular processes, such as proliferation, meta-bolic adaption, and differentiation, but excessive accumulation of ROS can cause pro-oxidant damage to cells and tissues. As such, ROS accumulation must be controlled by cellular and systemic AOP to avoid lipid peroxidation and the formation of IsoP. Dysfunctional inflammation associated with acute coliform mastitis results in an im-balance of the oxidant status, OS, and the formation of IsoP (Sordillo and Mavangira, 2014; Sordillo and Aitken, 2009; Smith and Malkowski, 2019). In this study, treatment with FM decreased 5-iso-iPF2α-VI, 8,12-iso-iPF2α-VI, and total IsoP in milk of the cows that survived, demonstrating a reduction in local OS. Localized OS is a key feature of acute coliform mastitis, as the elevated ROS production by neutrophils and macrophages recruited to the infection site causes significant OS (Lykkesfeldt and Svendsen, 2007; Mittal et al., 2014). Indeed, even though milk ROS was decreased with FM treatment among cows that died, it did not result in a decreased IsoP production. A possible explanation is that the extent of tissue damage among cows that died prior to FM administration

was too extensive for the animal to take advantage of the reported ex vivo improved epithelial barrier integrity of bovine mammary epithelial cells treated with FM (Sintes et al., 2020).

The resulting continuous influx of neutrophils and macrophages into infected mammary tissue may have resulted in the sustained IL-6 concentration observed and prevented the AOP to sufficiently neutralize ROS production by macrophages, resulting in sustained milk IsoP production. Lack of milk IsoP reduction among animals that died may also be tied to the lack of milk AOP increase, indicating a depleted antioxidant supply due to possibly prolonged acute local inflammation, lack of adequate feed intake (Sordillo and Aitken, 2009) or compromised liver function causing systemic oxidant status changes (Smith and Malkowski, 2019). However, from this study we cannot determine if decreased AOP among cows that died is a result or cause of excessive inflammation. Nonetheless, elevated pre-FM total plasma IsoP among cows that died compared to those that survived and the improved oxidant status from pre- to post-FM treatment show the potential of IsoP to not only be used as a biomarker to measure the extent of local and systemic inflammation, but to also measure efficacy of medical interventions. Certainly, the inconsistent nature of traditional inflammatory biomarkers such as cytokines and acute-phase proteins high-lights the potential of IsoP as an endpoint biomarker for inflammation in dairy cattle, not limited to acute coliform mastitis. Most importantly, quantification of IsoP highlights how defining the pre-existing inflammatory state and associated oxidant status are on the efficacy of FM treatment. Additional studies are needed to assess how local and systemic synthesis of IsoP and their possible bioactivity may impact disease progression.

Additional work relating to the differential production of specific IsoP may be of value. Limited knowledge exists on the specificity of IsoP production, but preferential production of E2- and D2-IsoP over F2-IsoP with depleted α-tocopherol (Milne et al., 2011) and variations of IsoP

production during mammary gland involution (Putman et al., 2018), are good indicators of regulated IsoP synthesis. In this study, only F2-IsoP were affected by FM treatment, whereas E2-IsoP did not change in milk and was not detected in blood. We were also not able to detect A- and D-IsoP variants in milk or blood. In humans and bovine, F2-IsoP were associated with severe OS and lipid peroxidation during exacerbated or chronic inflammation (Mavangira et al., 2016; Kuhn et al., 2018; Milne et al., 2007; Celi, 2010; Milne et al., 2011). Nevertheless, differential production of A-, D-, and E-IsoP may be essential for regulation of inflammation-mediated tissue repair or possibly act as anti-inflammatory mediators. Indeed, Putman et al., 2018 observed greatest A2-IsoP concentrations 2 days after cessation of lactation, whereas A1-IsoP was not detected until 12 days after involution. The lack of A- and D-IsoP in this study may be due to the unregulated inflammation and excess production of ROS compared to non-infectious and regulated inflammatory events. However, the lack of data on regulating mechanisms or bioactivity of the various IsoP limits our understanding, particularly in non-human species, and therefore additional research into IsoP production and bioactivity is essential.

2.5: CONCLUSIONS

This study highlights for the first time the importance of oxidant status and the severity of the pre-existing inflammatory state on the efficacy of FM during coliform mastitis. Additionally, we offer unique insights into potential biomarkers to determine and improve the efficacy of FM treatment for endotoxemia caused by coliform mastitis. Ability of FM to eliminate blood NEFAs and total IsoP elevations in cows that died compared to those that survived from pre- to post-treatment, as well as a reduction in milk ROS from pre- to post-FM treatment, indicate that the FM treatment was effective in reducing signs of inflammation. However, the lack of IsoP reduction in milk among cows that died, compared to the reduction in not only total IsoP but specific IsoP

linked to OS by excessive inflammation, highlights the extent of the local tissue damage. Degree of blood–milk barrier compromise may therefore be crucial for survivability, and treatment with FM does not reduce inflammation sufficiently to ameliorate excessive tissue damage. Additional NSAIDs are currently being examined to improve inflammatory responses and milk production during mastitis and onset of lactation. However, inhibition of proper inflammatory function (Caldeira et al., 2021) and lack of effect on haptoglobin concentrations (Barragan et al., 2020) further highlight the need for improved markers of inflammation and anti-inflammatory treatment. A better understanding of the inflammatory state of cows at the time of NSAID treatment has the potential to improve the clinical outcomes of severe coliform mastitis with systemic involvement.

CHAPTER 3: The Effect of Cyclooxygenase Inhibition on Endocannabinoid and Oxylipid Profiles during Naturally Occurring Acute Coliform Mastitis in Holstein Dairy Cows

3.1: INTRODUCTION

Infection of the mammary gland, or mastitis, is the single most expensive infectious disease in the US dairy industry, with over $2 billion in annual deficits incurred by loss of milk production and potential death of the animal (NAHMS, 2014; Rollin et al., 2015). Mastitis caused by coliform bacteria can be especially severe due to targeted breakdown of the blood-milk barrier (Bruckmaier and Wellnitz, 2017). During acute infections, excessive recruitment of leukocytes and macrophages, due to overproduction of pro-inflammatory cytokines and lipid mediators by immune mediating cells, can lead to break down of the endo- and epithelial cells, excessive local inflammation, tissue damage, and increases the potential for systemic involvement (Ryman et al., 2015; Sordillo, 2018). The importance of the cyclooxygenase (COX) pathway during inflammatory events lies with the production of potent lipid-based inflammatory mediators or oxylipids, such as prostaglandins (PG), leukotrienes, and thromboxanes. Predominantly pro-inflammatory, excessive production of COX-2 metabolites is a key factor in the development of systemic inflammation associated with endotoxemia (Sordillo, 2018). Usage of the non-steroidal anti-inflammatory drug (NSAID) flunixin meglumine (FM) to inhibit COX, with the goal of reducing pro-inflammatory mediator synthesis, is common in North America (NAHMS, 2014). However, even with medical intervention, over 30% of naturally occurring acute coliform mastitis cases result in death of the animal (Nakajima et al., 1997; Erskine et al., 1988; Walker et al., 2021), indicating that further optimization of the inflammatory response is necessary. Lack of longitudinal studies of naturally occurring acute coliform mastitis limits our understanding of the underlying physiological states influencing NSAID efficacy, and how pre-treatment conditions influence

oxylipid production. Indeed, recent work with the COX pathway revealed that inhibition may only be beneficial with proper timing (Sintes et al., 2020). Other factors, such as metabolism and inactivation of the NSAID through the cytochrome P450 (CYP450) group of enzymes, may greatly influence the effect of the drug on COX-derived oxylipids.

Closely tied to the COX pathway and oxylipids is a lipid-based mediator network with dedicated receptors, called the endocannabinoid system (ECS). Humans have exploited the anti-inflammatory and analgesic properties of the ECS for centuries by ingesting and inhaling cannabis plants rich in exocannabinoids (EX), such as delta-9 tetrahydrocannabinol (THC) and cannabidiol (CBD) (Crocq, 2020). Research has focused on the endogenous analogs to THC and CBD, arachidonoylethanolamide (AEA) and 2-arachidonoyl-glyverol (2-AG), respectively, which were discovered in the 1990s. Today a plethora of endocannabinoids (EC) with varying bioactivity have been documented, such a palmitoylethanolamide (PEA) and oleoylethanolamide (OEA). Inflammatory modulation through the ECS has the potential to limit activation and recruitment of neutrophils and macrophages, thereby reducing production of reactive oxygen species (ROS) (Rahaman and Ganguly, 2021), one of the key contributors to dysfunctional inflammatory responses during coliform mastitis. The effect of EX and EC activation of CB2 on inflammation, and CB1 on neural and vasculature, is well documented in humans and rodents and effects of the ECS on inflammation and immune mediating cells is also dosage and timing dependent (Cabral et al., 2015). In bovine, ECS research has focused on reproduction, and only recently shifted towards energy metabolism and inflammatory conditions (Zachut et al., 2018, Kuhla et al., 2020, Bonsale at al., 2018). However, EC concentrations in circulation during an inflammatory event with systemic involvement, such as coliform mastitis, have not been documented.

In addition to direct activity of EC, metabolism through the lipoxygenase (LOX), COX, and cytochrome P450 (CYP450) pathways yields bioactive mediators with yet untapped potential to modulate inflammatory responses (de Bus et al., 2019). Specifically, AEA and 2-AG, having arachidonic acid (AA) at their core, are the ideal substrate for COX-2 and are metabolized into prostaglandin-ethanolamides, or prostamides (PG-EA), and PG-glycerols (PG-G), respectively. Prostamides and PG-G and possess unique actions, differing from their AA derived PG counterparts. However, there is a lack of understanding of PG-EA and PG-G biosynthesis regulation and inflammatory modulatory effects, particularly in non-human species. Inhibition of COX-2 may reduce the concentrations of AEA and 2-AG derived mediators with unknown consequences to the inflammatory mechanism. Conversely, analgesic effects of NSAIDs have been partially attributed to greater EC concentrations, specifically CB1 activation by AEA, following COX inhibition (Guindon et al., 2006). However, CB1 activation via AEA also induces ROS production and apoptotic signaling in several cell types (Han et al., 2009; Rajesh et al., 2010), highlighting the sensitivity of the ECS. More recent studies in bovine describe EC concentrations, receptor, and enzyme mRNA expression in adipose and reproductive tissues during inflammatory events (Zachut et al., 2018; Bonsale et al., 2018).

Even though the presence of the bovine ECS has been established, inflammatory involvement and effects of NSAID treatment on EC and metabolite concentrations remains unknown. In the present study we determined the longitudinal change of fatty acid, oxylipid, EC, and PG-EA/-G concentrations within plasma of Holstein dairy cows suffering from naturally occurring acute coliform mastitis. We showed that fatty acid concentrations were affected by NSAID treatment and that CYP450 derived oxylipids exhibited the greatest changes among cows that succumbed to the infection. Additionally, 2-AG was elevated pre-FM treatment among cows

that succumbed to the infection compared to those that survived and that 2-AG concentrations were not affected by NSAID administration in either outcome group. Furthermore, AEA concentrations increased from pre- to post-FM treatment among cows that succumbed to the infection, whereas AEA concentrations among cows that survived were not affected by NSAID administration. Effects of FM treatment on prostamide concentrations varied between infection outcome groups and PG-Gs were not detected in plasma, most likely due to their rapid degradation *in vivo*. Our results highlight the importance of the CYP450 enzymatic pathway for the efficacy of NSAD treatment during coliform mastitis. We also provide initial evidence of the role of the ECS in mastitis, which could be used to improve our understanding of anti-inflammatory and analgesic therapies.

3.2: MATERIALS AND METHODS

Reagents

Acetonitrile, methanol, and formic acid of liquid chromatography–MS grade were purchased from SigmaAldrich (St. Louis, MO). Deuterated and nondeuterated endocannabinoid and respective metabolite standards were purchased from Cayman Chemical (Ann Arbor, MI). Butylated hydroxy toluene (BHT) was purchased from Acros (Waltham, MA), 156 EDTA and tri-phenylphosphine were purchased from SigmaAldrich, and indomethacin was purchased from Cayman Chemical.

Animals and Design

This study was approved by the Michigan State University Institutional Animal Care and Use Committee (IACUC). All animals were Holstein dairy cattle housed at a commercial dairy in mid-Michigan. Animals were enrolled in the study when suffering from systemic coliform mastitis after on-farm protocol dictated that veterinary care, including treatment with the NSAID flunixin

meglumine was necessary. Cows in the coliform mastitis group had positive E. coli milk cultures (>100 colony forming units) and exhibited at least 2 signs of systemic clinical disease. Initial blood samples were collected immediately before treatment with a single dose of flunixin meglumine (2.2 mg/kg IV), ceftiofur sodium (2.2 mg/kg SC), and oral electrolyte fluids according to standard farm treatment protocols (pre-FM treatment); 8 hours post treatment (post-FM treatment); and again, immediately before the animal succumbed to the infection or recovered and was returned to the milking herd or sold (Resolution). One animal succumbed to the infection within 4 hours of the post-FM treatment sample and no third sample collection was possible. A total of eight individually matched control (MC) animals were chosen based on the enrolled systemic coliform animals and matched for days in milk (DIM), lactation number (LAC), and phenotype (number of milking quarters). Mean days in milk (DIM) for systemically infected animals was 101.63 (± 50.3) and the mean lactation number was 3.125 (± 0.687). Animals were deemed healthy based on negative bacterial milk cultures, no overt clinical signs, and a somatic cell count of <200,000 cells/mL.

Case Definition

Signs of acute systemic coli-form mastitis included increased core body temperature (>39.2°C), tachycardia (heart rate > 80 beats/minute), tachypnea (respiratory rate > 30 breaths/minute), episcleral injection, local signs of mammary gland inflammation including discoloration, swelling, heat and pain on palpation, and typical serum-like watery milk.

Blood Sample Collection

Blood samples were collected with evacuated tubes containing serum separator and EDTA. Pre-treatment samples of systemic coliform infected animals were collected from the jugular vein, all subsequent blood samples from the same animal were collected from the coccygeal vein. Blood

samples from healthy matched control animals was taken from the coccygeal vein and occurred within 14 days of initial pre-treatment sample from the paired systemically infected animal. Blood collection at each sampling point consisted of two 10mL EDTA tubes and two 15mL serum separator tubes. After transport on ice, EDTA tubes were treated with 4uL/mL of antioxidant/reducing agent (ARA) before centrifugation at 3000 rpm for 15 minutes at 4°C. Serum separator tubes sat at room temp until properly coagulated, before being placed on ice and centrifuged at 3000 rpm for 15 minutes at 4°C. After processing, 1 mL of serum and plasma was aliquoted into 1.5/2 mL microcentrifuge tubes and snap frozen in liquid nitrogen before being stored at -80C.

Solid Phase Extraction (SPE) of Blood

Blood samples were extracted and analyzed using methods published previously by Mavangira et al. 2016. Briefly, plasma (2mL) samples were mixed with an antioxidant reducing agent mixture (4µL of antioxidant reducing agent/1mL of sample) to prevent degradation of preformed oxylipids and prevent ex vivo lipid peroxidation as described previously the antioxidant reducing agent mixture consisted of 50% methanol, 25% ethanol, and 25% water with 0.9mM of BHT, 0.54mM EDTA, 3.2mM TPP, and 5.6mM indomethacin.

Plasma extractions were done using an Oasis plasma protocol on an Extrahera robot by Biotage (Charlotte, NC, USA). The samples, including formic acid, ARA, and Internal Standard were loaded into Oasis HLB 12 cc 500 mg LP extraction columns (Waters, Milford, MA, USA) and eluted using a 90:10 acetonitrile (ACN) and methanol (MeOH). Once the samples were eluted, they were evaporated using a Savant SpeedVac, resuspended in 150µL of 4:1 MeOH and ddH2O, filtered through an Amicon Ultrafree-MC filter (Sigma-Aldrich, St. Louis, MO, USA) and transferred to a chromatography vial with insert and stored at -20ºC until LC/MS/MS analysis.

LC/MS/MS Analysis

Details of LC/MS/MS analysis for oxylipids and fatty acids are described in Mavangira et al., 2016. In short, the quantification of analytes was accomplished on a Waters Xevo-TQ-S tandem quadrupole mass spectrometer (Water Corp., Milford, MA, USA) using multiple reaction monitoring (MRM). Chromatography separation was performed with an Ascentis Express C18 HPLC column (10 cm × 2.1 mm; 2.7 μm particles, Sigma-Aldrich, St. Louis, MO, USA) held at 50 °C, and the autosampler was held at 10 °C. Mobile phase A was water containing 0.1 % formic acid, and mobile phase B was acetonitrile. Flow rate was fixed at 0.3 mL/ min. Liquid chromatography separation took 15 min per sample. MRM parameters including cone voltage, collision voltage, precursor ion, production, and dwell time were optimized based on Waters QuanOptimize software (Waters Corp., Milford, MA, USA) by flow injection of pure standard for each individual compound.

The details of LC/MS/MS analysis for endocannabinoids and prostaglandin-ethanolamides and -glycerols are described in Williams et al., 2007. In short, the quantification of analytes was accomplished on a Q-Exactive Quadrupole-Orbitrap mass spectrometer (Thermo Fisher Scientific, Waltham, MA, USA) using multiple reaction monitoring (MRM). Chromatography separation was performed with an Acquity BEH C18 HPLC column (10 cm × 2.1 mm; 2.7 μm particles, Waters Corp., Milford, MA, USA) held at 40 °C, and the autosampler was held at 10 °C. Mobile phase A was water containing 0.1 % formic acid, and mobile phase B was acetonitrile. Flow rate was fixed at 0.3 mL/ min. Liquid chromatography separation took 15 min per sample. MRM parameters including cone voltage, collision voltage, precursor ion, production, and dwell time were optimized based on Xcalibur Data Acquisition and Interpretation software (Thermo Fisher

Scientific, Waltham, MA, USA) by flow injection of pure standard for each individual compound. Prostaglandin-glycerols (PG-G) were not detected in blood samples.

Statistical Analysis

All statistics were calculated using SAS9.4 (SAS institute Inc., Cary, NC). For pairwise comparison the Wilcoxon Rank-Sum score was used and means with standard error of the mean (SEM) were reported. Multiple comparisons of timepoints over the course of the infection were done using a two-way ANOVA, with uneven time-points, repeated measures, and Tukey-Kramer adjustment. Non-normally distributed data was either Log10 or square root transformed and back transformed for graphical representation. Of the eight animals with acute coliform mastitis that were enrolled in this study, four animals survived. Therefore, inclusive and individual analyses of the infection outcome groups were performed. Multiple comparisons were sliced by time and treatment, for the analysis of individual infection outcome groups.

3.3: RESULTS

Infection outcome alters fatty acid concentrations

The analysis of all animals for plasma fatty acid concentrations showed that all fatty acids quantified were elevated among cows suffering from acute coliform mastitis pre-FM treatment compared to their healthy matched control animals (Table 3.1a). Analysis of each infection outcome showed that cows that survived the infection, lauric, myristic, adrenic, palmitoleic, palmitic, α-linoleic, oleic, and stearic acid were elevated pre-FM treatment compared to their healthy matched control animals (Table 3.1b). Among cows that succumbed to the infection, lauric, myristic, palmitic, adrenic, arachidonic, docosahexaenoic, eicosapentaenoic, linoleic, oleic, and palmitic

Table 3.1: Fatty acid concentrations of Holstein dairy cows affected with acute coliform mastitis pre-FM treatment compared to their healthy matched control animals.

a) All animals (survival and death)

			Concentrations						
			Matched Control (N=8)			Pre-FM treatment (N=8)			
Fatty acid			Mean		SEM	Mean		SEM	*P*-value
Lauric acid***	C12:0	saturated	0.399	±	0.0564	2.555	±	0.5633	0.0009
Myristic acid***	C14:0	saturated	36.153	±	4.3775	419.0338	±	104.3474	0.0007
Palmitic acid***	C16:0	saturated	75.928	±	15.7936	335.015	±	40.0661	0.0009
Stearic acid**	C18:0	saturated	25.239	±	3.5984	46.225	±	6.0883	0.0054
Adrenic acid**	C22:4 (n-6)	unsaturated	0.059	±	0.0122	0.465	±	0.1856	0.0018
Arachidonic acid**	C20:4 (n-6)	unsaturated	0.729	±	0.0994	4.4125	±	1.7172	0.0028
Dihomo-linolenic acid**	C20:6 (n-6)	unsaturated	0.141	±	0.0252	0.725	±	0.2599	0.0073
Docosahexaenoic acid*	C22:6 (n-3)	unsaturated	0.039	±	0.0123	0.3325	±	0.2318	0.0114
Docosapentaenoic acid*	C22:5 (n-3)	unsaturated	1.155	±	0.1378	4.0438	±	1.2489	0.0039
Eicosapentaenoic acid**	C20:5 (n-3)	unsaturated	1.026	±	0.1493	4.58	±	1.0712	0.0101
Linoleic acid**	C18:2 (n-6)	unsaturated	24.770	±	5.0898	180.535	±	47.3500	0.0011
Oleic acid**	C18:1 (n-9)	unsaturated	49.270	±	19.6500	461.8188	±	61.9511	0.0014
Palmitoleic acid***	C16:1 (n-7)	unsaturated	21.165	±	3.6386	574.5713	±	148.7449	0.0009
α-linoleic acid**	C18:3 (n-3)	unsaturated	9.243	±	1.9686	37.8475	±	6.7378	0.0019

* p<0.05, ** p<0.01, *** p<0.001.

b) Survival only

			Concentrations						
			Matched Control (N=8)			Pre-FM treatment (N=8)			
Fatty acid			Mean		SEM	Mean		SEM	*P*-value
Lauric acid*	C12:0	saturated	0.338	±	0.0614	2.015	±	0.4205	0.0304
Myristic acid*	C14:0	saturated	29.010	±	5.5518	284.42	±	61.5574	0.0301
Palmitic acid*	C16:0	saturated	84.770	±	33.0065	312.7525	±	42.6251	0.0300
Stearic acid*	C18:0	saturated	26.283	±	4.0063	43.795	±	1.9327	0.0298
Arachidonic acid*	C22:4 (n-6)	unsaturated	0.060	±	0.0100	0.2275	±	0.0480	0.0265
Oleic acid*	C18:1 (n-9)	unsaturated	45.133	±	24.7402	387.88	±	89.6542	0.0366
Palmitoleic acid*	C16:1 (n-7)	unsaturated	20.180	±	6.3885	331.75	±	58.3104	0.0304
α-linoleic acid*	C18:3 (n-3)	unsaturated	7.573	±	1.6324	31.385	±	5.9857	0.0311

* p<0.05, ** p<0.01, *** p<0.001.

c) Death only

			Concentrations						
			Matched Control (N=8)			Pre-FM treatment (N=8)			
Fatty acid			Mean		SEM	Mean		SEM	*P*-value
Lauric acid*	C12:0	saturated	0.460	±	0.0926	3.095	±	1.0533	0.0364
Myristic acid*	C14:0	saturated	43.295	±	4.9593	553.6475	±	186.9293	0.0152
Palmitic acid*	C16:0	saturated	67.085	±	4.7420	357.2775	±	73.1031	0.0251
Adrenic acid*	C22:4 (n-6)	unsaturated	0.058	±	0.0243	0.7025	±	0.3477	0.0295
Arachidonic acid*	C20:4 (n-6)	unsaturated	0.778	±	0.1622	6.27	±	3.3280	0.0304
Docosahexaenoic acid*	C22:6 (n-3)	unsaturated	0.038	±	0.0125	0.5725	±	0.4598	0.0294
Eicosapentaenoic acid*	C20:5 (n-3)	unsaturated	1.255	±	0.1004	5.4775	±	1.8344	0.0403
Linoleic acid*	C18:2 (n-6)	unsaturated	25.903	±	8.4561	246.0875	±	79.1325	0.0388
Oleic acid*	C18:1 (n-9)	unsaturated	53.408	±	34.3281	535.7575	±	78.9170	0.0286
Palmitoleic acid*	C16:1 (n-7)	unsaturated	22.150	±	4.5083	567.3925	±	62.9085	0.0229

* p<0.05, ** p<0.01, *** p<0.001.

acid were elevated pre-FM treatment when compared to their healthy matched control animals (Table 3.1c). Analysis of all animals for fatty acid concentrations across the sampling time points showed that palmitoleic acid concentrations decreased from pre-FM treatment to resolution ($p=0.0294$), but pre-FM was not different from post-FM treatment, nor was post-FM treatment different from resolution (Table 3.2a). Palmitic acid concentrations of all animals were not different from pre- to post-FM treatment or resolution but decreased from post-FM treatment to resolution ($p=0.0187$). Oleic acid concentrations were lower among all animals at resolution than at pre- and post-FM treatment sampling time points ($p=0.011$ and $p=0.0413$, respectively) and no change was observed from pre- to post-FM treatment.

The discrete analysis of the infection outcomes revealed that among cows that survived the infection there was no change across the sampling time points for any of the fatty acids recorded. Among cows that succumbed to the infection, palmitoleic, linoleic and oleic acid exhibited variations across the sampling time points (Table 3.2b). Palmitoleic and oleic acid concentrations decreased from pre-FM treatment to resolution ($p=0.0120$ and $p=0.0262$, respectively), but were unchanged from pre- to post-FM treatment as well as from post-FM treatment to resolution. Linoleic acid concentrations decreased from pre- to post-FM treatment ($p=0.0342$) and resolution ($p=0.0264$). Between outcome groups, only linoleic acid was elevated pre-FM treatment among cows that succumbed to the infection compared to those that survived ($p=0.0496$). There was no difference between outcome groups at any other time points for any of the fatty acids recorded in this study.

Table 3.2: Inclusive and discrete multiple comparison of fatty acid concentrations of Holstein dairy cows affected with acute coliform mastitis.

a) All animals (survival and death)

			Concentrations								
			Pre-FM treatment (N=8)			Post-FM treatment (N=8)			Resolution (N=7)		
Fatty acid			Mean		SEM	Mean		SEM	Mean		SEM
Palmitic acid	C16:0	saturated	335.02[ab]	±	60.3938	371.22[a]	±	60.3938	152.35[b]	±	63.8898
Oleic Acid	C18:1 (n-9)	unsaturated	461.82[a]	±	65.1364	364.37[a]	±	65.1364	169.4[b]	±	68.6983
Palmitoleic Acid	C16:1 (n-7)	unsaturated	449.57[a]	±	63.1963	363.31[ab]	±	63.1963	197.2[b]	±	66.9932

[a -d] Means within a row with different superscripts are different ($p<0.05$)

b) Death only

			Concentrations								
			Pre-FM treatment (N=8)			Post-FM treatment (N=8)			Resolution (N=7)		
Fatty acid			Mean		SEM	Mean		SEM	Mean		SEM
Linoleic Acid	C18:2 (n-6)	unsaturated	246.09[a]	±	42.0412	61.1475[b]	±	42.0412	50.4958[b]	±	48.438
Oleic Acid	C18:1 (n-9)	unsaturated	535.76[a]	±	95.3563	352.11[ab]	±	95.3563	142.62[b]	±	106.89
Palmitoleic Acid	C16:1 (n-7)	unsaturated	567.39[a]	±	84.7096	384.37[ab]	±	84.7096	136.01[b]	±	96.48

[a -d] Means within a row with different superscripts are different ($p<0.05$)

CYP450 derived oxylipids are most affected by flunixin meglumine

The inclusive analysis of all animals showed that of the 32 oxylipids that were recorded, eight were elevated and three decreased among cows suffering from acute coliform mastitis pre-FM treatment compared to their healthy matched controls (Table 3.3a). The oxylipids that were elevated among cows suffering from acute coliform mastitis were 13-oxoODE, 9-oxoODE, 20-HETE, 6-keto PGF1α, 8,9-EET, 11,12-DHET, 14,15-DHET, and 14,15-EET. The oxylipids that exhibited decreased concentrations among cows with acute coliform mastitis include PGE2, ReD2, and 9,10-DiHOME. The discrete analysis of each infection outcome groups revealed that among animals that survived the infection only PGE2 exhibited a concentration difference, being decreased pre-FM treatment among animals suffering from acute coliform mastitis compared to their healthy matched control (Table 3.3b). Among animals that succumbed to the infection, only

Table 3.3: Products of fatty acid metabolism of Holstein dairy cows affected with acute coliform mastitis pre-FM treatment compared to their healthy matched control animals.

a) All animals (survival and death)

			Concentrations						
			Matched Control (N=8)			Pre-FM treatment (N=8)			
Pathway	Substrate	Oxylipid	Mean		SEM	Mean		SEM	*P*-value
COX	AA	6-keto-PGF1α**	0.566	±	0.1806	2.3625	±	0.4476	0.0073
COX	AA	PGE2*	20.438	±	6.8902	1.625	±	1.3548	0.0215
CYP450	AA	11,12-DHET*	1.638	±	0.1711	3.175	±	0.7188	0.0455
CYP450	AA	14,15-DHET**	1.875	±	0.1601	3.875	±	0.6739	0.0038
CYP450	AA	14,15-EET*	0.101	±	0.0180	0.325	±	0.1031	0.0113
CYP450	AA	20-HETE*	1.4	±	0.2053	3.3375	±	0.6995	0.0236
CYP450	AA	8,9-EET*	0.078	±	0.0214	0.2163	±	0.0529	0.0483
CYP450	LA	9,10-DiHOME**	2.563	±	0.5148	0.9875	±	0.1652	0.0031
LOX	DHA	ReD2*	1.550	±	0.1488	0.6575	±	0.2361	0.0387
LOX	LA	13-oxo-ODE*	3.038	±	0.9331	7.725	±	1.9535	0.0312
LOX	LA	9-oxo-ODE*	3.688	±	0.5416	13.075	±	3.8102	0.0462

* p<0.05, ** p<0.01, *** p<0.001.

b) Survival only

			Concentrations						
			Matched Control (N=4)			Pre-FM treatment (N=4)			
Pathway	Substrate	Oxylipid	Mean		SEM	Mean		SEM	*P*-value
COX	AA	PGE2*	29.1[a]	±	9.4700	2.7875[b]	±	2.7375	0.0265

* p<0.05, ** p<0.01, *** p<0.001.

c) Death only

			Concentrations						
			Matched Control (N=4)			Pre-FM treatment (N=4)			
Pathway	Substrate	Oxylipid	Mean		SEM	Mean		SEM	*P*-value
COX	AA	6-keto-PGF1α*	0.558	±	0.3052	3.05	±	0.3926	0.0304
CYP450	AA	11,12-DHET*	1.450	±	0.2021	4.525	±	1.0820	0.0291
CYP450	AA	14,15-DHET*	1.800	±	0.1780	4.975	±	1.0881	0.0304
CYP450	AA	20-HETE*	1.350	±	0.2255	4.1	±	1.2241	0.0305
CYP450	DHA	19,20-DiHDPA*	0.775	±	0.0629	1.9	±	0.5260	0.0294
CYP450	LA	9,10-DiHOME*	2.425	±	0.3772	0.85	±	0.2062	0.0284
LOX	LA	9-oxo-ODE*	3.175	±	0.7729	15.975	±	6.1054	0.0303

* p<0.05, ** p<0.01, *** p<0.001.

Table 3.4: Inclusive and discrete multiple comparison of plasma oxylipid concentrations, and corresponding enzymatic synthesis pathway with fatty acid substrate, of Holstein dairy cows affected with acute coliform mastitis.

a) All animals (survival and death)

			Concentrations								
			Pre-FM treatment (N=8)			Post-FM treatment (N=8)			Resolution (N=7)		
Pathway	Substrate	Oxylipid	Mean		SEM	Mean		SEM	Mean		SEM
COX	AA	6-keto-PGF1α	2.3625[a]	±	0.3708	0.8788[b]	±	0.3708	0.541[b]	±	0.3957
CYP450	EPA	14,15-DiHETE	6.55[a]	±	0.7736	4.000[b]	±	0.7736	4.5535[ab]	±	0.8232
CYP450	EPA	17,18-DIHETE	58.5625[a]	±	6.4499	42.275[b]	±	6.4499	36.8122[b]	±	6.7594
CYP450	LA	9,10-EpOME	0.1513[ab]	±	0.0325	0.1025[a]	±	0.0325	0.1765[b]	±	0.0337

[a -d] Means within a row with different superscripts are different ($p<0.05$)

b) Death only

			Concentrations								
			Pre-FM treatment (N=4)			Post-FM treatment (N=4)			Resolution (N=3)		
Pathway	Substrate	Oxylipid	Mean		SEM	Mean		SEM	Mean		SEM
COX	AA	6-keto-PGF1α	3.05[a]	±	0.4963	0.5825[b]	±	0.4963	0.9814[b]	±	0.5603
CYP450	AA	8,9-DHET	1.25[a]	±	0.1682	0.875[ab]	±	0.1682	0.4834[b]	±	0.1912
CYP450	EPA	14,15-DiHETE	8.5[a]	±	0.9597	4.375[b]	±	0.9597	4.7506[ab]	±	1.1047
CYP450	EPA	17,18-DIHETE	76.65[a]	±	6.7834	51.1[b]	±	6.7834	40.1772[b]	±	7.7503
CYP450	LA	12,13-EpOME	0.25[a]	±	0.07878	0.175[a]	±	0.07878	0.5986[b]	±	0.0906

[a -d] Means within a row with different superscripts are different ($p<0.05$)

9,10-DiHOME exhibited lower concentrations pre-FM treatment when compared to their healthy matched control (Table 3.3c). Whereas 9-oxo-ODE, 20-HETE, 6-keto-PGF1α, 11,12-DHET, 14,15-DHET, and 19,20-DiHPDA concentrations were elevated pre-FM treatment among cows that succumbed to the infection, compared to their healthy matched controls. The inclusive analysis of all animals across the three sampling time points revealed that 6-keto PGF1α concentrations decreased from pre- to post-FM treatment ($p=0.0215$) and pre-FM treatment to resolution ($p=0.0122$) but were not different from post-FM treatment to resolution (Table 3.4a). 9,10-EpOME concentrations increased from post-FM treatment to resolution ($p=0.0440$) but were unchanged from pre- to post-FM treatment and from pre-FM treatment to resolution. 14,15-DiHETE concentrations were decreased from pre- to post-FM treatment ($p=0.0425$) but were not different from pre- or post-FM treatment to resolution. Lastly, 17,18-DiHETE exhibited decreased plasma

concentrations from pre- to post-FM treatment and pre-FM treatment to resolution (p=0.0459 and p=0.0390, respectively). The discrete analysis of each infection outcome group revealed that among cows that survived the infection, none of the 32 oxylipids evaluated exhibited any concentrations changes. Conversely, cows that succumbed to the infection had decreased 6-keto PGF1α from pre- to post-FM treatment (p=0.0020) and from pre- FM treatment to resolution (p=0.0296) (Table 3.4b). 8,9-DHET concentrations decreased from pre-FM treatment to resolution (p=0.0216) but were unchanged from pre- to post-FM treatment and from post-FM treatment to resolution. Whereas 12,13-EpOME concentrations were unchanged from pre- to post-FM treatment but increased at resolution compared to both pre- and post-FM concentrations (p=0.0332

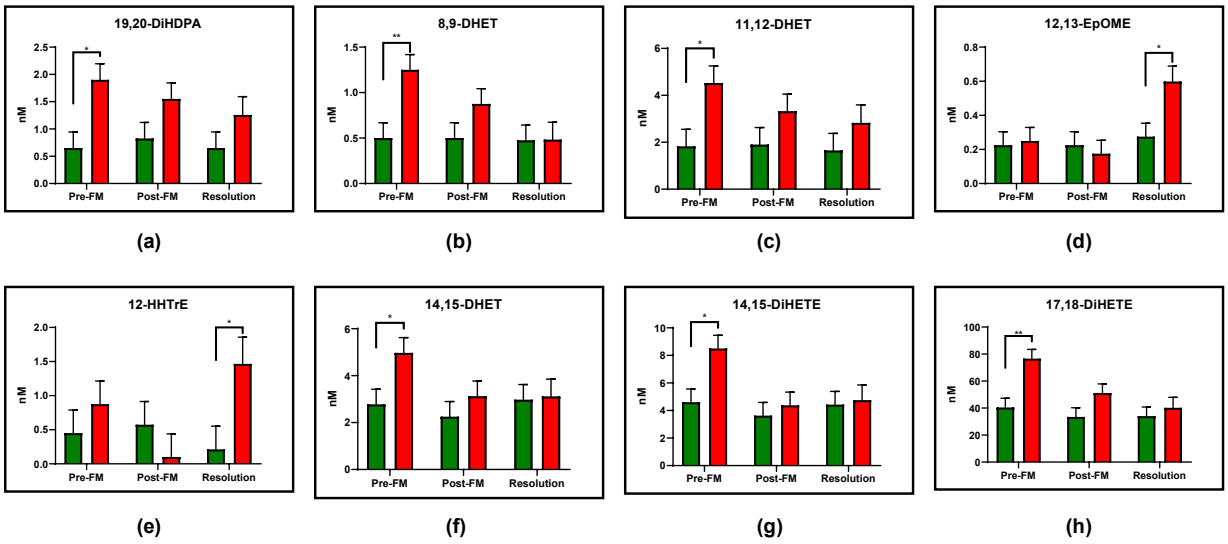

Figure 3.1: Concentrations (mean ± SEM) of plasma oxylipids of Holstein dairy cows suffering from naturally occurring acute coliform mastitis, treated with flunixin meglumine (FM), compared between the infection outcome groups (green bars = survived; red bars = died), at each sample timepoint: **(a)** 19,20-DiHDPA; **(b)** 8,9-DHET; **(c)** 11,12-DHET; **(d)** 12,13-EpOME; **(e)** 12-HHTrE; **(f)** 14,15-DHET; **(g)** 14,15-DiHETE; **(h)** 17,18-DiHETE.

*p<0.05, **p<0.01, ***p<0.001.

and p=0.0181, respectively). Both 14,15-DiHETE and 17,18-DiHETE concentrations were decreased from pre- to post-FM treatment (p=0.0151 and p=0.0228, respectively), but only 17,18-DiHETE concentrations remained decreased at resolution compared to pre-FM treatment (p=0.0094).

Evaluation of oxylipid concentration differences between outcome groups at each of the three sampling time points revealed that cows that succumbed to the infection had elevated pre-FM treatment plasma concentrations of 8,9-DHET, 11,12-DHET, 14,15-DHET, 14,15-DiHETE, 17,18-DiHETE, and 19,20-DiHDPA (p=0.0092, p=0.0236, p=0.0354, p=0.0151, p=0.0031, and p=0.0122, respectively) compared to cows that survived (Figure 3.2). Whereas 12,13-EpOME and 12-HHTrE concentrations were elevated at resolution among cows that succumbed to the infection (p=0.0209 and p=0.0343, respectively) compared to cows that survived.

Oxylipid Ratios

The inclusive analysis of all animals revealed that the ratio of 13-HODE/13-oxoODE was decreased pre-FM treatment among cows suffering from acute coliform mastitis compared to their healthy matched controls (Table 3.5a). The discrete analysis of each infection outcome group showed that only among cows that succumbed to the infection, the ratio of 13-HODE/13-oxoODE was decreased pre-FM treatment compared to the healthy matched control animals (Table 3.5b). No difference in oxylipid ratios was detected pre-FM treatment among cows that survived the infection and their healthy matched controls. The inclusive analysis of all animals showed that across the sampling time points the ratio of 9-HODE/9-oxoODE increased from pre- to post-FM treatment (p=0.0054) and from pre-FM treatment to resolution (p=0.0379).

Table 3.5: Oxylipid ratios (upstream/downstream) of Holstein dairy cows affected with acute coliform mastitis pre-FM treatment compared to their healthy matched control animals.

a) All animals (survival and death)

	Concentrations						
	Matched Control (N=8)			Pre-FM treatment (N=8)			
Metabolites	Mean		SEM	Mean		SEM	*P*-value
13-HODE/13-oxoODE*	9.377	±	1.5423	4.8903	±	0.6987	0.0136

* p<0.05, ** p<0.01, *** p<0.001.

b) Death only

	Concentrations						
	Matched Control (N=8)			Pre-FM treatment (N=8)			
Metabolites	Mean		SEM	Mean		SEM	*P*-value
13-HODE/13-oxoODE*	12.127	±	2.3386	4.9718	±	0.6525	0.0294

* p<0.05, ** p<0.01, *** p<0.001.

Table 3.6: Inclusive and discrete multiple comparison of oxylipid ratios (upstream/downstream) across the three sample time points.

a) All animals (survival and death)

	Concentrations								
	Pre-FM treatment (N=8)			Post-FM treatment (N=8)			Resolution (N=7)		
Metabolites	Mean		SEM	Mean		SEM	Mean		SEM
9-HODE/9-oxoODE	3.6485[a]	±	1.198	9.642[b]	±	1.198	8.4892[b]	±	1.2789
13-HODE/13-	4.8903[a]	±	1.0926	9.8485[b]	±	1.0926	9.605[b]	±	1.1674

[a -d] Means within a row with different superscripts are different (p<0.05)

b) Survival only

	Concentrations								
	Pre-FM treatment (N=4)			Post-FM treatment (N=4)			Resolution (N=4)		
Metabolites	Mean		SEM	Mean		SEM	Mean		SEM
9-HODE/9-oxoODE	3.3176[a]	±	1.5633	7.5441[ab]	±	1.5633	10.0981[b]	±	1.5633

[a -d] Means within a row with different superscripts are different (p<0.05)

c) Death only

	Concentrations								
	Pre-FM treatment (N=4)			Post-FM treatment (N=4)			Resolution (N=3)		
Metabolites	Mean		SEM	Mean		SEM	Mean		SEM
9-HODE/9-oxoODE	3.9794[a]	±	1.5633	11.74[b]	±	1.5633	6.372[a]	±	1.7728

[a -d] Means within a row with different superscripts are different (p<0.05)

The ratio of 9-HODE/9-oxoODE was not different from post-FM treatment to resolution (Table 3.6a). The ratio of 13-HODE/13-oxoODE of all animals exhibited similar patterns, with an increased ratio from pre- to post-FM treatment ($p=0.0129$) and from pre-FM treatment to resolution ($p=0.0278$), with no change from post-FM treatment to resolution. The discrete analysis of each infection outcome group showed that only the ratio of 9-HODE/9-oxoODE changed across the three sampling time points for those cows that survived and those that succumbed to the infection (Table 3.6b and c). Among cows that survived, the ratio of 9-HODE/9-oxoODE increased from pre-FM treatment to resolution ($p=0.0176$) but was not different from pre- to post-FM treatment, or from post-FM treatment to resolution. Conversely, among cows that succumbed to the infection the ratio of 9-HODE/9-oxoODE increased from pre- to post-FM treatment ($p=0.0026$) and decreased again from post-FM treatment to resolution ($p=0.0443$).

Coliform mastitis alters endocannabinoid biosynthesis

The inclusive analysis of all animals showed that AEA, PEA, OEA, EPEA, and dihomo-γ-linolenoyl-EA were elevated among all infected animals compared to their healthy matched controls (Table 3.7a). The discrete analysis of each infection outcome group showed that cows that survived the infection had elevated pre-FM treatment concentrations of AEA, PEA, OEA, and dihomo-γ-linolenoyl-EA compared to their healthy matched controls (Table 3.7b). The only EC that was decreased pre-FM treatment among animals that survived compared to their healthy matched controls was 2-AG. Among cows that succumbed to the infection, AEA, PEA, OEA, and dihomo-γ-linolenoyl-EA concentrations were elevated pre-FM treatment compared to their healthy matched control animals (Table 3.7c).

Table 3.7: Blood endocannabinoids of Holstein cows with acute coliform mastitis pre-flunixin meglumine (FM) treatment and their healthy matched control animals.

a) All animals (survival and death)

	Concentrations						
	Healthy Matched Control (N=8)			Acute coliform mastitis pre-FM treatment (N=8)			
Endocannabinoid	Mean		SEM	Mean		SEM	*P*-value
AEA***	0.498	±	0.0529	3.1938	±	0.4346	0.0009
PEA**	0.825	±	0.0597	1.9517	±	0.5097	0.0014
OEA***	19.946	±	2.0376	40.0748	±	4.4472	0.0009
EPEA*	0.01	±	0.0000	0.247	±	0.1152	0.0352
Dihomo-γ-linolenoyl-EA***	0.52	±	0.1025	3.2696	±	0.7090	0.0009

* p<0.05, ** p<0.01, *** p<0.001.

b) Survival only

	Concentrations						
	Healthy Matched Control (N=4)			Acute coliform mastitis pre-FM treatment (N=4)			
Endocannabinoid	Mean		SEM	Mean		SEM	*P*-value
AEA*	0.4603	±	0.0553	3.3746	±	0.3764	0.0304
2-AG*	8.514	±	0.3770	2.2115	±	0.5357	0.0297
PEA*	0.831	±	0.0331	1.289	±	0.0998	0.0316
OEA*	19.566	±	3.9246	34.186	±	2.4774	0.0371
Dihomo-γ-linolenoyl-EA*	0.368	±	0.0996	2.9374	±	0.5028	0.0307

* p<0.05, ** p<0.01, *** p<0.001.

c) Death only

	Concentrations						
	Healthy Matched Control (N=4)			Acute coliform mastitis pre-FM treatment (N=4)			
Endocannabinoid	Mean		SEM	Mean		SEM	*P*-value
AEA*	0.535	±	0.0953	3.013	±	0.8473	0.0336
PEA*	0.819	±	0.1245	2.6144	±	0.9538	0.0294
OEA*	20.326	±	1.9689	45.9636	±	7.9395	0.0352
Dihomo-γ-linolenoyl-EA*	0.673	±	0.1536	3.6017	±	1.4212	0.0304

* p<0.05, ** p<0.01, *** p<0.001.

Across sampling time points, the inclusive analysis of all animals showed no change among any of the selected EC. The discrete analysis of each infection outcome group showed that only AEA concentrations changed among cows that survived the infection (Table 3.8a), with concentrations decreasing from pre- and post-FM treatment to resolution (p=0.0011 and p=0.0015, respectively). Among cows that succumbed to the infection, AEA concentrations increased from

pre- to post-FM treatment and resolution (p=0.0003 and p=0.0022, respectively) (Table 3.8b). Additionally, OEA concentrations among cows that succumbed to the infection decreased from pre-FM treatment to resolution (p=0.0299) but were not different from pre- to post-FM treatment or from post-FM treatment to resolution.

Table 3.8: Blood endocannabinoid concentrations over the course of acute systemic coliform mastitis with flunixin meglumine (FM) treatment in Holstein cows.

a) Survival only

	Concentrations								
	Pre-FM treatment (N=4)			Post-FM treatment (N=4)			Resolution (N=4)		
Endocannabinoi	Mean		SEM	Mean		SEM	Mean		SEM
AEA	3.3746[a]	±	0.874	2.4492[a]	±	0.874	0.3048[b]	±	0.874

[a -d] Means within a row with different superscripts are different (p<0.05)

b) Death only

	Concentrations								
	Pre-FM treatment (N=4)			Post-FM treatment (N=4)			Resolution (N=3)		
Endocannabinoi	Mean		SEM	Mean		SEM	Mean		SEM
AEA	3.0129[a]	±	0.874	5.6748[b]	±	0.874	6.0256[b]	±	0.909
OEA	45.9638[a]	±	6.111	33.5015[ab]	±	6.111	19.307[b]	±	6.972
α-LEA	0.3055[a]	±	0.062	0.158[b]	±	0.062	0.1874[ab]	±	0.068

Lastly, α-LEA concentrations decreased from pre- to post-FM treatment among cows that succumbed to the infection (p=0.0419) but were not different from pre- or post-FM treatment to resolution. Between the infection outcome groups, only AEA and 2-AG exhibited concentration differences at any of the sampling time points (Figure 3.3), with AEA concentrations being increased among cows that succumbed to the infection at post-FM treatment and resolution (p=0.0243 and p=0.0008, respectively), and 2-AG concentrations being elevated among cows that succumbed to the infection at all three sampling time points (p=0.0178, p=0.0222, and p=0.0018; respectively).

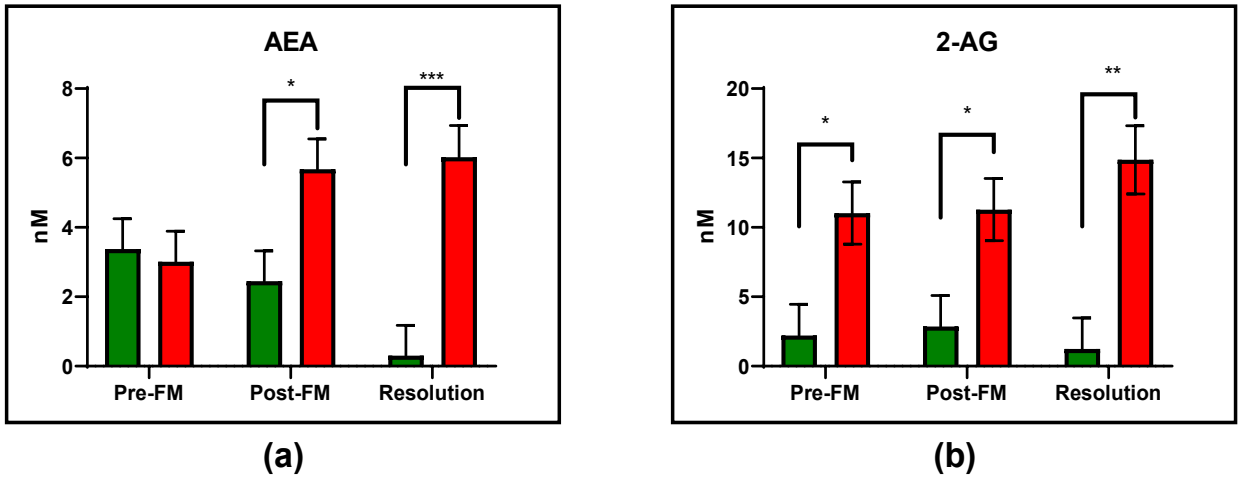

Figure 3.2. Concentrations (mean ± SEM) of blood EC compared between the infection outcome groups (green bars = survived; red bars = died) at each sample timepoint: **(a)** arachidonoylethanolamide (AEA) was elevated among cows that died post-FM treatment and at resolution, but not pre-FM treatment; **(b)** 2-arachidonoyl-glycerol (2-AG) was elevated at all three sample timepoints among cows that died.

* $p<0.05$, ** $p<0.01$, *** $p<0.001$.

Infection outcome affects prostamide biosynthesis during coliform mastitis

In inclusive and individual analysis of both infection outcome groups showed that PGE1-EA was not elevated among infected animals compared to their healthy matched controls. The inclusive analysis of all animals showed that cows suffering from acute coliform mastitis had elevated plasma PGE2-EA concentrations pre-FM treatment compared to their healthy matched control animals (Table 3.9a). However, neither outcome group by itself exhibited any changes in PGE2-EA concentrations pre-FM treatment compared to their healthy matched controls. The inclusive analysis of all animals showed that PGD2-EA concentrations were elevated pre-FM treatment compared to the healthy matched controls. The discrete analysis of each outcome groups

revealed that PGD2-EA concentrations were elevated among animals that survived and those that did not, compared to their healthy matched controls (Table 3.9b and c). The inclusive analysis of all animals showed increased pre-FM treatment concentrations of PGF2α-EA compared to the healthy matched control animals, but only those animals that succumbed to the infection exhibited elevated PGF2α-EA concentrations pre-FM treatment compared to their healthy matched controls.

Table 3.9: Blood prostaglandin-ethanolamide (PG-EA) concentrations of Holstein cows with acute coliform mastitis pre-flunixin meglumine (FM) treatment and their healthy matched control animals.

a) All Animals (survival and death)

	Concentrations						
	Healthy Matched Control			Acute coliform mastitis			
Prostamide	Mean		SEM	Mean		SEM	*P*-value
PGE2-EA**	0.01[a]	±	0.0000	1.164[b]	±	0.3342	0.0045
PGD2-EA***	0.01[a]	±	0.0000	0.3179[b]	±	0.0043	0.0004
PGF2a-EA**	0.170[a]	±	0.0647	1.6663[b]	±	0.5525	0.009

* p<0.05, ** p<0.01, *** p<0.001.

b) Survival only

	Concentrations						
	Healthy Matched Control			Acute coliform mastitis			
Prostamide	Mean		SEM	Mean		SEM	*P*-value
PGD2-EA*	0.01[a]	±	0.0000	0.3088[b]	±	0.0019	0.0202

* p<0.05, ** p<0.01, *** p<0.001.

c) Death only

	Concentrations						
	Healthy Matched Control			Systemic coliform mastitis			
Prostamide	Mean		SEM	Mean		SEM	*P*-value
PGD2-EA*	0.01[a]	±	0.0000	0.3269[b]	±	0.0053	0.0211
PGF2a-EA*	0.19[a]	±	0.1127	2.9603[b]	±	0.5384	0.0294

* p<0.05, ** p<0.01, *** p<0.001.

The inclusive analysis of all animals across the sampling time points revealed that PGE2-EA decreased from pre- to post-FM treatment (p=0.0077) but did not change from pre- or post-FM to resolution (Table 3.10a). Concentrations of PGD2-EA among all animals decreased from pre- to post-FM treatment and resolution (p<0.0001 and p<0.0001, respectively). During the

individual analysis of the infection outcome groups, only animals that succumbed to the infection had decreased PGE2-EA concentrations from pre- to post-FM treatment (p=0.0109), which remained depressed at resolution (Table 3.10c). Whereas concentrations of PGD2-EA decreased from pre- to post-FM treatment and resolution for both infection outcome groups (survival: p<0.0001 and p<0.0001, respectively; death: p<0.0001 and p<0.0001, respectively). Between outcome groups, cows that succumbed to the infection had greater post-FM treatment concentrations of PGE1-EA (p=0.0300) (Figure 3.4a), greater pre-FM treatment concentrations of PGD2-EA (p=0.0002) (Figure 4b), and greater PGF2α-EA concentrations at all three sampling time points compared to the cows that survived (p=0.0014, p=0.0003, and p=0.0001, respectively) (Figure 3.4c).

Table 3.10: Blood prostaglandin-ethanolamide (PG-EA) concentrations over the course of acute systemic coliform mastitis with flunixin meglumine (FM) treatment in Holstein cows.

a) All animals (survival and death)

	Concentrations								
	Pre-FM treatment (N=8)			Post-FM treatment (N=8)			Resolution (N=7)		
Prostamide	Mean		SEM	Mean		SEM	Mean		SEM
PGE2-EA	1.164[a]	±	0.2235	0.01[b]	±	0.2235	0.3241[ab]	±	0.239
PGD2-EA	0.3179[a]	±	0.002563	0.01[b]	±	0.002563	0.01[b]	±	0.00274

[a -d] Means within a row with different superscripts are different (p<0.05)

b) Survival only

	Concentrations								
	Pre-FM treatment (N=4)			Post-FM treatment (N=4)			Resolution (N=4)		
Prostamide	Mean		SEM	Mean		SEM	Mean		SEM
PGD2-EA	0.3088[a]	±	0.002379	0.01[b]	±	0.002379	0.01[b]	±	0.00237

[a -d] Means within a row with different superscripts are different (p<0.05)

c) Death only

	Concentrations								
	Pre-FM treatment (N=4)			Post-FM treatment (N=4)			Resolution (N=3)		
Prostamide	Mean		SEM	Mean		SEM	Mean		SEM
PGE2-EA	1.5518[a]	±	0.3038	0.01[b]	±	0.3038	0.01[b]	±	0.3508
PGD2-EA	0.327[a]	±	0.002379	0.01[b]	±	0.002379	0.01[b]	±	0.00274

[a -d] Means within a row with different superscripts are different (p<0.05)

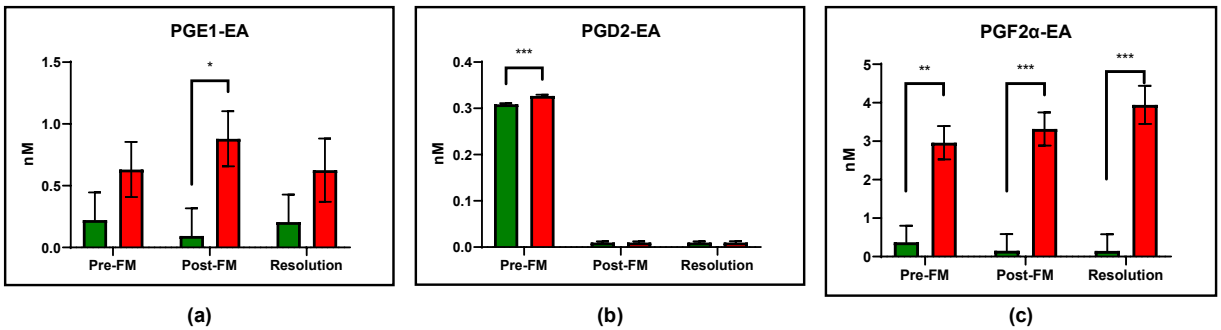

Figure 3.3. Concentrations (mean ± SEM) of blood PG-EA compared between the infection outcome groups (green bars = survived; red bars = died) at each sample timepoint: **(a)** prostaglandin-E1-ethanolamide (PGE1-EA) was elevated post-FM treatment among cows that died, but was not different from cows that survived at the pre-FM treatment and resolution timepoints; **(b)** prostaglandin-D2-ethanolamide (PGD2-EA) concentrations were elevated among cows that died pre-FM treatment, but there was no difference at the post-FM or resolution timepoints; **(c)** prostaglandin-F2-α-ethanolamide (PGF2α -EA) was elevated among cows that died at all three timepoints.

* $p<0.05$, ** $p<0.01$, *** $p<0.001$.

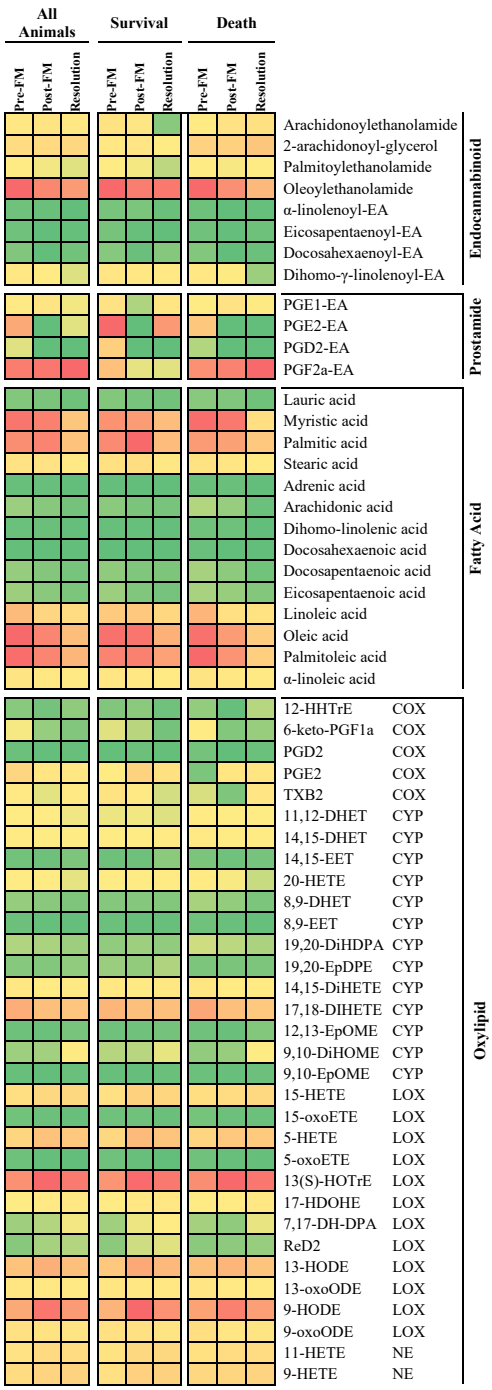

Figure 3.4: Heat map (Red – greatest concentrations, Green – lowest) of mean plasma concentrations of endocannabinoids, prostamides, fatty acids, and oxylipids of Holstein dairy cows suffering from naturally occurring acute coliform mastitis. Synthesis pathway of oxylipids listed in alphabetical order concentrations.

3.4: DISCUSSION

Differences in fatty acid, oxylipid, EC and prostamide concentrations before and after NSAID administration, among dairy cattle the succumbed to naturally occurring acute coliform mastitis compared to those that did not, implies underlying physiological states that may determine the efficacy of medical interventions. Currently, efficacy of NSAID treatments in dairy cattle is focused on select inflammatory markers and oxylipids. However, we have already shown that products of lipid peroxidation by free radicals, or isoprostanes, may hold greater insight into the inflammatory status of dairy cattle affected with acute coliform mastitis (Walker et al., 2021). Further highlighting the importance of a broader analysis of inflammatory mediators, we showed that animals that succumbed to the infection exhibited a greater degree of fatty acid mobilization and subsequent reduction of fatty acid concentrations following NSAID treatment, compared to those animals that survived. Additionally, the majority of oxylipids affected by coliform mastitis and NSAID treatment were CYP450 derived and among animals that succumbed to the infection. Lack of NSAID effect on oxylipid ratios among cows that survived is indicative of a better regulated pro- and antioxidant environment. Increased AEA concentrations post-FM treatment among cows that succumbed to the infection may contribute to the elevated oxygenated metabolites of oxylipids among cows that succumbed to the infection, and elevated 2-AG among cows that succumbed to the infection at all three time points supports a greater degree of lipid mobilization due to a dysregulated metabolic state. Additionally, the varying effects of NSAID treatment on prostamide and oxylipid concentrations highlights the importance of non-COX targets of FM and the implications of underlying physiological states on the efficacy of NSAID treatments.

Infection outcome alters fatty acid concentrations

Increased lipolysis during acute coliform mastitis leads to elevated concentrations of circulating non-esterified fatty acids (NEFA) which can induce COX-2, ROS production and release of proinflammatory cytokines. Metabolic stress during peak lactation is considered a major contributor to dysfunctional inflammatory responses to pathogens in dairy cows (Sordillo et al., 2009) and we demonstrated that the animals that succumbed to the infection in this study had elevated pre-FM treatment NEFA concentrations compared to those animals that survived (Walker et al., 2021). We now showed a difference in fatty acid profile among dairy cows that survived and those that did not, with classically anti-inflammatory n-3 unsaturated fatty acids EPA and DHA being elevated pre- FM treatment only among animals that succumbed, and the n-3 unsaturated α-linoleic acid being elevated only among animals that survived. Effect of specific fatty acid profiles may play a crucial role in enzyme activity. The discovery of allosteric modulation of the COX enzymes highlights the importance of relative fatty acid concentrations and substrate availability (Smith and Malkowski 2019). For example, particular relative concentrations of EPA and AA may increase the production of pro-inflammatory AA derived oxylipids, due to allosteric modulation of the COX active site to preferentially bind AA over other substrates, thereby negating the anti-inflammatory properties of EPA derived oxylipids.

The lack of NSAID treatment effect, or any changes in fatty acid concentrations observed in this study among dairy cows that survived the infection implies the presence of underlying metabolic dysregulation prior to medical intervention among those animals that succumbed to the infection. Only among animals that succumbed to the infection did fatty acid concentrations change across the time course of the study. However, only linoleic acid concentration was decreased after 8 hours of FM treatment among animals that succumbed to the infection, whereas oleic and palmitoleic

acid only decreased at resolution compared to pre-FM concentrations, indicating that the reduction in fatty acid concentrations is not due to direct action of FM, but may be due to breakdown of regulatory mechanisms of lipolysis and other homeostatic processes.

CYP450 derived oxylipids are most affected by flunixin meglumine

Differences in synthesis of CYP450 derived oxylipids recorded in this study and lack of changes among COX derived oxylipids implies that the CYP450 group of enzymes plays a crucial role in oxylipid production during acute coliform mastitis. Specifically, the interaction of FM and the CYP450 enzymatic pathway is of interest in this study, as the largest proportion of oxylipid concentration changes are CYP450 derived. Indeed, animals that succumbed to the infection had elevated pre-FM CYP450 derived oxylipids, whereas animals that survived had no changes in pre-FM CYP450 derived oxylipids, but exhibited decreased PGE2, compared to their healthy matched controls. Furthermore, in the survival group, there was no change observed among any of the 32 oxylipids, indicating that NSAID treatment did not affect the synthesis of oxylipids among animals that survived. Expression of CYP450 enzymes is widespread and highly variable in bovine tissue (Kuhn et al., 2020). Metabolism and inactivation of FM occurs through CYP450 enzymes (Knych et al., 2021) and therefore, excessive CYP450 expression and activity, not only in hepatic tissue, may alter the drug's half-life and ability to reduce mediator synthesis through the COX pathway (Howard et al., 2015). Interestingly, 9,10-DiHOME was the only CYP450 derived oxylipid not elevated among infected animals, but concentrations were decreased compared to healthy matched control animals. Production of DiHOME occurs during oxidative burst in inflammatory cells and reduced concentrations of 9,10-DiHOME among animals that succumbed to the infection may therefore be indicative of compromised immune cell function, reduced oxidative burst capabilities, and diminished clearance of pathogens. However, 9,10-DiHOME concentrations did not change

over the time course of the infection, and effect of NSAID treatment is therefore not discernable. The reduced concentrations of PGE2 among animals that survived the infection is crucial, as PGE2 is crucial to the regulation of activation, maturation, migration, and cytokine production of several immune cells involved in innate immunity (Agard et al., 2013). Decreased PGE2 among the animals that survived may therefore be indicative of less immune cell recruitment and activation pre-FM treatment. Lack of 9,10-DiHOME elevation among animals that succumbed to the infection and decreased PGE2 among animals that survived, further implies functional differences of immune cells between the infection outcome groups. Dysfunctional immune cells may lead to lack of pathogen clearance and recruitment of additional immune cells, exasperating the inflammatory response and potential for localize tissue damage and systemic involvement.

Oxylipid Ratios

Oxylipids are unique in their function during inflammation and downstream metabolites can possess opposite effects relative to their precursors. Ability of 9- and 13-HODE to activate PPARγ results in pro-inflammatory effects, whereas the dehydrogenation product of 9- and 13-HODE, 9- and 13-oxoODE, exhibits anti-inflammatory effects with PPARγ activation (Altman et al., 2007, Vangaveti et al., 2010). Increased ratio of up- / downstream oxylipids among both outcome groups may be indicative of NSAID action within immune cells. Animals that succumbed to the infection had a significantly elevated ratio of 9-HODE/9-oxoODE eight hours after FM administration, whereas animals that survived did not reach a similar ratio until the resolution time point. More immediate effects on oxylipid ratios among animals that succumbed to the infection implies that FM effects were more immediate, likely due to pre-existing differences in immune cell number and function. Overall, the oxylipid ratios indicate a pre-existing difference in oxylipid synthesis and possibly also immune cell function.

Coliform mastitis alters endocannabinoid biosynthesis

Differences in plasma EC and metabolite concentrations were not only detected post-FM treatment, but also before the NSAID was administered, indicating differential synthesis and metabolism of EC based on underlying factors, such as metabolic state and degree of inflammation. Increased AEA concentrations from pre- to post-FM treatment among cows that succumbed to the infection may be indicative of decreased expression and activity of the degradation enzyme fatty acid amide hydrolase (FAAH). Among dairy cows suffering from endometritis, uterine FAAH mRNA expression was decreased (Bonsale et al., 2018) and mRNA expression of FAAH within the central nervous system was decreased among dairy cows affected by metabolic stress during the onset of- and peak lactation (Kuhla et al., 2020). Elevated AEA during inflammatory events may act to resolve inflammation by reducing IL-6, IL-12, and IL-13 production by macrophages (Correa et al., 2011), limit TNFα released by neutrophils, and inhibit neutrophil recruitment to infection sites (Berdyshev et al., 1998). However, the effects of AEA on immune mediating cells are highly variable and dependent on timing, concentrations, and differential activation of downstream pathways, demonstrated by AEA induced ROS and IL-10 production in macrophages (Correa et al., 2011; Takenouchi et al., 2012), as well as chemotaxis and respiratory burst in neutrophils. Indeed, monocyte to macrophage differentiation not only increases CB1 expression, but may be dependent on CB1 activation by AEA (Han et al., 2009) and elevated AEA concentrations observed post-FM treatment among cows that succumbed to the infection in this study, may contribute to the exasperated inflammatory response and inability to resolve inflammation in a timely manner due to prolonged recruitment and activation of macrophages and neutrophils. Furthermore, prolonged elevated AEA may also contribute to endothelial cell dysfunction, a hallmark of coliform mastitis, due to increased ROS production and

cell death via initiation of apoptotic pathways (Rajesh et al., 2010). In this study increase in AEA concentrations from pre- to post-FM treatment observed among cows that succumbed to the infection may also be due to the well documented decrease in FAAH expression, elevated circulating fatty acids due to adipose mobilization, and inhibition of the COX pathways due to NSAID treatment. Interestingly, several NSAIDs, such as ibuprofen and flurbiprofen, were documented to also inhibit FAAH activity (Dongdem et al., 2022). Even though activity of FM on FAAH has yet to be documented, off-target effects of FM cannot be excluded.

Elevated 2-AG concentrations at all three sampling time points among cows that succumbed to the infection is indicative of metabolic dysregulation. Indeed, previously published data from this study shows that non-esterified fatty acid (NEFA) concentrations were significantly elevated among cows that succumbed to the infection, compared to those that survived (Walker et al., 2021). Elevated 2-AG concentrations may contribute to the dysfunctional inflammatory state of cows that succumbed to the infection, as 2-AG increases expression of adhesion molecules, chemokines, and migration of macrophages (Kishimoto et al., 2004) and neutrophils (Chouinard et al., 2011). However, the importance of proper timing is highlighted by 2-AG induced decrease in neutrophil degranulation and ROS release (Balenga et al., 2011), as well as decreased production of TNFα and neutrophil recruitment to infection sites (Chouinard et al., 2011). Furthermore, metabolism of 2-AG to PG-Gs is a key step towards resolution of the inflammatory response, as PGD2-G reduced mRNA expression of macrophage inflammatory protein-1α in murine models (Alhouayek et al., 2018). Excessive 2-AG synthesis among cows that succumbed to the infection may therefore also be an attempt of the organism to synthesize pro-resolving mediators through the now inhibited COX pathway. However, similar to AEA, the dual nature of the ECS is

highlighted by the activation of macrophages by picomolar concentrations of the COX metabolite PGE2-G (Nirodi et al., 2004), that we were not able to quantify in this study.

Infection outcome affects prostamide biosynthesis during coliform mastitis

Greater degrees of prostamide synthesis pre-FM treatment among cows that succumbed to the infection are indicative of increased COX-2 activity and substrate availability, compared to those that survived. Interestingly, FM treatment did not reduce PGF2α-EA concentrations among cows that succumbed to the infection whereas PGD2-EA and PGE2-EA concentrations were decreased among both infection outcome groups, possibly due to inhibition of specific prostaglandin synthases by FM. Failure to reduce PGF2α-EA concentrations among cows that succumbed to the infection is detrimental to the analgesic properties of NSAID administration, as PGF2α-EA exerts proalgesic effects in mice models (Woodward et al., 2013). Additionally, elimination of PGD2-EA synthesis with FM administration highlights the potential detrimental effects of NSAID treatment, as PGD2-EA was shown to exert anti-inflammatory effects in murine models of colitis (Alhouayek et al., 2018). Furthermore, PGE2-EA reduces TNFα production in monocytes (Brown et al., 2013), and elimination of the PGD2-EA and PGE2-EA may also inhibit proper resolution of the inflammatory response. Differential effects of FM treatment on prostamide concentrations may be due to FM inhibiting specific prostaglandin synthases as well as the COX enzymes. Our understanding of the bovine ECS may therefore benefit from future *in-vitro* studies regarding the specific targets of FM within immune mediating cells. Lastly, shunting of substrate to the lipoxygenase and CYP450 pathways of lipid metabolism may also be occurring. Metabolism of AEA and 2-AG via the LOX and CYP450 pathways yields hydroxyeicosatetraenoic acid-ethanolamides (HETE-EA) (van der Stelt et al., 2000) and epoxyicosatrienoyl-ethanolamides (EET-EA) (Urquhart et al., 2015), respectively. However, this study did not quantify these

metabolites. Future research should therefore be focused on completing the ECS profile via metabolites through the LOX and CYP pathways. Nonetheless, the effects of acute coliform mastitis and FM treatment on prostamide synthesis via the COX pathways recorded in this study, give some insight into FM function and underlying mechanisms influencing the efficacy of the NSAID.

3.5: CONCLUSIONS

This study, for the first time, gave insight into the biosynthesis of endocannabinoids and their metabolites in Holstein dairy cows suffering from naturally occurring acute coliform mastitis. Particularly interesting are the EC and oxylipid concentration differences pre-treatment, among animals that succumbed to the infection and those that survived. Differential effects of NSAID treatment dependent on the infection outcome are indicative of the importance of the timing of medical interventions and degree of dysregulated inflammation prior to NSAID administration. Indeed, 2-AG concentrations of cows suffering from acute coliform mastitis may be a potent biomarker for efficacy of NSAID administration, as animals that survived had lower concentrations of 2-AG pre- treatment, not only compared to those that succumbed to the infection, but also compared to their healthy matched control animals. The role AEA plays in inflammation may also be of great interest and benefit to future studies, seeing as FM administration resulted in elevated AEA concentrations among cows that succumbed to the infection only, suggesting a discrepancy in underlying biosynthesis and degradation pathways among outcome groups, prior to NSAID administration. Lastly, lack of concentrations differences of CYP450 derived oxylipids among animals that survived highlights the importance of the CYP450 enzymatic pathway on FM mediated effects. Additional research into non-COX targets of FM is imperative to defining

adequate timing of FM administration and provide greater insight into establishing therapeutic strategies of the NSAID.

CHAPTER 4: Anandamide Alters Barrier Integrity of Bovine Vascular Endothelial Cells during Endotoxin Challenge

4.1: INTRODUCTION

Infection of the mammary gland, or mastitis, is one of the diseases with the greatest impact on animal welfare and dairy cow health in North America (NAHMS, 2014; Rollin et al., 20151,2). Infections caused by coliform bacteria can be particularly severe, with a negative impact on cow well-being and a mortality rate of over 30% (Nakajima et al., 1997; Erskine et al., 1988; Walker et al., 2021). Effective clearance of the pathogen is highly dependent on a properly regulated inflammatory response, with rapid onset and timely resolution, to prevent excessive mammary secretory tissue damage. However, acute infections are associated with overproduction of pro-inflammatory oxylipids, excessive leukocyte infiltration into infected tissue, and excessive reactive oxygen species' (ROS) production that may lead to oxidative stress, damaging healthy tissues.

Breakdown of the epi- and endothelial monolayers is part of the pathology of coliform mastitis in dairy cows (Bruckmaier and Wellnitz, 2017). Stimulation of the Toll-like receptor 4 (TLR4) by the coliform derived bacterial endotoxin lipopolysaccharide (LPS), results in increased expression of adhesion molecules, as well as increased production of inflammatory mediators, such as oxylipids, cytokines, and ROS. Inflammatory responses during coliform mastitis include synthesis of pro- and anti-inflammatory oxylipids that were recently characterized in in vitro models of endothelial inflammation. Increased synthesis of specific oxylipids contributes to endothelial cell dysfunction and reduction in barrier integrity (Ryman et al., 2016), whereas others improve integrity and act to resolve inflammation (Rittchen at al., 2022).

Closely tied to oxylipids, are a class of potent lipid-based inflammatory mediators called endocannabinoids (EC). As part of the endocannabinoid system (ECS), EC and dedicated cannabinoid receptors-1 and -2 (CB1/2), are involved in several physiological processes, such as energy homeostasis, cellular metabolism, pain, and inflammation (Kaur et al., 2016). Fluctuations of EC plasma concentrations during inflammatory events in dairy cows has recently been demonstrated (Bonsale et al., 2018) and elevated concentrations of arachidonoylethanolamide, or anandamide (AEA) associated with non-steroidal anti-inflammatory drug (NSAID) treatment in murine models, is theorized to contribute to the analgesic effects of the drugs (Buisseret et al., 2019). Considering that in isolated endothelial and other immune mediating cells, effects of AEA not only vary by tissue type but are highly time and concentration dependent (Cabral et al., 2015), increased AEA concentrations can lead to elevated ROS production, mitochondrial dysfunction, prolonged activation of macrophages and neutrophils, as well as induction of apoptotic signaling via cannabinoid receptors 1 and 2 (CB1/2) (Rahaman and Ganguly, 2021). Therefore, untimely elevation of AEA may contribute to the dysfunctional inflammatory response through prolonged pro-inflammatory signaling in dairy cows. As administration of NSAIDs in dairy cattle suffering from acute coliform mastitis occurs only when symptoms have become systemic, the increase in AEA concentration associated with NSAID treatment may result in further deterioration of the endothelial barrier. However, studies pertaining to the effects of the ECS on endothelial barrier function have focused on pre-treatment with EC and concurrent LPS challenge and EC administration, which does not consider the possibility of significant changes in ECS receptor and enzyme expression that are well documented in immune mediating cells (Rahaman and Ganguly, 2021).

Therefore, we set out to characterize the effects of AEA on BAEC function and barrier integrity, during LPS challenge. We demonstrate that the ECS is not only present in BAEC, but that expression of key genes is altered by LPS challenge. We also demonstrate that CB1 activation by AEA concentrations as low as 0.5 M, are detrimental to BAEC function and monolayer barrier integrity, during LPS challenge. Lastly, we demonstrate that AEA induces ROS production and the likelihood of oxidative stress in BAEC without LPS challenge, while apparent mitochondrial dysfunction results from AEA treatment of BAEC during LPS challenge, leading to activation of apoptotic pathways.

4.2: MATERIALS AND METHODS

Reagents

High performance liquid chromatography (HPLC) grade acetonitrile, HPLC-grade methanol, formic acid, glycerol, transferrin, insulin, heparin, sodium selenite, Hanks buffered salt solution (HBSS) powder, collagenase, lipopolysaccharide (LPS) (O111:B4), 156 EDTA, and tri-phenylphosphine were purchased from Sigma-Aldrich (Burlington, MA, USA). Deuterated and nondeuterated isoprostane standards, indomethacin, 2,20-azobis-2-methyl-propanimidamide dihydrochloride (AAPH), arachidonoylethanolamide (AEA) and AM251 were purchased from Cayman Chemical (Ann Arbor, MI, USA). Butylated hydroxy toluene (BHT) was purchased from Acros (Waltham, MA, USA). Fetal bovine serum was purchased from Hyclone Laboratories, Inc. (Logan, UT, USA) and 4-(2-hydroxyethyl)-1-piperazineethanesulfonic acid (HEPES) buffer, and dimethyl sulfoxide (DMSO) were purchased from Corning Inc. (Corning, NY, USA). HAM's F-12k was purchased from Irvine Scientific (St. Santa Ana, CA, USA). Antibiotics/antimycotics, trypsin-EDTA, bovine collagen, and ProLong-Gold antifade were from Life Technologies (Carlsbad, CA, USA). Predesigned and custom-made bovine TaqMan primers were purchased

from Applied Biosystems (Foster City, CA, USA). 40,6-diamidino-2-phenylindole (DAPI) was purchased from Molecular Probes (Eugene, OR, USA), and von Willebrand's factor was purchased from Agilent Technologies (Santa Clara, CA, USA).

Primary Cell Isolation

Endothelial barrier function was assessed using primary bovine aortic endothelial cells collected as described previously (Aherne et al., 1995). Briefly, for BAEC isolation, a 10 cm full-circumference section of descending aorta, just distal to the branch of the subclavian artery, was collected at a commercial abattoir and immediately submerged in HBSS with 0.05 mg/mL gentamicin on ice. Once transported to the laboratory for processing, aorta samples were cut lengthwise and laid flat in a solution of 2 mg/mL collagenase in Krebs-Ringer bicarbonate with 4% BSA and allowed to incubate at 37 °C for 10 min. After each incubation, the collagenase solution was collected and the luminal sides of tissues were rinsed with HBSS, collecting the rinse solution. The rinse solution was added to collected collagenase and samples were centrifuged at 160 μg for 10 min at 15 °C. Resulting cellular pellets were plated in T25 cell culture flasks until confluent in Ham's F12K medium containing 10% fetal bovine serum, 10 mM HEPES buffer, 0.25% sodium bicarbonate, 2 mM L-glutamine, 1% 1:1 antibiotic:antimycotic, 100 μg/mL heparin, 10 μg/mL insulin, 5 μg/mL transferrin, and 40 ng/mL sodium selenite. Cells were detached via incubation with 0.05% trypsin, diluted serially, and plated in 96-well plates. To exclude fibroblasts and other cell types, wells containing only colonies derived from a single cell were selected for propagation. Wells were selected by typical endothelial cobblestone morphology for further propagation and confirmed by von Willebrand factor staining. Cells were frozen at passage 3, grown to passage 6 for RNA isolation, representing the earliest passage at which cells could realistically be used for assays, and discarded after passage 9.

Experimental Design

Cells were plated at 1 x 10^5 cells/well in 96 well plates, and 1 x 10^6 cell/well in 6 well plates, and grown to confluency in 5% FBS Ham's F12k media containing 20 mM HEPES, antibiotics and antimycotics (100 U/mL consisting of penicillin, streptomycin, and amphotericin B), heparin (100 µg/mL), insulin (10 µg/mL), transferrin (5 µg/mL), and sodium selenite (10 ng/mL), for 18 h before media was changed to serum free media for 2 h (Figure 4.1). Treatments were as follows: untreated media control, vehicle control with 0.05% ethanol by volume, positive control of either 25 ng/mL LPS or 3 mM AAPH as an agonist, physiologically relevant doses of AEA (0.5, 1, and 5 µM), 1 µM of the CB1 antagonist AM251, and co-culture of either agonist and AEA, with and without AM251. To mimic coliform infections, cells were pre-treated with 25 ng/mL LPS + vehicle for 8 h before addition of AEA and AM251. Results were recorded at 2, 4, 8, 12, and 24 h post-AEA addition, with the 4 h time point showing the greatest change in results. Only the 4 h time point is presented here; the remaining time points can be found in the Supplemental Data. All experiments were carried out with an N = 6.

Real-Time PCR

Collection of cells was initiated by washing twice with HBSS and 300 µL of buffer RLT (Qiagen, Germantown, MD, USA) was added for cell lysis. Buffer RLT was collected and stored at -20 °C for no longer than one month before processing. Extraction of RNA occurred utilizing a Promega Maxwell RSC Instrument following the manufacturer's protocol. RNA quantity and quality were evaluated using a NanoDrop ND-1000 spectrophotometer (Thermo Fisher Scientific,Waltham, MA, USA).

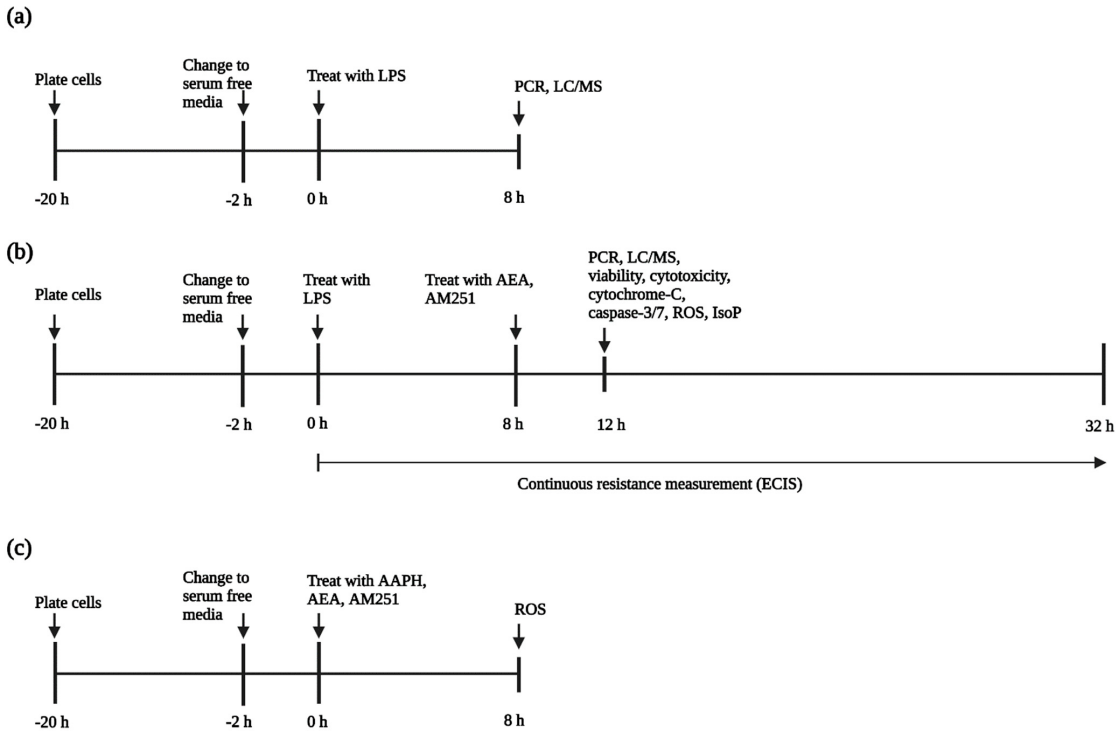

Figure 4.1: Experimental design to determine the effect of arachidonoylethanolamide (AEA) on bovine aortic endothelial cells (BAEC) (N = 6). (a) Initial experiment to establish presence of genes related to the endocannabinoid system and concentrations of AEA in response to lipopolysaccharide (LPS) challenge; (b) Experimental design to establish effect of AEA on gene expression, isoprostane production, viability, cytotoxicity, cytochrome-C release, and caspase 3/7 activation in BAEC; (c) Experimental design to establish effect of AEA on reactive oxygen species' (ROS) production without LPS challenge. Figure created with Biorender.com.

For cDNA generation, RNA was diluted with nuclease-free water to standardize all samples. A master mix of 10x reverse-transcription buffer, 25x dNTP, 10x random primers, Multiscribe reverse transcriptase, RNase inhibitor, and RNase nuclease-free water from a high-capacity cDNA reverse-transcription kit with RNase inhibitor (all kit components from Applied

Biosystems, Vilnius, Lithuania), was added at an equal volume to diluted RNA. Samples were placed in a PTC-200 Peltier Thermo Cycler (MJ Research, Waltham, MA, USA), which ran as follows: stage 1, 25 °C for 10 min; stage 2, 37 °C for 2 h; stage 3, 85 °C for 5 min; stage 4, hold at 4 °C.

Real-time PCR was carried out with predesigned TaqMan primers and FAM-MGB probes (Applied Biosystems, Pleasanton, CA, USA). All primers and probes were used in a 7500 Fast Real-time PCR system (Applied Biosystems). Genes were evaluated in triplicate with 2x TaqMan Gene Expression Master Mix (Applied Biosystems), 20x Custom TaqMan Gene Expression Assay Mix (Applied Biosystems), sample cDNA (50 ng/well for tissues, 100 ng/well for cells), and nuclease free water for a total of 10 µL per reaction well. A 20x pre-designed TaqMan Gene Expression Assay for RPS9 was used as endogenous control (Applied Biosystems). Thermal cycling conditions for the Fast 2-step PCR system were as follows: stage 1, 95 °C for 20 s; stage 2, 95 °C for 3 s; stage 3, 60 °C for 30 s, with 40 cycles of stages 2 and 3. Data were recorded and compiled using ExpressionSuite Software version 1.0.4 (Applied Biosystems) and analyzed using DataAssist Software version 3.01 (Applied Biosystems, Foster City, CA, USA). Data from in vitro cell samples, having no standard cell type for comparison, are expressed as $2^{-\Delta\Delta CT}$. Efficiency (E) of PCR was calculated based on the slope of a standard curve of tissue samples, serially diluted. The slope of the standard curve was used to calculate E, using the equation $E = (10^{-1/slope} - 1) \times 100$.

Reactive Oxygen Species

Quantification of ROS production was carried out using the commercially available OxiSelect fluorometric ROS assay (Cell Biolabs, San Diego, CA, USA). Briefly, BAEC were cultured in 96-well, black walled and clear bottom plates following the experimental design and

the assay was carried out following manufacturer's recommendations. Cells were preloaded with DCF-DA at 100 μM in serum-free media for 15 min before treatments were added. The assay utilizes a non-fluorescent probe, 20,70-dichlorodihydrofluorescein diacetate (DCFH-DA), which is cleaved by cellular deacetylases and is oxidized by ROS to yield the fluorescent and stable 20,70-Dichlorodihydrofluorescein (DCF) product. Temporal ROS production was determined by measuring fluorescence using a BioTek Synergy H1 plate reader (Agilent, Santa Clara, CA, USA) at 480 nm excitation and 530 nm emission wavelengths. Results were analyzed as the fold change in fluorescence signal over untreated controls.

Viability and Cytotoxicity

Evaluation of AEA effects on viability and cytotoxicity of BAEC was carried out using commercially available assay kits from Promega (Promega, Madison, WI, USA). Briefly, for multiplex evaluation of viability and cytotoxicity, BAEC were cultured for 18 h in 96-well white wall, flat bottom plates and treated following the experimental design. Viability was evaluated using the Promega CellTiter-Glo Assay, following the manufacturer's recommendations. The assay is based on the principle that the amount of ATP generated is proportional to the number of viable cells. Luminescence was read on a BioTek Synergy H1 plate reader (Agilent, Santa Clara, CA, USA). A complimentary cytotoxicity assay from Promega was employed as a multiplex assay on the same plate and cells as the CellTiter-Glo assay.

Mitochondrial Function

Cytochrome-C release

Quantification of cytochrome-C released in response to AEA treatment in BAEC challenged with LPS was carried out using the Promega Cytochrome-C Assay (Promega, Madison, WI, USA). Briefly, BAEC were cultured in white 96-well plates following the experimental design

and the assay was carried out following manufacturer's recommendations. Luminescence was read on a BioTek Synergy H1 plate reader (Agilent, Santa Clara, CA, USA).

Apoptosis via caspase 3/7

Effect of AEA on apoptosis via caspase 3/7 of BAEC challenged with LPS was determined via a commercially available Promega Caspase-Glo 3/7 kit (Promega, Madison, WI, USA). Briefly, BAEC were plated in a white flat bottom 96-well plate and treated according to the experimental design, and the assay was carried out according to the manufacturer's recommendations. Caspase activation of the substrate releases aminoluciferin and subsequent interaction of the free aminoluciferin with luciferase results in a luminescent signal proportional to caspase 3/7 activity. Luminescence was read on a BioTek Synergy H1 plate reader (Agilent, Santa Clara, CA, USA).

Targeted Lipidomic Analyses

Solid Phase Extraction (SPE) of cultured endothelial cells

Cell pellet samples collected from cell culture experiments, previously stored at -80 C, were thawed while on ice and protected from light. Initially, cell pellet samples were hydrolyzed by incubating with a 3 M potassium hydroxide solution at 45 °C for 45 min, allowed to cool to room temperature before being acidified with hydrogen chloride to a pH range of 2–3. The cell pellet samples were centrifuged at 4816 x g for 45 min at 4 °C and the supernatant was extracted in Phenomenex 8B S100 FCH extraction cartridges. After determining that cell pellet hydrolysis did not change detection of target metabolites, the hydrolysis step was not included in processing samples from subsequent experiments. After thawing, samples were centrifuged (4000 x g, 30 min, 4 °C), and combined with HPLC-grade water and formic acid to achieve 20% methanol and maintain 0.1% formic acidification, respectively. Samples were extracted with SPE cartridges

(Waters Oasis HLB 12 cc, 500 mg LP) preconditioned with methanol followed by HPLC-grade water, washed with 20% methanol solution and cartridges were dried for 15 min under full vacuum. A 7.5 mL 1:1 mixture of methanol and acetonitrile was used to elute extracted samples from the cartridges into glass tubes pre-coated with 10 µL of 20% glycerol in methanol followed by a 30 s drying under full vacuum. Samples were dried in a Savant SpeedVac (ThermoQuest, Holbrook, NY, USA) with an initial heating phase at 45 °C, residues suspended in 150 µL of a 4:1 (v:v) methanol and water mixture, and centrifuged (14,000 x g, 5 min, 4 °C). The supernatant (120 µL) was transferred to an autosampler vial with a low volume insert and stored at -80 °C before LC–MS/MS analyses.

LC/MS/MS Analysis

Details of LC/MS/MS analysis of isoprostanes are described in Mavangira et al., 2016 (Mavangira et al., 2016). In short, the quantification of analytes was accomplished on a Waters Xevo-TQ-S tandem quadrupole mass spectrometer (Water Corp., Milford, MA, USA) using multiple reaction monitoring (MRM). Chromatography separation was performed with an Ascentis Express C18 HPLC column (10 cm x 2.1 mm; 2.7 µm particles, Sigma-Aldrich, St. Louis, MO, USA) held at 50 °C, and the autosampler was held at 10 °C. Mobile phase A was water containing 0.1% formic acid, and mobile phase B was acetonitrile. Flow rate was fixed at 0.3 mL/ min. Liquid chromatography separation took 15 min per sample. MRM parameters including cone voltage, collision voltage, precursor ion, production, and dwell time were optimized based on Waters QuanOptimize software (Waters Corp., Milford, MA, USA) by flow injection of pure standards for each individual compound.

The details of LC/MS/MS analysis for endocannabinoids are described in Williams et al., 2007. In short, the quantification of analytes was accomplished on a Q-Exactive Quadrupole-

Orbitrap mass spectrometer (Thermo Fisher Scientific,Waltham, MA, USA) using multiple reaction monitoring (MRM). Chromatographic separation was performed with an Acquity BEH C18 UPLC column (10 cm x 2.1 mm; 1.7 μm particles, Waters Corp., Milford, MA, USA) held at 40 °C, and the autosampler was held at 10 °C. Mobile phase A was water containing 0.1% formic acid, and mobile phase B was acetonitrile. Flow rate was fixed at 0.3 mL/min. Liquid chromatography separation took 15 min per sample. MRM parameters including cone voltage, collision voltage, precursor ion, production, and dwell time were optimized based on Xcalibur Data Acquisition and Interpretation software (Thermo Fisher Scientific, Waltham, MA, USA) by flow injection of pure standard for each individual compound.

Endothelial Barrier Function Assessment

For assessment of endothelial barrier integrity, BMEC were plated on bovine collagen coated 96-well plates with gold electrodes and cultured for 18 h. Electric currents passing through the monolayer were continuously measured by the Electric Cell-Substrate Impedance Sensing Z-theta system (ECIS Z-Q, Applied Biophysics, Inc., Troy, NY, USA). Approximately 2 h prior to treatment addition, media were changed to serum free media. Trans endothelial resistance (TER) across the monolayer was monitored up to 32 h after LPS addition. TER was normalized to the time point immediately prior to LPS addition.

Statistical Analysis

For statistical analyses all data sets were tested for normality and variance, before t-test using proc "t-test" procedure and one- or two-way ANOVAs were performed using the proc mixed procedure, with or without repeated measures where appropriate using the SAS9.4 software (SAS Institute Inc., Cary, NC, USA). A Tukey adjustment for multiple comparisons was performed with a $p \leq 0.05$ considered significant when all-pairwise comparisons were performed; otherwise, a

Dunnett's post-hoc correction was performed for comparison of different treatments to the untreated control. For statistical analyses, undetected measures of variables in a treatment class were presented as undetected and assigned a zero value for statistical analyses.

4.3: RESULTS

LPS Alters ECS Related Gene Expression and AEA Biosynthesis in BAEC

Analysis by RT-qPCR revealed that gene expression of CB1/2 and NAPE-PLD was elevated with LPS challenge ($p = 0.0016$, $p = 0.0003$, and $p = 0.0010$, respectively), whereas expression of FAAH decreased with LPS challenge compared to the media control ($p = 0.0010$). Addition of 0.5 μM AEA did not alter gene expression of CB1/2, NAPE-PLD, or FAAH, with and without 25 ng/mL LPS. (Figure 4.2a–d). Exposure of BAEC to LPS also increased intracellular and extracellular AEA concentrations ($p < 0.0001$ and $p < 0.0001$, respectively). Extra- and intracellular AEA concentrations did not change with addition of 0.5 μM AEA without LPS compared to the media only treatment. In the presence of 25 ng/mL LPS, 0.5 μM AEA does not alter extra- or intracellular AEA concentrations compared to the LPS control.

AEA Alters Endothelial Barrier Function

Assessment of the trans-endothelial resistance (TER) via ECIS showed that without LPS pre-treatment, 0.5, 1, and 5 μM AEA did not alter barrier integrity compared to the media control (Figure 4.3). In BAEC pre-treated with LPS, addition of 0.5 M of AEA increased TER at 10 h ($p = 0.0457$). Treatment concentrations of 1 and 5 μM AEA were detrimental to BAEC TER. Addition of 1 μM AEA resulted in decreased TER at 28, 29, 30, 31, and 32 h compared to the LPS control ($p = 0.0410$, $p = 0.0107$, $p = 0.0024$, $p = 0.0028$, and $p = 0.0003$, respectively), and with 5 μM AEA, TER was decreased at 10, 11, and 12 h ($p = 0.0376$, $p = 0.0306$, and $p = 0.0298$, respectively), and again at 25, 26, 27, 28, 29, 30, 31, and 32 h ($p = 0.0282$, $p = 0.0302$, $p = 0.0268$,

$p = 0.0083$, $p = 0.0020$, $p = 0.0003$, $p < 0.0001$, and $p < 0.0001$, respectively) compared to the LPS control.

CB1 Mediates AEA Induced Changes in Endothelial Barrier Function

Treatment with 1 μM of the CB1 antagonist AM251 eliminated the 2 h TER increase associated with 0.5 μM AEA treatment in BAEC challenged with LPS (Figure 4.4a). Starting at 15 h, TER of BAEC pre-treated with LPS significantly increased with addition of 0.5 μM AEA + 1 μM AM251 compared to the 0.5 μM AEA only treatment. Treatment of LPS challenged BAEC with 0.5 μM AEA and 1 μM AM251 increased TER starting at 15 h compared to the AEA treatment alone and remained significantly greater throughout the 32 h timepoint ($p < 0.05$). Addition of 1 μM AM251 to 0.5 μM AEA increased barrier integrity over the LPS control at 20 h in BAEC pre-treated with LPS ($p = 0.0460$).

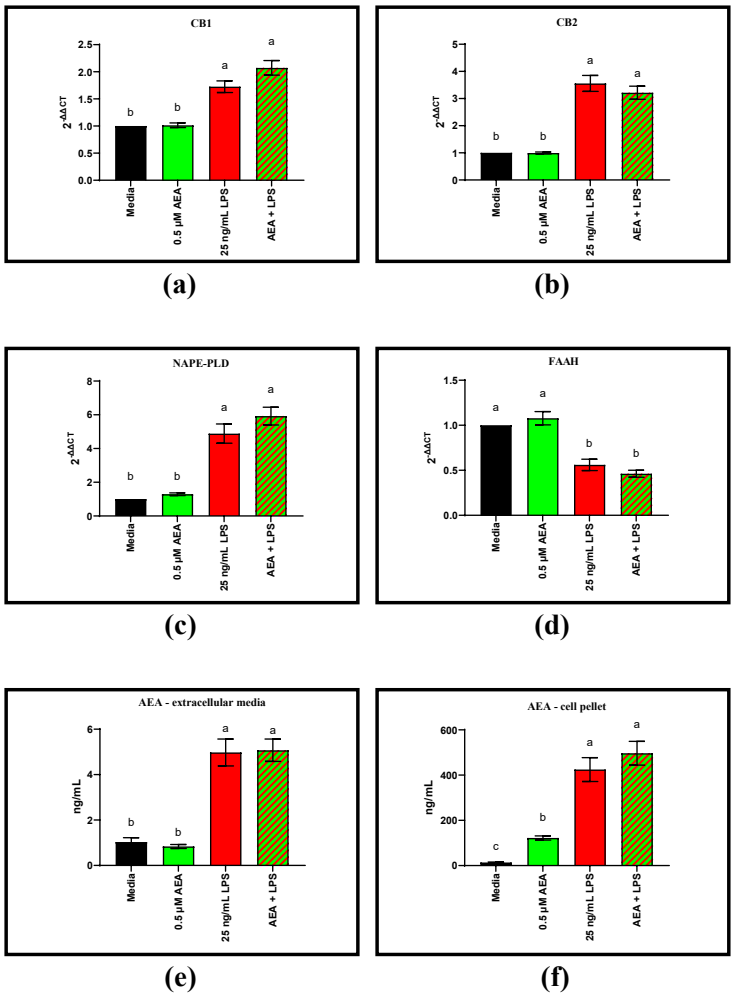

Figure 4.2. Gene expression via RT-qPCR of endocannabinoid receptors and arachidonoylethanolamide (AEA) associated genes in bovine aortic endothelial cells (BAEC) (N = 6). Extracellular and cellular AEA concentrations quantified via LC/MS. All results were recorded 8 h following lipopolysaccharide (LPS) challenge and/or 05. μM AEA: (a) gene expression of cannabinoid receptor-1 (CB1); (b) gene expression of CB2; (c) gene expression of N-acyl phosphatidylethanolamine phospholipase-D (NAPE-PLD); (d) gene expression of fatty acid amide hydrolase (FAAH); (e) extracellular media concentration of AEA; (f) cell pellet concentration of AEA. Statistical analysis: one-way ANOVA, Tukey's adjustment. a–c: Means with different superscripts are different ($p < 0.05$).

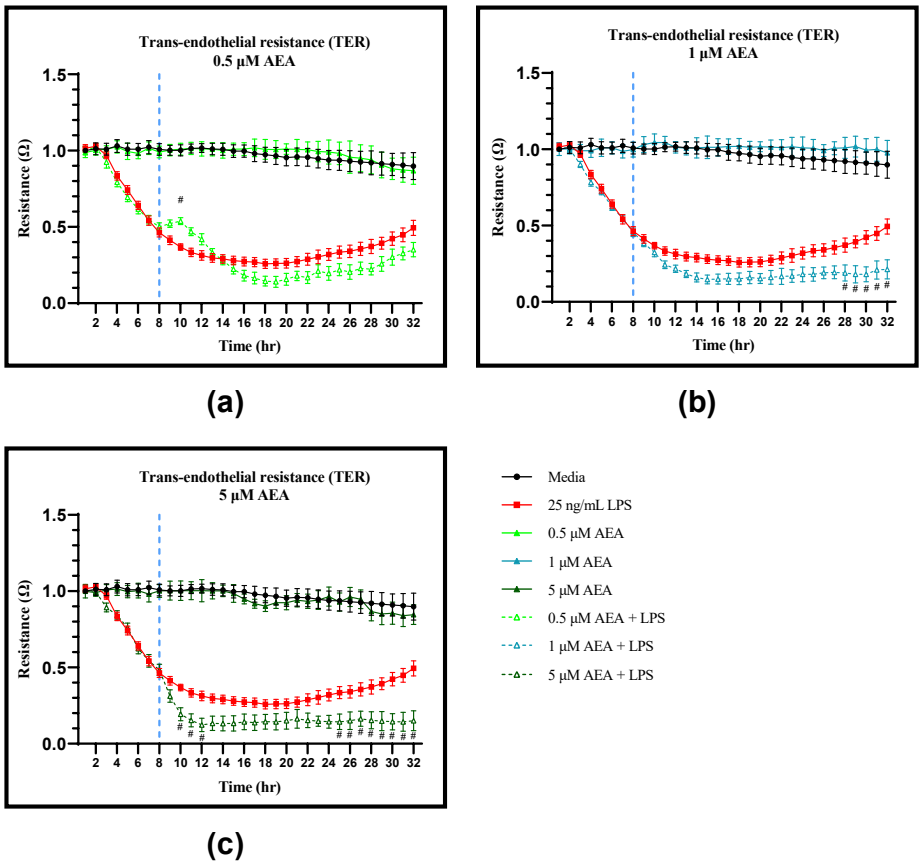

Figure 4.3. Analysis of trans-endothelial resistance (TER) utilizing electric cell-substrate impedance sensing (ECIS) of bovine aortic endothelial cells (BAEC) (N = 6) treated with (a) 0.5, (b) 1, and (c) 5 µM arachidonoylethanolamide (AEA), with and without 25 ng/mL lipopolysaccharide (LPS) pretreatment. Statistical analysis: two-way ANOVA, Tukey's adjustment. # $p < 0.05$ for AEA + LPS compared to LPS control.

Similarly, LPS pre-treated BAEC had greater TER with the addition of 1 µM AM251 to 1 and 5 µM AEA, not only over the AEA only treatment, but TER of AEA and AM251 treatments was consistently greater than that of the LPS control (Figure 4.4b and c). Addition of 1 µM AM251 to 1 µM AEA increased TER compared to 1 µM AEA alone, starting at 11 h through to the 32 h

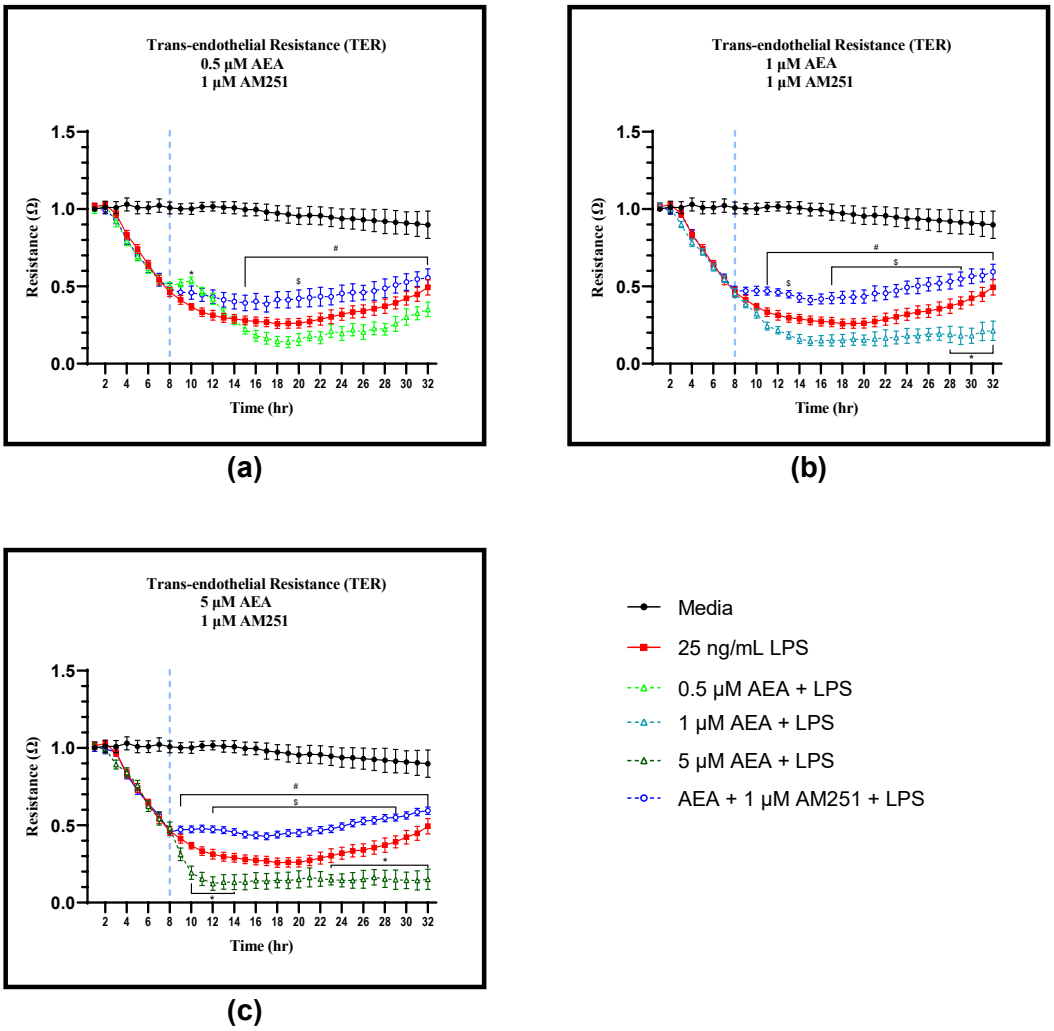

Figure 4.4. Trans-endothelial resistance (TER) of bovine aortic endothelial cells (BAEC) (N = 6) treated with 0.5, 1, and 5 µM AEA and 1 µM CB1 antagonist AM251 and 25 ng/mL lipopolysaccharide (LPS) pre-treatment. BAEC were treated with LPS at 0 h and AEA/AM251 at 8 h: (a) 0.5 µM AEA, 1 µM AM251, 25 ng/mL LPS; (b) 1 µM AEA, 1 µM AM251, 25 ng/mL LPS; (c) 5 µM AEA, 1 µM AM251, 25 ng/mL LPS. Statistical analysis: two-way ANOVA, Tukey's adjustment. *$p < 0.05$ significantly different to LPS control. #$p < 0.05$ AEA + AM251 + LPS treatment significantly different to corresponding AEA + LPS only treatment. \$ $p < 0.05$ AEA + AM251 + LPS treatment significantly different to LPS control.

timepoint ($p < 0.05$). Additionally, TER increased with 1 μM AEA and AM251 over the LPS control at 13 h ($p = 0.0429$) and again from 17 to 29 h ($p < 0.05$). Addition of 1 μM AM251 to 5 μM AEA increased TER of LPS pre-treated BAEC over 5 μM AEA only, starting at 9 h through to the 32 h time point ($p < 0.05$). Lastly, treatment with 5 μM AEA and 1 μM AM251 showed greater TER compared to the LPS control from 12 to 29 h ($p < 0.05$). By itself, 1 μM AM251 did not alter TER, with and without LPS (Graph S1).

RT-qPCR analysis of gene expression of ICAM-1 and VCAM-1 in BAEC not challenged with LPS was not altered by 0.5, 1, and 5 μM AEA treatment doses at 4 hours, compared to the media control (Figure 4.5a and b). In BAEC pre-treated with LPS, only 5 μM AEA increased ICAM-1 mRNA gene expression over the LPS control ($p = 0.0012$), while VCAM-1 mRNA gene expression did not change with any AEA treatment concentration compared to the LPS control. However, in BAEC pre-treated with LPS mRNA gene expression of ICAM-1 was elevated following 4 h of 5 μM AEA treatment compared to 0.5 μM AEA ($p < 0.0001$). Similarly, expression of VCAM-1 in response to 4 h of 5 μM AEA treatment was greater than that of 0.5 and 1 μM AEA treatments ($p = 0.0027$ and $p = 0.0007$, respectively). Expression of the ICAM-1 de-creased with the addition of 1 μM of the CB1 antagonist AM251 to 0.5 μM AEA, com-pared to the 0.5 μM AEA only treatment ($p = 0.0495$). Expression of the VCAM-1 was not altered by 0.5 μM AEA and 1 μM AM251.

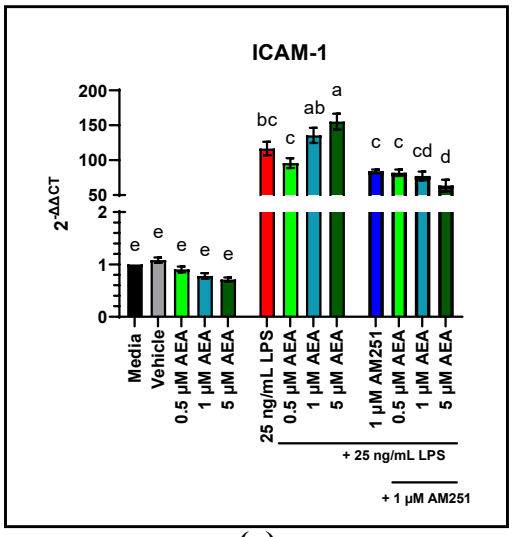

(a)

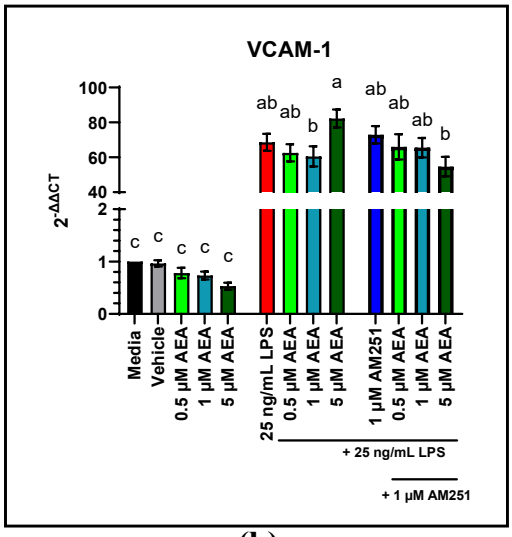

(b)

Figure 4.5. RT-qPCR analysis of gene expression of intracellular adhesion molecule-1 (ICAM-1) and vascular cell adhesion molecule-1 (VCAM-1) in response to 0.5, 1, and 5 µM arachidonoylethanolamide (AEA) and 1 µM AM251 treatment in bovine aortic endothelial cells (BAEC) (N = 6), with and without 25 ng/mL lipopolysaccharide (LPS) challenge: (**a**) expression of ICAM-1 following AEA and 1 µM AM251 treatment; (**b**) expression of VCAM-1 following AEA and 1 µM AM251 treatment. Statistical analysis: one-way ANOVA, Tukey's adjustment. a–e: Means with different superscripts are different ($p < 0.05$).

AEA Induced Endothelial Mitochondrial Dysfunction Is CB1 Mediated

AEA concentrations of 0.5 μM elevated ATP production in BAEC challenged with 25 ng/mL LPS compared to LPS alone ($p = 0.0055$) (Figure 4.6a). Addition of the CB1 antagonist AM251 did not alter ATP production in response to 0.5 μM AEA. Addition of 1 μM AEA did not alter ATP production, and addition of 1 μM AM251 to 1 μM AEA did not affect ATP release compared to the 1 μM AEA only treatment. However, 5 μM AEA decreased ATP release, compared to LPS alone ($p = 0.0108$) and addition of 1 μM AM251 increased ATP production compared to the 5 μM AEA only treatment ($p = 0.0029$).

Cytotoxicity was not affected by 0.5 and 1 μM AEA, but increased with 5 μM AEA compared to the LPS control ($p = 0.0156$) (Figure 4.6b). Addition of the CB1 antagonist AM251 reduced cytotoxicity of 5 μM AEA compared to AEA alone ($p = 0.0045$).

Cytochrome-C release from the mitochondria increased with all AEA doses used (0.5, 1, and 5 μM) compared to the LPS control ($p = 0.0185$, $p < 0.0001$, and $p = 0.0001$, respectively) (Figure 4.6c). The CB1 antagonist AM251 decreased cytochrome-C release at 1 μM concentration, compared to the LPS control ($p = 0.0115$) and addition of 1 μM AM251 to 0.5, 1, and 5 μM AEA reduced cytochrome-C release compared to the corresponding AEA only treatments ($p = 0.0006$, $p = 0.0005$, and $p = 0.0045$, respectively).

Activation of caspase 3/7 increased with the addition of all three concentrations of AEA (0.5, 1, and 5 μM) compared to the LPS control ($p = 0.0004$, $p < 0.0001$, and $p < 0.0001$, respectively) (Figure 4.6d). Addition of the CB1 antagonist AM251 reduced caspase 3/7 activation for all AEA treatment concentrations (0.5, 1, and 5 μM) compared to their respective AEA only treatments ($p = 0.0006$, $p < 0.0001$, and $p = 0.0225$, respectively).

Production of ROS is increased with LPS antagonism compared to the untreated control ($p < 0.0001$) (Figure 4.6e). Increase in ROS production with AEA treatment is not significant. However, addition of AM251 significantly reduced ROS production of LPS challenged BAEC treated with 5 μM AEA ($p = 0.0480$). Interestingly, addition of 1 and 5 μM AEA increased ROS production without LPS compared to the untreated control ($p = 0.0404$ and $p = 0.0068$, respectively. Production of IsoP without LPS challenge was increased with all AEA doses (0.5, 1, and 5 μM) ($p = 0.006$, $p < 0.0001$, and $p < 0.0001$, respectively) (Figure 4.6f). Addition of AM251 reduced IsoP production of LPS challenged BAEC treated with 1 and 5 μM AEA ($p < 0.0001$ and $p < 0.0001$, respectively), whereas IsoP production of 0.5 μM AEA was unchanged. The remaining time points for ATP-production, cytotoxicity, cytochrome-C release, caspase 3/7 activation, ROS, and IsoP production can be found in the Supplemental Data (Tables S1–S6, respectively).

AEA Induced ROS and IsoP Production in BAEC Is CB1 Mediated

Concentrations as low as 0.5 μM AEA induce ROS production in BAEC ($p < 0.0001$) (Figure 4.7a). Addition of 1 μM of the CB1 antagonist AM251 eliminated ROS production of 0.5 μM AEA ($p < 0.0001$). Production of ROS was dosage dependent and significantly elevated at 0.5 μM, 1 and 5 μM AEA compared to the media control ($p < 0.0001$, $p < 0.0001$, and $p < 0.0001$, respectively) (Figure 4.7b). Addition of 1 μM AM251 reduced ROS production of all three AEA doses compared to their respective AEA only treatments ($p = 0.0002$, $p < 0.0001$, and $p < 0.0001$, respectively). Total IsoP concentrations were also elevated over media control with 0.5 μM AEA addition ($p = 0.0002$) (Figure 4.7c). Addition of AM251 to 0.5 μM AEA eliminated IsoP production compared to the AEA only treatment ($p = 0.0002$). Total IsoP production is also dosage dependent, with 0.5 μM, 1 and 5 μM of AEA inducing IsoP production ($p = 0.0002$, $p < 0.0001$, and $p < 0.0001$, respectively) (Figure 4.7d). Addition of AM251 eliminates 0.5 μM AEA IsoP

production ($p = 0.0002$), but only reduces total IsoP of 1 and 5 μM AEA ($p < 0.0001$ and $p < 0.0001$, respectively).

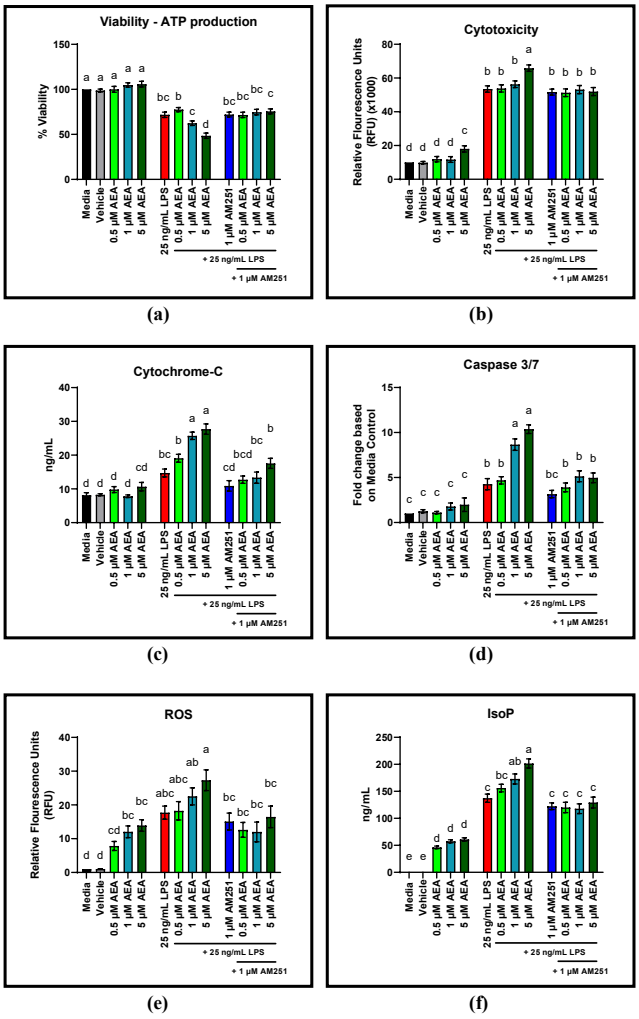

Figure 4.6. Viability via ATP release, cytotoxicity, cytochrome-c, and caspase 3/7 in bovine aortic endothelial cells (BAEC) (N = 6) treated with 0.5, 1, and 5 μM AEA and 1 μM CB1 antagonist AM251 for 4 h, in the absence and presence of 25 ng/mL lipopolysaccharide (LPS) challenge: (a) Viability via ATP production following AEA and 1 μM AM251 treatment; (b) Cytotoxicity following AEA and 1 μM AM251 treatment; (c) Cytochrome-C release following AEA and 1 μM AM251 treatment; (d) Caspase 3/7 activation following AEA and 1 μM AM251 treatment; (e) ROS production following AEA and 1 μM AM251 treatment; (f) IsoP production following AEA and 1 μM AM251 treatment. Statistical analysis: one-way ANOVA, Tukey's adjustment. a–e: Means with different superscripts are different ($p < 0.05$).

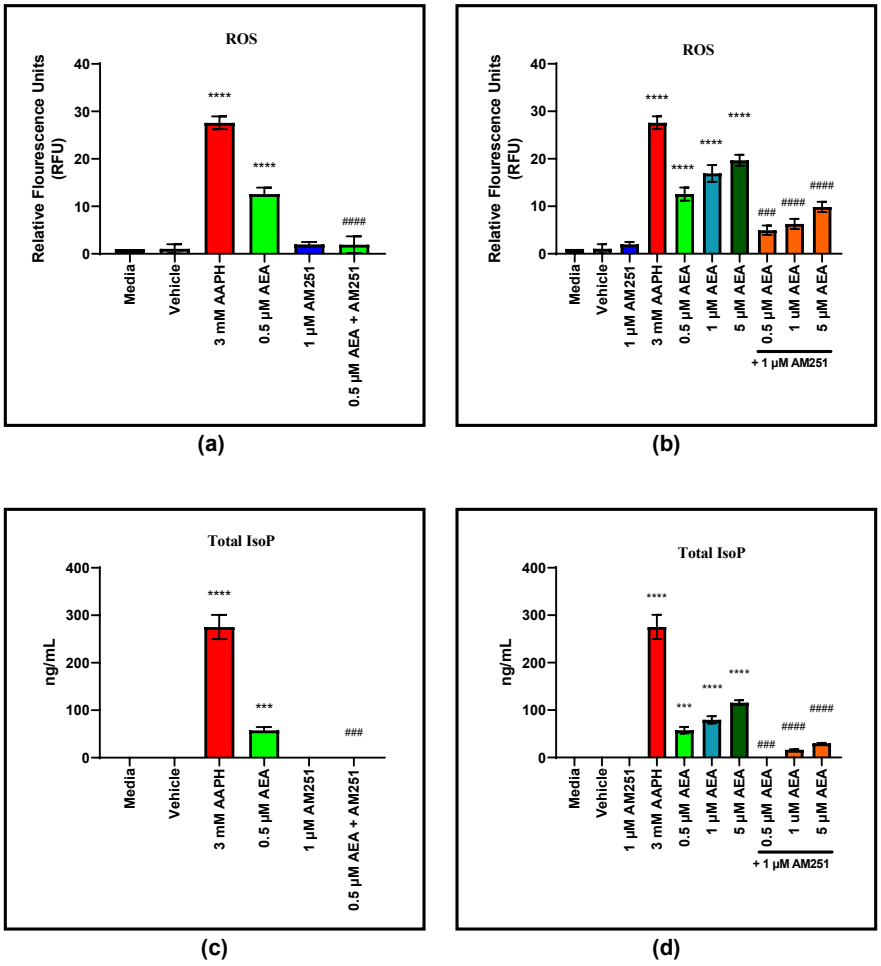

Figure 4.7. Reactive oxygen species (ROS) and isoprostane (IsoP) production of bovine aortic endothelial cells (BAEC) (N = 6) treated with AEA: (a) Involvement of cannabinoid receptor-1 and -2 (CB1/2) in ROS production of 0.5 µM AEA. CB1 antagonist: 1 µM AM251; (b) Dosage dependent ROS production of BAEC treated with AEA only, and combined with AM251; (c) Involvement of CB1/2 in total IsoP production of 0.5 µM AEA. CB1 antagonist: 1 µM AM251; (d) Dosage dependent total IsoP production of BAEC treated with AEA only and combined with AM251. Statistical analysis: one-way ANOVA, Tukey's adjustment. * Significantly different to corresponding media control (*** $p \leq 0.001$, **** $p \leq 0.0001$); # Significantly different to AEA treatment of corresponding concentration (### $p \leq 0.001$, #### $p \leq 0.0001$).

4.4: DISCUSSION

In this study, we demonstrate that coliform mastitis endothelial barrier damage may include ECS activation as a mechanistic component. The activation of the endothelial endocannabinoid receptor CB1 mediates effects of AEA on endothelial barrier integrity and mitochondrial function. Addition of AEA altered gene expression of adhesion molecules, induced ROS production, increased cytochrome-C release, and activation of apoptotic pathways via caspase 3/7. However, treatment of endothelial cells with AEA without LPS challenge did increase ROS production and the likelihood of oxidative stress, but did not alter barrier function or activation of apoptotic pathways, indicating that inflammatory state and timing of AEA increase are crucial.

Basal expression of CB1 and 2 in this study indicates the involvement of the ECS in non-inflammatory functions of BAEC. Non-inflammatory models utilizing AEA in nonbovine species support the involvement of the ECS in a variety of processes in vascular endothelial cells, such as regulation of vascular tone (Stanley et al., 2015) and angiogenesis (Rieck et al., 2021). Increased gene expression of the cannabinoid receptors following treatment with an antagonist such as LPS was demonstrated in many cell types, not just immune mediating cells. Expression patterns of ECS related genes observed in this study agree with endometrial expression of ECS related genes in Holstein dairy cows suffering from endometritis (Bonsale et al., 2018) and expression of hypothalamic ECS genes in Holstein dairy cows experiencing metabolic stress due to onset of lactation (Kuhla et al., 2021). Therefore, elevated synthesis or release of AEA and receptor expression reported in this study, support involvement of the ECS in inflammatory regulation of BAEC.

Treatment of BAEC with up to 5 μM AEA without LPS challenge did not alter TER, whereas in the presence of LPS even nanomolar concentrations altered TER. Lack of change in

gene expression of ICAM and VCAM-1 with 0.5 and 1 μM AEA addition stands in contrast to decreased expression of the adhesion genes in human blood-brain barrier treated with AEA in an ischemia/reperfusion model (Hind et al., 2015). Simultaneous treatment with LPS and AEA may have different results to our study, not only due to cell type, but also timing. As LPS increases not only AEA concentrations but also CB1 expression and addition of AEA before or with LPS antagonism may result in degradation of AEA to arachidonic acid and subsequent metabolism to oxylipids, affecting expression of adhesion molecules. Additionally, supraphysiological concentrations of AEA may stimulate non-CB receptors, particularly prior to the upregulation of CB receptors following LPS antagonism. Furthermore, as demonstrated in this study, supraphysiological concentrations of 5 μM or greater of AEA may affect the survivability of endothelial cells, and the relative expression of adhesion molecules may no longer be the greatest contributor to changes in TER. Indeed, in human primary coronary artery endothelial cells, AEA induced a concentration- and time-dependent activation of MAPK, cell death, and ROS generation (Rajesh et al., 2010).

Even though ROS production was not significantly different with addition of AEA in this study, we did observe a numerical increase that was dose dependent, and addition of AM251 significantly reduced ROS production of 1 and 5 μM AEA, indicating that activation of the CB1 receptor by AEA does contribute to overall ROS production and possible mitochondrial dysfunction. Furthermore, addition of 1 and 5 μM AEA to LPS challenged BAEC increased IsoP production compared to the LPS control, which was ameliorated by the addition of AM251. Elevated IsoP production is an indicator for oxidative stress, or damage to healthy tissue by free radicals, such as ROS. Even though the effect of IsoP on bovine vascular endothelial cells remains elusive (Putman et al., 2022), increased ROS production is associated with endothelial dysfunction

(Kuhn et al., 2021). Elevated IsoP production associated with addition of 1 and 5 μM AEA may therefore be a key contributor to decreased TER observed at these concentrations. Increased release of cytochrome-c associated with 0.5, 1, and 5 μM AEA treatment of LPS challenged BAEC is indicative of mitochondrial dysfunction and initiation of apoptotic pathways. Elevated cytochrome-C release of LPS challenged BAEC treated with AEA was ameliorated by addition of the CB1 antagonist AM251, reducing subsequent activation of caspase 3/7 apoptotic pathways. However, 5 μM of AEA did not increase cytochrome-C release over 1 μM of AEA, but activation of caspase 3/7 did increase compared to the 1 μM AEA treatment, indicating activation of caspase 3/7 in a mitochondrial independent manner at micromolar concentrations of AEA. Interestingly, without LPS antagonism, even nano-molar concentrations of AEA are sufficient to induce ROS production and subsequent production of IsoP, indicating the presence of oxidative stress in BAEC. Presence of IsoP with only AEA addition, no LPS or other antagonist, highlights the sensitivity of mitochondrial metabolism to CB1 activation. Increased concentration of AEA following LPS exposure in BAEC and reduced expression of the AEA degradation enzyme FAAH may therefore be sufficient to increase cytochrome-c release with addition of only 0.5 μM AEA in this model of endotoxemia associated inflammation.

The compounding of increased AEA concentrations and CB1 expression may therefore lead to detrimental effects on barrier integrity and endothelial cell function following any additional AEA increase, for example by NSAIDs. Elevated AEA following NSAID treatment has been recorded in several models, in vivo and in vitro, and has been associated with analgesic and anti-inflammatory effects in several cell types. However, treatment of bovine mammary epithelial cells with the NSAID flunixin meglumine (FM), the only FDA approved NSAID for endotoxemia associated with acute coliform mastitis, significantly reduced TER for up to 10 h post treatment

(Sintes et al., 2020). Elevated systemic AEA, decreased barrier integrity following NSAID treatment, and the data from this study showing that even nanomolar concentrations are sufficient to induce ROS production and alter TER, indicate that untimely increase in AEA concentrations during endotoxin challenge may be detrimental to endo- and perhaps even epithelial barrier integrity. However, further studies are needed to determine if elevated AEA associated with NSAID treatment is detrimental to the inflammatory response and endothelial function, and if timing is a factor.

Interestingly, 0.5 μM AEA treatment increased TER at 2 h but did not exhibit any changes in ICAM/VCAM expression or other parameters that were evaluated (see Supplemental Data). The increase in TER observed may be due to morphological changes, as the endogenous analog of AEA, N-arachidonoyl-L-serin modulates the cytoskeleton (actin) of the human cerebral microvascular endothelium (Kino et al., 2016). Detrimental effects on endothelial cell function associated with 1 and 5 μM AEA treatment in this study may eliminate any potential TER increase. However, without morphological analysis, possibly through immunostaining, the cause of the 2 h increase in TER associated with 0.5 μM AEA cannot be speculated on here.

Future studies should focus on the involvement of CB2 and non-CB receptors, such as TRPV1. Non-published data from this study shows that antagonism of CB2 alters BAEC barrier function independently of AEA addition, and the data was therefore not included in this publication. However, AEA is capable of activating CB2 and modifying the effects of CB2 activation by other agonists via allosteric modulation, particularly at supraphysiological concentrations greater than 5 μM (Smith and Malkowski, 2019). Furthermore, elevated AEA, by separate addition or associated with NSAID treatment, may provide additional AEA as a substrate for metabolism into active mediators, such as prostaglandin ethanolamides, or prostamides, and

other ethanolamide derivates of cyclooxygenase, lipoxygenase, and cytochrome p450 pathways. Several AEA derived mediators have already been shown to modulate inflammation [Van der Stelt et al., 2000; Rouzer and Marnett, 2011; Urquhart et al., 2015).

Overall, addition of AEA had detrimental effects on BAEC barrier integrity, elevated ROS production, leading to mitochondrial dysfunction highlighted by cytochrome-C release, and activation of apoptotic pathways, namely caspase 3/7. Reports on anti- and pro-inflammatory effects of AEA are numerous, and indication of pro-inflammatory effects in BAEC pre-treated with LPS are shown here. Nonetheless, further studies on timing and concentration dependent effects of AEA on BAEC function are needed, as activation of CB1 by AEA can reduce or increase ROS production, depending on cell type, timing of administration, and concentration.

There are limitations to our study design and functional assays. Utilization of the ECIS as a functional assay of endothelial barrier function allows for real-time determination of barrier integrity and advanced modeling thanks to multiple frequency electrical resistance and capacitance measurements. However, the embedded electrodes impede imaging of the cells after completion of the ECIS assay. Therefore, the mechanism causing increases in TER at 2 h post 0.5 μM AEA could not be determined with the data presented in this study. Future studies should determine the morphological changes associated with CB1 activation by AEA.

4.5: CONCLUSIONS

Increased AEA concentrations during coliform mastitis further deteriorates endothelial barrier integrity. Treatment of endothelial cells with AEA at physiological concentrations (0.5 μM) results in ROS production, increasing likelihood of oxidative stress and activation of apoptotic pathways. However, dynamic concentrations of cannabinoids and expression of related genes emphasizes the importance of timing of endocannabinoid treatment. Additional studies pertaining

to the timing of concentration ranges of endocannabinoids and endocannabinoid related drugs are necessary to determine the true effect of AEA and other endocannabinoids on endothelial barrier function. Improved endothelial barrier function is a crucial facet of improving welfare and reducing mortality and cost associated with coliform mastitis.

Supplementary Materials: The following supporting information can be downloaded at: https://www.mdpi.com/article/10.3390/antiox11081461/s1, Table S1: Viability (ATP-production) of BAEC treated with AEA and AM251, with and without LPS (2, 8, 12, and 24 h); Table S2: Cytotoxicity of BAEC treated with AEA and AM251, with and without LPS (2, 8, 12, and 24 h); Table S3: Cytochrome-C release of BAEC treated with AEA and AM251, with and without LPS (2, 8, 12, and 24 h); Table S4: Caspase-3/7 activation of BAEC treated with AEA and AM251, with and without LPS (2, 8, 12, and 24 h); Table S5: ROS production of BAEC treated with AEA and AM251, with and without LPS (2, 8, 12, and 24 h); Table S6: IsoP production of BAEC treated with AEA and AM251, with and without LPS (2, 8, 12, and 24 h); Table S7: ICAM-1 gene expression of BAEC treated with AEA and AM251, with and without LPS (2, 8, 12, and 24 h); Table S8: VCAM-1 gene expression of BAEC treated with AEA and AM251, with and without LPS (2, 8, 12, and 24 h); Figure S1: Trans-endothelial resistance of BAEC treated with 1 μM AM251, with and without LPS.

CONCLUSIONS

This dissertation illustrates the involvement of the ECS in inflammation and oxidative stress during naturally occurring acute coliform mastitis. We demonstrate for the first time that ECs may be potent inflammatory biomarkers and that EC concentrations are affected not only by coliform mastitis itself but are dependent on survival and death of the animal. Furthermore, we also demonstrate for the first time that the ECS is present in bovine vascular endothelial cells and the involvement of AEA in vascular endothelial cell barrier and mitochondrial function. We provide evidence that AEA alters endothelial cell viability, ROS production, barrier integrity, and mitochondrial function. We also provide evidence that supraphysiological concentrations of AEA are not necessary to elicit endothelial cell responses.

Our in vitro model describes how AEA may be a contributing factor to the decreased endothelial barrier integrity observed following NSAID treatment which is CB1 mediated. We thereby provide a better understanding of the efficacy of medical interventions utilized to treat coliform mastitis and potential novel therapeutic targets within the ECS. Manipulation of the ECS via selective receptor inhibition may improve endothelial function and overall inflammatory response during coliform mastitis, improving cow well-being, and decreasing mortality rate.

With the findings in this dissertation, we provide new knowledge gaps of the inflammatory involvement of the ECS, specifically AEA. There is a need to further characterize the effect of elevated AEA during inflammatory events in dairy cattle, particularly the timing of AEA concentration increases. Additionally, the mechanism of CB1 activation by AEA must be further investigated. Internalization and translocation of CB1 following activation, transport of AEA into the cytosol via transport proteins, and AEA synthesis and release from storage vesicles following CB1 activation by AEA have all been shown in immune cells of various species. Lastly, the effects

of AEA and CB1 on oxidative stress may be of great interest, not only during active infections, but to oxidant balance during high stress periods, such as onset of lactation, with the hopes of eliminating an underlying cause of dysregulated inflammation. However, research should not be limited to AEA and 2-AG. Ideally, profiling of EC should be as comprehensive as possible, including non-arachidonic acid-based EC and active metabolites of EC synthesized through the cyclooxygenase, lipoxygenase, and cytochrome p450 pathways.

REFERENCES

Ahn, K. H., Mahmoud, M. M., Shim, J. Y., & Kendall, D. A. (2013). Distinct roles of β-arrestin 1 and β-arrestin 2 in ORG27569-induced biased signaling and internalization of the cannabinoid receptor 1 (CB1). The Journal of biological chemistry, 288(14), 9790–9800. https://doi.org/10.1074/jbc.M112.438804

Aitken, S. L., Corl, C. M., & Sordillo, L. M. (2011). Immunopathology of mastitis: insights into disease recognition and resolution. Journal of mammary gland biology and neoplasia, 16(4), 291–304. https://doi.org/10.1007/s10911-011-9230-4

Aitken, S. L., Corl, C. M., & Sordillo, L. M. (2011). Pro-inflammatory and pro-apoptotic responses of TNF-α stimulated bovine mammary endothelial cells. Veterinary immunology and immunopathology, 140(3-4), 282–290. https://doi.org/10.1016/j.vetimm.2011.01.016

Akopian, A. N., Ruparel, N. B., Jeske, N. A., Patwardhan, A., & Hargreaves, K. M. (2009). Role of ionotropic cannabinoid receptors in peripheral antinociception and antihyperalgesia. Trends in pharmacological sciences, 30(2), 79–84. https://doi.org/10.1016/j.tips.2008.10.008

Alhouayek, M., Buisseret, B., Paquot, A., Guillemot-Legris, O., & Muccioli, G. G. (2018). The endogenous bioactive lipid prostaglandin D2-glycerol ester reduces murine colitis via DP1 and PPARγ receptors. FASEB journal : official publication of the Federation of American Societies for Experimental Biology, 32(9), 5000–5011. https://doi.org/10.1096/fj.201701205R

Amulic, B., Cazalet, C., Hayes, G. L., Metzler, K. D., & Zychlinsky, A. (2012). Neutrophil function: from mechanisms to disease. Annual review of immunology, 30, 459–489. https://doi.org/10.1146/annurev-immunol-020711-074942

Andersson, H., D'Antona, A. M., Kendall, D. A., Von Heijne, G., & Chin, C. N. (2003). Membrane assembly of the cannabinoid receptor 1: impact of a long N-terminal tail. Molecular pharmacology, 64(3), 570–577. https://doi.org/10.1124/mol.64.3.570

Artegoitia, V. M., Foote, A. P., Lewis, R. M., King, D. A., Shackelford, S. D., Wheeler, T. L., & Freetly, H. C. (2016). Endocannabinoids concentrations in plasma associated with feed efficiency and carcass composition of beef steers. Journal of animal science, 94(12), 5177–5181. https://doi.org/10.2527/jas.2016-1025

Awumey, E. M., Hill, S. K., Diz, D. I., & Bukoski, R. D. (2008). Cytochrome P-450 metabolites of 2-arachidonoylglycerol play a role in Ca2+-induced relaxation of rat mesenteric arteries. American journal of physiology. Heart and circulatory physiology, 294(5), H2363–H2370. https://doi.org/10.1152/ajpheart.01042.2007

Balan, S., Saxena, M., & Bhardwaj, N. (2019). Dendritic cell subsets and locations. International review of cell and molecular biology, 348, 1–68. https://doi.org/10.1016/bs.ircmb.2019.07.004

Balenga, N. A., Aflaki, E., Kargl, J., Platzer, W., Schröder, R., Blättermann, S., Kostenis, E., Brown, A. J., Heinemann, A., & Waldhoer, M. (2011). GPR55 regulates cannabinoid 2 receptor-mediated responses in human neutrophils. Cell research, 21(10), 1452–1469. https://doi.org/10.1038/cr.2011.60

Baranowska-Kuczko, M., Kozłowska, H., Kozłowski, M., Schlicker, E., Kloza, M., Surażyński, A., Grzęda, E., & Malinowska, B. (2014). Mechanisms of endothelium-dependent relaxation evoked by anandamide in isolated human pulmonary arteries. Naunyn-Schmiedeberg's archives of pharmacology, 387(5), 477–486. https://doi.org/10.1007/s00210-014-0961-9

Barragan, A. A., Hovingh, E., Bas, S., Lakritz, J., Byler, L., Ludwikowski, A., Takitch, S., Zug, J., & Hann, S. (2020). Effects of postpartum acetylsalicylic acid on metabolic status, health, and production in lactating dairy cattle. Journal of dairy science, 103(9), 8443–8452. https://doi.org/10.3168/jds.2019-17966

Basavarajappa B. S. (2007). Critical enzymes involved in endocannabinoid metabolism. Protein and peptide letters, 14(3), 237–246. https://doi.org/10.2174/092986607780090829

Berdyshev, E. V., Boichot, E., Germain, N., Allain, N., Anger, J. P., & Lagente, V. (1997). Influence of fatty acid ethanolamides and delta9-tetrahydrocannabinol on cytokine and arachidonate release by mononuclear cells. European journal of pharmacology, 330(2-3), 231–240. https://doi.org/10.1016/s0014-2999(97)01007-8

Berdyshev, E., Boichot, E., Corbel, M., Germain, N., & Lagente, V. (1998). Effects of cannabinoid receptor ligands on LPS-induced pulmonary inflammation in mice. Life sciences, 63(8), PL125–PL129. https://doi.org/10.1016/s0024-3205(98)00324-5

Biernacki, M., Ambrożewicz, E., Gęgotek, A., Toczek, M., Bielawska, K., & Skrzydlewska, E. (2018). Redox system and phospholipid metabolism in the kidney of hypertensive rats after FAAH inhibitor URB597 administration. Redox biology, 15, 41–50. https://doi.org/10.1016/j.redox.2017.11.022

Biringer R. G. (2021). Endocannabinoid signaling pathways: beyond CB1R and CB2R. Journal of cell communication and signaling, 15(3), 335–360. https://doi.org/10.1007/s12079-021-00622-6

Blankman, J. L., Simon, G. M., & Cravatt, B. F. (2007). A comprehensive profile of brain enzymes that hydrolyze the endocannabinoid 2-arachidonoylglycerol. Chemistry & biology, 14(12), 1347–1356. https://doi.org/10.1016/j.chembiol.2007.11.006

Bodiga, S., Gruenloh, S. K., Gao, Y., Manthati, V. L., Dubasi, N., Falck, J. R., Medhora, M., & Jacobs, E. R. (2010). 20-HETE-induced nitric oxide production in pulmonary artery endothelial cells is mediated by NADPH oxidase, H2O2, and PI3-kinase/Akt. American journal of physiology. Lung cellular and molecular physiology, 298(4), L564–L574. https://doi.org/10.1152/ajplung.00298.2009

Boivin, B., Vaniotis, G., Allen, B. G., & Hébert, T. E. (2008). G protein-coupled receptors in and on the cell nucleus: a new signaling paradigm?. Journal of receptor and signal transduction research, 28(1-2), 15–28. https://doi.org/10.1080/10799890801941889

Bonsale, R., Seyed Sharifi, R., Dirandeh, E., Hedayat, N., Mojtahedin, A., Ghorbanalinia, M., & Abolghasemi, A. (2018). Endocannabinoids as endometrial inflammatory markers in lactating Holstein cows. Reproduction in domestic animals = Zuchthygiene, 53(3), 769–775. https://doi.org/10.1111/rda.13169

Borregaard N. (2010). Neutrophils, from marrow to microbes. Immunity, 33(5), 657–670. https://doi.org/10.1016/j.immuni.2010.11.011

Bouaboula, M., Poinot-Chazel, C., Bourrié, B., Canat, X., Calandra, B., Rinaldi-Carmona, M., Le Fur, G., & Casellas, P. (1995). Activation of mitogen-activated protein kinases by stimulation of the central cannabinoid receptor CB1. The Biochemical journal, 312 (Pt 2)(Pt 2), 637–641. https://doi.org/10.1042/bj3120637

Brailoiu, G. C., Oprea, T. I., Zhao, P., Abood, M. E., & Brailoiu, E. (2011). Intracellular cannabinoid type 1 (CB1) receptors are activated by anandamide. The Journal of biological chemistry, 286(33), 29166–29174. https://doi.org/10.1074/jbc.M110.217463

Bruckmaier, R. M., & Wellnitz, O. (2017). TRIENNIAL LACTATION SYMPOSIUM/BOLFA: Pathogen-specific immune response and changes in the blood-milk barrier of the bovine mammary gland. Journal of animal science, 95(12), 5720–5728. https://doi.org/10.2527/jas2017.1845

Buisseret, B., Alhouayek, M., Guillemot-Legris, O., & Muccioli, G. G. (2019). Endocannabinoid and Prostanoid Crosstalk in Pain. Trends in molecular medicine, 25(10), 882–896. https://doi.org/10.1016/j.molmed.2019.04.009

Cabral, G. A., Raborn, E. S., Griffin, L., Dennis, J., & Marciano-Cabral, F. (2008). CB2 receptors in the brain: role in central immune function. British journal of pharmacology, 153(2), 240–251. https://doi.org/10.1038/sj.bjp.0707584

Cabral, G. A., Ferreira, G. A., & Jamerson, M. J. (2015). Endocannabinoids and the Immune System in Health and Disease. Handbook of experimental pharmacology, 231, 185–211. https://doi.org/10.1007/978-3-319-20825-1_6

Caldeira, M. O., Bruckmaier, R. M., & Wellnitz, O. (2021). Effects of local or systemic administration of meloxicam on mammary gland inflammatory responses to lipopolysaccharide-induced mastitis in dairy cows. Journal of dairy science, 104(1), 1039–1052. https://doi.org/10.3168/jds.2020-18691

Catanzaro, G., Rapino, C., Oddi, S., & Maccarrone, M. (2009). Anandamide increases swelling and reduces calcium sensitivity of mitochondria. Biochemical and biophysical research communications, 388(2), 439–442. https://doi.org/10.1016/j.bbrc.2009.08.037

Celi P. (2011). Biomarkers of oxidative stress in ruminant medicine. Immunopharmacology and immunotoxicology, 33(2), 233–240. https://doi.org/10.3109/08923973.2010.514917

Cencioni, M. T., Chiurchiù, V., Catanzaro, G., Borsellino, G., Bernardi, G., Battistini, L., & Maccarrone, M. (2010). Anandamide suppresses proliferation and cytokine release from primary human T-lymphocytes mainly via CB2 receptors. PloS one, 5(1), e8688. https://doi.org/10.1371/journal.pone.0008688

Chang, Y. H., Lee, S. T., & Lin, W. W. (2001). Effects of cannabinoids on LPS-stimulated inflammatory mediator release from macrophages: involvement of eicosanoids. Journal of cellular biochemistry, 81(4), 715–723. https://doi.org/10.1002/jcb.1103

Chemin, J., Monteil, A., Perez-Reyes, E., Nargeot, J., & Lory, P. (2001). Direct inhibition of T-type calcium channels by the endogenous cannabinoid anandamide. The EMBO journal, 20(24), 7033–7040. https://doi.org/10.1093/emboj/20.24.7033

Cheng, J., Ou, J. S., Singh, H., Falck, J. R., Narsimhaswamy, D., Pritchard, K. A., Jr, & Schwartzman, M. L. (2008). 20-hydroxyeicosatetraenoic acid causes endothelial dysfunction via eNOS uncoupling. American journal of physiology. Heart and circulatory physiology, 294(2), H1018–H1026. https://doi.org/10.1152/ajpheart.01172.2007

Chiurchiù, V., Battistini, L., & Maccarrone, M. (2015). Endocannabinoid signalling in innate and adaptive immunity. Immunology, 144(3), 352–364. https://doi.org/10.1111/imm.12441

Chiurchiù, V., Lanuti, M., De Bardi, M., Battistini, L., & Maccarrone, M. (2015). The differential characterization of GPR55 receptor in human peripheral blood reveals a distinctive expression in monocytes and NK cells and a proinflammatory role in these innate cells. International immunology, 27(3), 153–160. https://doi.org/10.1093/intimm/dxu097

Chiurchiù, V., Cencioni, M. T., Bisicchia, E., De Bardi, M., Gasperini, C., Borsellino, G., Centonze, D., Battistini, L., & Maccarrone, M. (2013). Distinct modulation of human myeloid and plasmacytoid dendritic cells by anandamide in multiple sclerosis. Annals of neurology, 73(5), 626–636. https://doi.org/10.1002/ana.23875

Chiurchiù, V., Rapino, C., Talamonti, E., Leuti, A., Lanuti, M., Gueniche, A., Jourdain, R., Breton, L., & Maccarrone, M. (2016). Anandamide Suppresses Proinflammatory T Cell Responses In Vitro through Type-1 Cannabinoid Receptor-Mediated mTOR Inhibition in Human Keratinocytes. Journal of immunology (Baltimore, Md. : 1950), 197(9), 3545–3553. https://doi.org/10.4049/jimmunol.1500546

Chouinard, F., Lefebvre, J. S., Navarro, P., Bouchard, L., Ferland, C., Lalancette-Hébert, M., Marsolais, D., Laviolette, M., & Flamand, N. (2011). The endocannabinoid 2-arachidonoyl-glycerol activates human neutrophils: critical role of its hydrolysis and de novo leukotriene B4 biosynthesis. Journal of immunology (Baltimore, Md. : 1950), 186(5), 3188–3196. https://doi.org/10.4049/jimmunol.1002853

Chrousos G. P. (1995). The hypothalamic-pituitary-adrenal axis and immune-mediated inflammation. The New England journal of medicine, 332(20), 1351–1362. https://doi.org/10.1056/NEJM199505183322008

Coleman, R. A., & Haynes, E. B. (1986). Monoacylglycerol acyltransferase. Evidence that the activities from rat intestine and suckling liver are tissue-specific isoenzymes. The Journal of biological chemistry, 261(1), 224–228.

Contreras, G. A., & Sordillo, L. M. (2011). Lipid mobilization and inflammatory responses during the transition period of dairy cows. Comparative immunology, microbiology and infectious diseases, 34(3), 281–289. https://doi.org/10.1016/j.cimid.2011.01.004

Contreras, G. A., Strieder-Barboza, C., de Souza, J., Gandy, J., Mavangira, V., Lock, A. L., & Sordillo, L. M. (2017). Periparturient lipolysis and oxylipid biosynthesis in bovine adipose tissues. PloS one, 12(12), e0188621. https://doi.org/10.1371/journal.pone.0188621

Contreras, G. A., Raphael, W., Mattmiller, S. A., Gandy, J., & Sordillo, L. M. (2012). Nonesterified fatty acids modify inflammatory response and eicosanoid biosynthesis in bovine endothelial cells. Journal of dairy science, 95(9), 5011–5023. https://doi.org/10.3168/jds.2012-5382

Cordeiro R. M. (2014). Reactive oxygen species at phospholipid bilayers: distribution, mobility and permeation. Biochimica et biophysica acta, 1838(1 Pt B), 438–444. https://doi.org/10.1016/j.bbamem.2013.09.016

Correa, F., Hernangómez-Herrero, M., Mestre, L., Loría, F., Docagne, F., & Guaza, C. (2011). The endocannabinoid anandamide downregulates IL-23 and IL-12 subunits in a viral model of multiple sclerosis: evidence for a cross-talk between IL-12p70/IL-23 axis and IL-10 in microglial cells. Brain, behavior, and immunity, 25(4), 736–749. https://doi.org/10.1016/j.bbi.2011.01.020

Crocq M. A. (2020). History of cannabis and the endocannabinoid system. Dialogues in clinical neuroscience, 22(3), 223–228. https://doi.org/10.31887/DCNS.2020.22.3/mcrocq

de Bus, I., Witkamp, R., Zuilhof, H., Albada, B., & Balvers, M. (2019). The role of n-3 PUFA-derived fatty acid derivatives and their oxygenated metabolites in the modulation of inflammation. Prostaglandins & other lipid mediators, 144, 106351. https://doi.org/10.1016/j.prostaglandins.2019.106351

De Schepper, S., De Ketelaere, A., Bannerman, D. D., Paape, M. J., Peelman, L., & Burvenich, C. (2008). The toll-like receptor-4 (TLR-4) pathway and its possible role in the pathogenesis of Escherichia coli mastitis in dairy cattle. Veterinary research, 39(1), 5. https://doi.org/10.1051/vetres:2007044

Derkinderen, P., Ledent, C., Parmentier, M., & Girault, J. A. (2001). Cannabinoids activate p38 mitogen-activated protein kinases through CB1 receptors in hippocampus. Journal of neurochemistry, 77(3), 957–960. https://doi.org/10.1046/j.1471-4159.2001.00333.x

Di Marzo V. (2008). The endocannabinoid system in obesity and type 2 diabetes. Diabetologia, 51(8), 1356–1367. https://doi.org/10.1007/s00125-008-1048-2

Di Marzo, V., De Petrocellis, L., Fezza, F., Ligresti, A., & Bisogno, T. (2002). Anandamide receptors. Prostaglandins, leukotrienes, and essential fatty acids, 66(2-3), 377–391. https://doi.org/10.1054/plef.2001.0349

Dirandeh, E., & Ghaffari, J. (2018). Effects of feeding a source of omega-3 fatty acid during the early postpartum period on the endocannabinoid system in the bovine endometrium. Theriogenology, 121, 141–146. https://doi.org/10.1016/j.theriogenology.2018.07.043

Do, Y., McKallip, R. J., Nagarkatti, M., & Nagarkatti, P. S. (2004). Activation through cannabinoid receptors 1 and 2 on dendritic cells triggers NF-kappaB-dependent apoptosis: novel role for endogenous and exogenous cannabinoids in immunoregulation. Journal of immunology (Baltimore, Md. : 1950), 173(4), 2373–2382. https://doi.org/10.4049/jimmunol.173.4.2373

Donalisio, C., Barbero, R., Cuniberti, B., Vercelli, C., Casalone, M., & Re, G. (2013). Effects of flunixin meglumine and ketoprofen on mediator production in ex vivo and in vitro models of inflammation in healthy dairy cows. Journal of veterinary pharmacology and therapeutics, 36(2), 130–139. https://doi.org/10.1111/j.1365-2885.2012.01396.x

Dong, L., Sharma, N. P., Jurban, B. J., & Smith, W. L. (2013). Pre-existent asymmetry in the human cyclooxygenase-2 sequence homodimer. The Journal of biological chemistry, 288(40), 28641–28655. https://doi.org/10.1074/jbc.M113.505503

Dong, L., Yuan, C., Orlando, B. J., Malkowski, M. G., & Smith, W. L. (2016). Fatty Acid Binding to the Allosteric Subunit of Cyclooxygenase-2 Relieves a Tonic Inhibition of the Catalytic Subunit. The Journal of biological chemistry, 291(49), 25641–25655. https://doi.org/10.1074/jbc.M116.757310

Dongdem, J. T., Helegbe, G. K., Opare-Asamoah, K., Wezena, C. A., & Ocloo, A. (2022). Assessment of NSAIDs as potential inhibitors of the fatty acid amide hydrolase I (FAAH-1) using three different primary fatty acid amide substrates in vitro. BMC pharmacology & toxicology, 23(1), 1. https://doi.org/10.1186/s40360-021-00539-1

Duan, S. Z., Usher, M. G., & Mortensen, R. M. (2009). PPARs: the vasculature, inflammation and hypertension. Current opinion in nephrology and hypertension, 18(2), 128–133. https://doi.org/10.1097/MNH.0b013e328325803b

d'Uscio, L. V., He, T., Santhanam, A. V., Tai, L. J., Evans, R. M., & Katusic, Z. S. (2014). Mechanisms of vascular dysfunction in mice with endothelium-specific deletion of the PPAR-δ gene. American journal of physiology. Heart and circulatory physiology, 306(7), H1001–H1010. https://doi.org/10.1152/ajpheart.00761.2013

El-Benna, J., Dang, P. M., Gougerot-Pocidalo, M. A., Marie, J. C., & Braut-Boucher, F. (2009). p47phox, the phagocyte NADPH oxidase/NOX2 organizer: structure, phosphorylation and implication in diseases. Experimental & molecular medicine, 41(4), 217–225. https://doi.org/10.3858/emm.2009.41.4.058

Eldeeb, K., Leone-Kabler, S., & Howlett, A. C. (2016). CB1 cannabinoid receptor-mediated increases in cyclic AMP accumulation are correlated with reduced Gi/o function. Journal of basic and clinical physiology and pharmacology, 27(3), 311–322. https://doi.org/10.1515/jbcpp-2015-0096

Erskine, R. J., Eberhart, R. J., Hutchinson, L. J., Spencer, S. B., & Campbell, M. A. (1988). Incidence and types of clinical mastitis in dairy herds with high and low somatic cell counts. Journal of the American Veterinary Medical Association, 192(6), 761–765.

Felder, C. C., Joyce, K. E., Briley, E. M., Mansouri, J., Mackie, K., Blond, O., Lai, Y., Ma, A. L., & Mitchell, R. L. (1995). Comparison of the pharmacology and signal transduction of the human cannabinoid CB1 and CB2 receptors. Molecular pharmacology, 48(3), 443–450.

Fernandes, A., Davoodi, S., Kaur, M., Veira, D., Melo, L., & Cerri, R. (2019). Effect of repeated intravenous lipopolysaccharide infusions on systemic inflammatory response and endometrium gene expression in Holstein heifers. Journal of dairy science, 102(4), 3531–3543. https://doi.org/10.3168/jds.2018-14616

Feske, S., Wulff, H., & Skolnik, E. Y. (2015). Ion channels in innate and adaptive immunity. Annual review of immunology, 33, 291–353. https://doi.org/10.1146/annurev-immunol-032414-112212

Flores-Otero, J., Ahn, K. H., Delgado-Peraza, F., Mackie, K., Kendall, D. A., & Yudowski, G. A. (2014). Ligand-specific endocytic dwell times control functional selectivity of the cannabinoid receptor 1. Nature communications, 5, 4589. https://doi.org/10.1038/ncomms5589

Furman, B., Pyne, N., Flatt, P., & O'Harte, F. (2004). Targeting beta-cell cyclic 3'5' adenosine monophosphate for the development of novel drugs for treating type 2 diabetes mellitus. A review. The Journal of pharmacy and pharmacology, 56(12), 1477–1492. https://doi.org/10.1211/0022357044805

Galiègue, S., Mary, S., Marchand, J., Dussossoy, D., Carrière, D., Carayon, P., Bouaboula, M., Shire, D., Le Fur, G., & Casellas, P. (1995). Expression of central and peripheral cannabinoid receptors in human immune tissues and leukocyte subpopulations. European journal of biochemistry, 232(1), 54–61. https://doi.org/10.1111/j.1432-1033.1995.tb20780.x

Gantz, I., Muraoka, A., Yang, Y. K., Samuelson, L. C., Zimmerman, E. M., Cook, H., & Yamada, T. (1997). Cloning and chromosomal localization of a gene (GPR18) encoding a novel seven transmembrane receptor highly expressed in spleen and testis. Genomics, 42(3), 462–466. https://doi.org/10.1006/geno.1997.4752

Garaude, J., Acín-Pérez, R., Martínez-Cano, S., Enamorado, M., Ugolini, M., Nistal-Villán, E., Hervás-Stubbs, S., Pelegrín, P., Sander, L. E., Enríquez, J. A., & Sancho, D. (2016). Mitochondrial respiratory-chain adaptations in macrophages contribute to antibacterial host defense. Nature immunology, 17(9), 1037–1045. https://doi.org/10.1038/ni.3509

Garcia, D. E., Brown, S., Hille, B., & Mackie, K. (1998). Protein kinase C disrupts cannabinoid actions by phosphorylation of the CB1 cannabinoid receptor. The Journal of neuroscience: the official journal of the Society for Neuroscience, 18(8), 2834–2841. https://doi.org/10.1523/JNEUROSCI.18-08-02834.1998

Gervasi, M. G., Osycka-Salut, C., Caballero, J., Vazquez-Levin, M., Pereyra, E., Billi, S., Franchi, A., & Perez-Martinez, S. (2011). Anandamide capacitates bull spermatozoa through CB1 and TRPV1 activation. PloS one, 6(2), e16993. https://doi.org/10.1371/journal.pone.0016993

Gervasi, M. G., Marczylo, T. H., Lam, P. M., Rana, S., Franchi, A. M., Konje, J. C., & Perez-Martinez, S. (2013). Anandamide levels fluctuate in the bovine oviduct during the oestrous cycle. PloS one, 8(8), e72521. https://doi.org/10.1371/journal.pone.0072521

Giacobbe, J., Marrocu, A., Di Benedetto, M. G., Pariante, C. M., & Borsini, A. (2021). A systematic, integrative review of the effects of the endocannabinoid system on inflammation and neurogenesis in animal models of affective disorders. Brain, behavior, and immunity, 93, 353–367. https://doi.org/10.1016/j.bbi.2020.12.024

Glass, M., & Northup, J. K. (1999). Agonist selective regulation of G proteins by cannabinoid CB(1) and CB(2) receptors. Molecular pharmacology, 56(6), 1362–1369. https://doi.org/10.1124/mol.56.6.1362

Godbole, A., Lyga, S., Lohse, M. J., & Calebiro, D. (2017). Internalized TSH receptors en route to the TGN induce local Gs-protein signaling and gene transcription. Nature communications, 8(1), 443. https://doi.org/10.1038/s41467-017-00357-2

Goldammer, T., Zerbe, H., Molenaar, A., Schuberth, H. J., Brunner, R. M., Kata, S. R., & Seyfert, H. M. (2004). Mastitis increases mammary mRNA abundance of beta-defensin 5, toll-like-receptor 2 (TLR2), and TLR4 but not TLR9 in cattle. Clinical and diagnostic laboratory immunology, 11(1), 174–185. https://doi.org/10.1128/cdli.11.1.174-185.2004

Goparaju, S. K., Ueda, N., Taniguchi, K., & Yamamoto, S. (1999). Enzymes of porcine brain hydrolyzing 2-arachidonoylglycerol, an endogenous ligand of cannabinoid receptors. Biochemical pharmacology, 57(4), 417–423. https://doi.org/10.1016/s0006-2952(98)00314-1

Graham, E. S., Angel, C. E., Schwarcz, L. E., Dunbar, P. R., & Glass, M. (2010). Detailed characterisation of CB2 receptor protein expression in peripheral blood immune cells from healthy human volunteers using flow cytometry. International journal of immunopathology and pharmacology, 23(1), 25–34. https://doi.org/10.1177/039463201002300103

Guellich, A., Damy, T., Conti, M., Claes, V., Samuel, J. L., Pineau, T., Lecarpentier, Y., & Coirault, C. (2013). Tempol prevents cardiac oxidative damage and left ventricular dysfunction in the PPAR-α KO mouse. American journal of physiology. Heart and circulatory physiology, 304(11), H1505–H1512. https://doi.org/10.1152/ajpheart.00669.2012

Guindon, J., De Léan, A., & Beaulieu, P. (2006). Local interactions between anandamide, an endocannabinoid, and ibuprofen, a nonsteroidal anti-inflammatory drug, in acute and inflammatory pain. Pain, 121(1-2), 85–93. https://doi.org/10.1016/j.pain.2005.12.007

Gyires, K., & Zádori, Z. S. (2016). Role of Cannabinoids in Gastrointestinal Mucosal Defense and Inflammation. Current neuropharmacology, 14(8), 935–951. https://doi.org/10.2174/1570159x14666160303110150

Han, K. H., Lim, S., Ryu, J., Lee, C. W., Kim, Y., Kang, J. H., Kang, S. S., Ahn, Y. K., Park, C. S., & Kim, J. J. (2009). CB1 and CB2 cannabinoid receptors differentially regulate the production of reactive oxygen species by macrophages. Cardiovascular research, 84(3), 378–386. https://doi.org/10.1093/cvr/cvp240

Han, M. S., White, A., Perry, R. J., Camporez, J. P., Hidalgo, J., Shulman, G. I., & Davis, R. J. (2020). Regulation of adipose tissue inflammation by interleukin 6. Proceedings of the National Academy of Sciences of the United States of America, 117(6), 2751–2760. https://doi.org/10.1073/pnas.1920004117

Hattori, H., Subramanian, K. K., Sakai, J., Jia, Y., Li, Y., Porter, T. F., Loison, F., Sarraj, B., Kasorn, A., Jo, H., Blanchard, C., Zirkle, D., McDonald, D., Pai, S. Y., Serhan, C. N., & Luo, H. R. (2010). Small-molecule screen identifies reactive oxygen species as key regulators of neutrophil chemotaxis. Proceedings of the National Academy of Sciences of the United States of America, 107(8), 3546–3551. https://doi.org/10.1073/pnas.0914351107

Henstridge, C. M., Balenga, N. A., Schröder, R., Kargl, J. K., Platzer, W., Martini, L., Arthur, S., Penman, J., Whistler, J. L., Kostenis, E., Waldhoer, M., & Irving, A. J. (2010). GPR55 ligands promote receptor coupling to multiple signalling pathways. British journal of pharmacology, 160(3), 604–614. https://doi.org/10.1111/j.1476-5381.2009.00625.x

Hernanz, R., Briones, A. M., Salaices, M., & Alonso, M. J. (2014). New roles for old pathways? A circuitous relationship between reactive oxygen species and cyclo-oxygenase in hypertension. Clinical science (London, England : 1979), 126(2), 111–121. https://doi.org/10.1042/CS20120651

Herradón, E., Martín, M. I., & López-Miranda, V. (2007). Characterization of the vasorelaxant mechanisms of the endocannabinoid anandamide in rat aorta. British journal of pharmacology, 152(5), 699–708. https://doi.org/10.1038/sj.bjp.0707404

Herzig, S., & Shaw, R. J. (2018). AMPK: guardian of metabolism and mitochondrial homeostasis. Nature reviews. Molecular cell biology, 19(2), 121–135. https://doi.org/10.1038/nrm.2017.95

Hill, M. N., & Tasker, J. G. (2012). Endocannabinoid signaling, glucocorticoid-mediated negative feedback, and regulation of the hypothalamic-pituitary-adrenal axis. Neuroscience, 204, 5–16. https://doi.org/10.1016/j.neuroscience.2011.12.030

Hind, W. H., Tufarelli, C., Neophytou, M., Anderson, S. I., England, T. J., & O'Sullivan, S. E. (2015). Endocannabinoids modulate human blood-brain barrier permeability in vitro. British journal of pharmacology, 172(12), 3015–3027. https://doi.org/10.1111/bph.13106

Hinson, R. M., Williams, J. A., & Shacter, E. (1996). Elevated interleukin 6 is induced by prostaglandin E2 in a murine model of inflammation: possible role of cyclooxygenase-2. Proceedings of the National Academy of Sciences of the United States of America, 93(10), 4885–4890. https://doi.org/10.1073/pnas.93.10.4885

Hiroyama, M., & Takenawa, T. (1998). Purification and characterization of a lysophosphatidic acid-specific phosphatase. The Biochemical journal, 336 (Pt 2)(Pt 2), 483–489. https://doi.org/10.1042/bj3360483

Hoeben, D., Burvenich, C., Trevisi, E., Bertoni, G., Hamann, J., Bruckmaier, R. M., & Blum, J. W. (2000). Role of endotoxin and TNF-alpha in the pathogenesis of experimentally induced coliform mastitis in periparturient cows. The Journal of dairy research, 67(4), 503–514. https://doi.org/10.1017/s0022029900004489

Hofmann, N. A., Barth, S., Waldeck-Weiermair, M., Klec, C., Strunk, D., Malli, R., & Graier, W. F. (2014). TRPV1 mediates cellular uptake of anandamide and thus promotes endothelial cell proliferation and network-formation. Biology open, 3(12), 1164–1172. https://doi.org/10.1242/bio.20149571

Howard, J. T., O'Nan, A. T., Maltecca, C., Baynes, R. E., & Ashwell, M. S. (2015). Differential Gene Expression across Breed and Sex in Commercial Pigs Administered Fenbendazole and Flunixin Meglumine. PloS one, 10(9), e0137830. https://doi.org/10.1371/journal.pone.0137830

Hsu, K. L., Tsuboi, K., Adibekian, A., Pugh, H., Masuda, K., & Cravatt, B. F. (2012). DAGLβ inhibition perturbs a lipid network involved in macrophage inflammatory responses. Nature chemical biology, 8(12), 999–1007. https://doi.org/10.1038/nchembio.1105

Hu, Y. W., Yang, J. Y., Ma, X., Chen, Z. P., Hu, Y. R., Zhao, J. Y., Li, S. F., Qiu, Y. R., Lu, J. B., Wang, Y. C., Gao, J. J., Sha, Y. H., Zheng, L., & Wang, Q. (2014). A lincRNA-DYNLRB2-2/GPR119/GLP-1R/ABCA1-dependent signal transduction pathway is essential for the regulation of cholesterol homeostasis. Journal of lipid research, 55(4), 681–697. https://doi.org/10.1194/jlr.M044669

Huang, N. L., Juang, J. M., Wang, Y. H., Hsueh, C. H., Liang, Y. J., Lin, J. L., Tsai, C. T., & Lai, L. P. (2010). Rimonabant inhibits TNF-α-induced endothelial IL-6 secretion via CB1 receptor and cAMP-dependent protein kinase pathway. Acta pharmacologica Sinica, 31(11), 1447–1453. https://doi.org/10.1038/aps.2010.126

Hussey, S. E., Lum, H., Alvarez, A., Cipriani, Y., Garduño-Garcia, J., Anaya, L., Dube, J., & Musi, N. (2014). A sustained increase in plasma NEFA upregulates the Toll-like receptor network in human muscle. Diabetologia, 57(3), 582–591. https://doi.org/10.1007/s00125-013-3111-x

Hutch, C. R., & Hegg, C. C. (2016). Cannabinoid receptor signaling induces proliferation but not neurogenesis in the mouse olfactory epithelium. Neurogenesis (Austin, Tex.), 3(1), e1118177. https://doi.org/10.1080/23262133.2015.1118177

Ingvartsen, K. L., & Moyes, K. (2013). Nutrition, immune function and health of dairy cattle. Animal : an international journal of animal bioscience, 7 Suppl 1, 112–122. https://doi.org/10.1017/S175173111200170X

Irannejad, R., Pessino, V., Mika, D., Huang, B., Wedegaertner, P. B., Conti, M., & von Zastrow, M. (2017). Functional selectivity of GPCR-directed drug action through location bias. Nature chemical biology, 13(7), 799–806. https://doi.org/10.1038/nchembio.2389

Jackson, A. R., Nagarkatti, P., & Nagarkatti, M. (2014). Anandamide attenuates Th-17 cell-mediated delayed-type hypersensitivity response by triggering IL-10 production and consequent microRNA induction. PloS one, 9(4), e93954. https://doi.org/10.1371/journal.pone.0093954

Jain, T., Wager-Miller, J., Mackie, K., & Straiker, A. (2013). Diacylglycerol lipaseα (DAGLα) and DAGLβ cooperatively regulate the production of 2-arachidonoyl glycerol in autaptic hippocampal neurons. Molecular pharmacology, 84(2), 296–302. https://doi.org/10.1124/mol.113.085217

Johns, D. G., Behm, D. J., Walker, D. J., Ao, Z., Shapland, E. M., Daniels, D. A., Riddick, M., Dowell, S., Staton, P. C., Green, P., Shabon, U., Bao, W., Aiyar, N., Yue, T. L., Brown, A. J., Morrison, A. D., & Douglas, S. A. (2007). The novel endocannabinoid receptor GPR55 is activated by atypical cannabinoids but does not mediate their vasodilator effects. British journal of pharmacology, 152(5), 825–831. https://doi.org/10.1038/sj.bjp.0707419

Kaplan, B. L., Ouyang, Y., Rockwell, C. E., Rao, G. K., & Kaminski, N. E. (2005). 2-Arachidonoyl-glycerol suppresses interferon-gamma production in phorbol ester/ionomycin-activated mouse splenocytes independent of CB1 or CB2. Journal of leukocyte biology, 77(6), 966–974. https://doi.org/10.1189/jlb.1104652

Kaur, R., Ambwani, S. R., & Singh, S. (2016). Endocannabinoid System: A Multi-Facet Therapeutic Target. Current clinical pharmacology, 11(2), 110–117. https://doi.org/10.2174/1574884711666160418105339

Kishimoto, S., Gokoh, M., Oka, S., Muramatsu, M., Kajiwara, T., Waku, K., & Sugiura, T. (2003). 2-arachidonoylglycerol induces the migration of HL-60 cells differentiated into macrophage-like cells and human peripheral blood monocytes through the cannabinoid CB2 receptor-dependent mechanism. The Journal of biological chemistry, 278(27), 24469–24475. https://doi.org/10.1074/jbc.M301359200

Kishimoto, S., Muramatsu, M., Gokoh, M., Oka, S., Waku, K., & Sugiura, T. (2005). Endogenous cannabinoid receptor ligand induces the migration of human natural killer cells. Journal of biochemistry, 137(2), 217–223. https://doi.org/10.1093/jb/mvi021

Kishimoto, S., Kobayashi, Y., Oka, S., Gokoh, M., Waku, K., & Sugiura, T. (2004). 2-Arachidonoylglycerol, an endogenous cannabinoid receptor ligand, induces accelerated production of chemokines in HL-60 cells. Journal of biochemistry, 135(4), 517–524. https://doi.org/10.1093/jb/mvh063

Kleinhenz, M. D., Weeder, M., Montgomery, S., Martin, M., Curtis, A., Magnin, G., Lin, Z., Griffin, J., & Coetzee, J. F. (2022). Short term feeding of industrial hemp with a high cannabidiolic acid (CBDA) content increases lying behavior and reduces biomarkers of stress and inflammation in Holstein steers. Scientific reports, 12(1), 3683. https://doi.org/10.1038/s41598-022-07795-z

Knych, H. K., Finno, C. J., Baden, R., Arthur, R. M., & McKemie, D. S. (2021). Identification and characterization of the enzymes responsible for the metabolism of the non-steroidal anti-inflammatory drugs, flunixin meglumine and phenylbutazone, in horses. Journal of veterinary pharmacology and therapeutics, 44(1), 36–46. https://doi.org/10.1111/jvp.12891

Kohno, M., Hasegawa, H., Inoue, A., Muraoka, M., Miyazaki, T., Oka, K., & Yasukawa, M. (2006). Identification of N-arachidonylglycine as the endogenous ligand for orphan G-protein-coupled receptor GPR18. Biochemical and biophysical research communications, 347(3), 827–832. https://doi.org/10.1016/j.bbrc.2006.06.175

Kratofil, R. M., Kubes, P., & Deniset, J. F. (2017). Monocyte Conversion During Inflammation and Injury. Arteriosclerosis, thrombosis, and vascular biology, 37(1), 35–42. https://doi.org/10.1161/ATVBAHA.116.308198

Kuhla, B., Kaever, V., Tuchscherer, A., & Kuhla, A. (2020). Involvement of Plasma Endocannabinoids and the Hypothalamic Endocannabinoid System in Increasing Feed Intake after Parturition of Dairy Cows. Neuroendocrinology, 110(3-4), 246–257. https://doi.org/10.1159/000501208

Kuhn, M. J., Putman, A. K., & Sordillo, L. M. (2020). Widespread basal cytochrome P450 expression in extrahepatic bovine tissues and isolated cells. Journal of dairy science, 103(1), 625–637. https://doi.org/10.3168/jds.2019-17071

Kuhn, M. J., Mavangira, V., Gandy, J. C., & Sordillo, L. M. (2018). Production of 15-F2t-isoprostane as an assessment of oxidative stress in dairy cows at different stages of lactation. Journal of dairy science, 101(10), 9287–9295. https://doi.org/10.3168/jds.2018-14669

Kumar, B. V., Connors, T. J., & Farber, D. L. (2018). Human T Cell Development, Localization, and Function throughout Life. Immunity, 48(2), 202–213. https://doi.org/10.1016/j.immuni.2018.01.007

Kumar, H., Kawai, T., & Akira, S. (2011). Pathogen recognition by the innate immune system. International reviews of immunology, 30(1), 16–34. https://doi.org/10.3109/08830185.2010.529976

Lauckner, J. E., Hille, B., & Mackie, K. (2005). The cannabinoid agonist WIN55,212-2 increases intracellular calcium via CB1 receptor coupling to Gq/11 G proteins. Proceedings of the National Academy of Sciences of the United States of America, 102(52), 19144–19149. https://doi.org/10.1073/pnas.0509588102

Lauckner, J. E., Jensen, J. B., Chen, H. Y., Lu, H. C., Hille, B., & Mackie, K. (2008). GPR55 is a cannabinoid receptor that increases intracellular calcium and inhibits M current. Proceedings of the National Academy of Sciences of the United States of America, 105(7), 2699–2704. https://doi.org/10.1073/pnas.0711278105

Lauffer, L. M., Iakoubov, R., & Brubaker, P. L. (2009). GPR119 is essential for oleoylethanolamide-induced glucagon-like peptide-1 secretion from the intestinal enteroendocrine L-cell. Diabetes, 58(5), 1058–1066. https://doi.org/10.2337/db08-1237

LeBlanc, S. J., Lissemore, K. D., Kelton, D. F., Duffield, T. F., & Leslie, K. E. (2006). Major advances in disease prevention in dairy cattle. Journal of dairy science, 89(4), 1267–1279. https://doi.org/10.3168/jds.S0022-0302(06)72195-6

Leo, L. M., & Abood, M. E. (2021). CB1 Cannabinoid Receptor Signaling and Biased Signaling. Molecules (Basel, Switzerland), 26(17), 5413. https://doi.org/10.3390/molecules26175413

Li, Y., Yin, R., Liu, J., Wang, P., Wu, S., Luo, J., Zhelyabovska, O., & Yang, Q. (2009). Peroxisome proliferator-activated receptor delta regulates mitofusin 2 expression in the heart. Journal of molecular and cellular cardiology, 46(6), 876–882. https://doi.org/10.1016/j.yjmcc.2009.02.020

Li, Y., Chen, X., Nie, Y., Tian, Y., Xiao, X., & Yang, F. (2021). Endocannabinoid activation of the TRPV1 ion channel is distinct from activation by capsaicin. The Journal of biological chemistry, 297(3), 101022. https://doi.org/10.1016/j.jbc.2021.101022

Liang, Y., Zhou, Y., & Shen, P. (2004). NF-kappaB and its regulation on the immune system. Cellular & molecular immunology, 1(5), 343–350.

Ligresti, A., Martos, J., Wang, J., Guida, F., Allarà, M., Palmieri, V., Luongo, L., Woodward, D., & Di Marzo, V. (2014). Prostamide F(2) α receptor antagonism combined with inhibition of FAAH may block the pro-inflammatory mediators formed following selective FAAH inhibition. British journal of pharmacology, 171(6), 1408–1419. https://doi.org/10.1111/bph.12410

Lipina, C., & Hundal, H. S. (2016). Modulation of cellular redox homeostasis by the endocannabinoid system. Open biology, 6(4), 150276. https://doi.org/10.1098/rsob.150276

Liu, J., Gao, B., Mirshahi, F., Sanyal, A. J., Khanolkar, A. D., Makriyannis, A., & Kunos, G. (2000). Functional CB1 cannabinoid receptors in human vascular endothelial cells. The Biochemical journal, 346 Pt 3(Pt 3), 835–840.

Liu, J., Wang, L., Harvey-White, J., Huang, B. X., Kim, H. Y., Luquet, S., Palmiter, R. D., Krystal, G., Rai, R., Mahadevan, A., Razdan, R. K., & Kunos, G. (2008). Multiple pathways involved in the biosynthesis of anandamide. Neuropharmacology, 54(1), 1–7. https://doi.org/10.1016/j.neuropharm.2007.05.020

Liu, J., Batkai, S., Pacher, P., Harvey-White, J., Wagner, J. A., Cravatt, B. F., Gao, B., & Kunos, G. (2003). Lipopolysaccharide induces anandamide synthesis in macrophages via CD14/MAPK/phosphoinositide 3-kinase/NF-kappaB independently of platelet-activating factor. The Journal of biological chemistry, 278(45), 45034–45039. https://doi.org/10.1074/jbc.M306062200

Liu, M., Zhang, C., Xu, X., Zhao, X., Han, Z., Liu, D., Bo, R., Li, J., & Liu, Z. (2021). Ferulic acid inhibits LPS-induced apoptosis in bovine mammary epithelial cells by regulating the NF-κB and Nrf2 signalling pathways to restore mitochondrial dynamics and ROS generation. Veterinary research, 52(1), 104. https://doi.org/10.1186/s13567-021-00973-3

Liu, X., Wu, Y., Zhou, D., Xie, Y., Zhou, Y., Lu, Y., Yang, R., & Liu, S. (2020). N-linoleyltyrosine protects PC12 cells against oxidative damage via autophagy: Possible involvement of CB1 receptor regulation. International journal of molecular medicine, 46(5), 1827–1837. https://doi.org/10.3892/ijmm.2020.4706

Lloyd, E. E., Gaubatz, J. W., Burns, A. R., & Pownall, H. J. (2007). Sustained elevations in NEFA induce cyclooxygenase-2 activity and potentiate THP-1 macrophage foam cell formation. Atherosclerosis, 192(1), 49–55. https://doi.org/10.1016/j.atherosclerosis.2006.06.014

Lykkesfeldt, J., & Svendsen, O. (2007). Oxidants and antioxidants in disease: oxidative stress in farm animals. Veterinary journal (London, England : 1997), 173(3), 502–511. https://doi.org/10.1016/j.tvjl.2006.06.005

Maccarrone M. (2017). Metabolism of the Endocannabinoid Anandamide: Open Questions after 25 Years. Frontiers in molecular neuroscience, 10, 166. https://doi.org/10.3389/fnmol.2017.00166

Maestroni G. J. (2004). The endogenous cannabinoid 2-arachidonoyl glycerol as in vivo chemoattractant for dendritic cells and adjuvant for Th1 response to a soluble protein. FASEB journal : official publication of the Federation of American Societies for Experimental Biology, 18(15), 1914–1916. https://doi.org/10.1096/fj.04-2190fje

Mai, P., Tian, L., Yang, L., Wang, L., Yang, L., & Li, L. (2015). Cannabinoid receptor 1 but not 2 mediates macrophage phagocytosis by G(α)i/o /RhoA/ROCK signaling pathway. Journal of cellular physiology, 230(7), 1640–1650. https://doi.org/10.1002/jcp.24911

Malysz, J., Daza, A. V., Kage, K., Grayson, G. K., Yao, B. B., Meyer, M. D., & Gopalakrishnan, M. (2009). Characterization of human cannabinoid CB2 receptor coupled to chimeric Galpha(qi5) and Galpha(qo5) proteins. European journal of pharmacology, 603(1-3), 12–21. https://doi.org/10.1016/j.ejphar.2008.11.047

Manning, A. M., Bell, F. P., Rosenbloom, C. L., Chosay, J. G., Simmons, C. A., Northrup, J. L., Shebuski, R. J., Dunn, C. J., & Anderson, D. C. (1995). NF-kappa B is activated during acute inflammation in vivo in association with elevated endothelial cell adhesion molecule gene expression and leukocyte recruitment. Journal of inflammation, 45(4), 283–296.

Marrs, W. R., Blankman, J. L., Horne, E. A., Thomazeau, A., Lin, Y. H., Coy, J., Bodor, A. L., Muccioli, G. G., Hu, S. S., Woodruff, G., Fung, S., Lafourcade, M., Alexander, J. P., Long, J. Z., Li, W., Xu, C., Möller, T., Mackie, K., Manzoni, O. J., Cravatt, B. F., … Stella, N. (2010). The serine hydrolase ABHD6 controls the accumulation and efficacy of 2-AG at cannabinoid receptors. Nature neuroscience, 13(8), 951–957. https://doi.org/10.1038/nn.2601

Matias, I., Pochard, P., Orlando, P., Salzet, M., Pestel, J., & Di Marzo, V. (2002). Presence and regulation of the endocannabinoid system in human dendritic cells. European journal of biochemistry, 269(15), 3771–3778. https://doi.org/10.1046/j.1432-1033.2002.03078.x

Matsuda, L. A., Lolait, S. J., Brownstein, M. J., Young, A. C., & Bonner, T. I. (1990). Structure of a cannabinoid receptor and functional expression of the cloned cDNA. Nature, 346(6284), 561–564. https://doi.org/10.1038/346561a0

Mavangira, V., Brown, J., Gandy, J. C., & Sordillo, L. M. (2020). 20-hydroxyeicosatetraenoic acid alters endothelial cell barrier integrity independent of oxidative stress and cell death. Prostaglandins & other lipid mediators, 149, 106425. https://doi.org/10.1016/j.prostaglandins.2020.106425

Mavangira, V., Gandy, J. C., Zhang, C., Ryman, V. E., Daniel Jones, A., & Sordillo, L. M. (2015). Polyunsaturated fatty acids influence differential biosynthesis of oxylipids and other lipid mediators during bovine coliform mastitis. Journal of dairy science, 98(9), 6202–6215. https://doi.org/10.3168/jds.2015-9570

Mavangira, V., Mangual, M. J., Gandy, J. C., & Sordillo, L. M. (2016). 15-F2t-Isoprostane Concentrations and Oxidant Status in Lactating Dairy Cattle with Acute Coliform Mastitis. Journal of veterinary internal medicine, 30(1), 339–347. https://doi.org/10.1111/jvim.13793

Mavangira, V., & Sordillo, L. M. (2018). Role of lipid mediators in the regulation of oxidative stress and inflammatory responses in dairy cattle. Research in veterinary science, 116, 4–14. https://doi.org/10.1016/j.rvsc.2017.08.002

McDougall, J. J., Muley, M. M., Philpott, H. T., Reid, A., & Krustev, E. (2017). Early blockade of joint inflammation with a fatty acid amide hydrolase inhibitor decreases end-stage osteoarthritis pain and peripheral neuropathy in mice. Arthritis research & therapy, 19(1), 106. https://doi.org/10.1186/s13075-017-1313-1

Milne, G. L., Dai, Q., & Roberts, L. J., 2nd (2015). The isoprostanes--25 years later. Biochimica et biophysica acta, 1851(4), 433–445. https://doi.org/10.1016/j.bbalip.2014.10.007

Milne, G. L., Yin, H., Brooks, J. D., Sanchez, S., Jackson Roberts, L., 2nd, & Morrow, J. D. (2007). Quantification of F2-isoprostanes in biological fluids and tissues as a measure of oxidant stress. Methods in enzymology, 433, 113–126. https://doi.org/10.1016/S0076-6879(07)33006-1

Milne, G. L., Yin, H., Hardy, K. D., Davies, S. S., & Roberts, L. J., 2nd (2011). Isoprostane generation and function. Chemical reviews, 111(10), 5973–5996. https://doi.org/10.1021/cr200160h

Mittal, M., Siddiqui, M. R., Tran, K., Reddy, S. P., & Malik, A. B. (2014). Reactive oxygen species in inflammation and tissue injury. Antioxidants & redox signaling, 20(7), 1126–1167. https://doi.org/10.1089/ars.2012.5149

Morak, M., Schmidinger, H., Riesenhuber, G., Rechberger, G. N., Kollroser, M., Haemmerle, G., Zechner, R., Kronenberg, F., & Hermetter, A. (2012). Adipose triglyceride lipase (ATGL) and hormone-sensitive lipase (HSL) deficiencies affect expression of lipolytic activities in mouse adipose tissues. Molecular & cellular proteomics : MCP, 11(12), 1777–1789. https://doi.org/10.1074/mcp.M111.015743

Moreno, E., Andradas, C., Medrano, M., Caffarel, M. M., Pérez-Gómez, E., Blasco-Benito, S., Gómez-Cañas, M., Pazos, M. R., Irving, A. J., Lluís, C., Canela, E. I., Fernández-Ruiz, J., Guzmán, M., McCormick, P. J., & Sánchez, C. (2014). Targeting CB2-GPR55 receptor heteromers modulates cancer cell signaling. The Journal of biological chemistry, 289(32), 21960–21972. https://doi.org/10.1074/jbc.M114.561761

Mukhopadhyay, P., Rajesh, M., Bátkai, S., Patel, V., Kashiwaya, Y., Liaudet, L., Evgenov, O. V., Mackie, K., Haskó, G., & Pacher, P. (2010). CB1 cannabinoid receptors promote oxidative stress and cell death in murine models of doxorubicin-induced cardiomyopathy and in human cardiomyocytes. Cardiovascular research, 85(4), 773–784. https://doi.org/10.1093/cvr/cvp369

Muller, C., & Reggio, P. H. (2020). An Analysis of the Putative CBD Binding Site in the Ionotropic Cannabinoid Receptors. Frontiers in cellular neuroscience, 14, 615811. https://doi.org/10.3389/fncel.2020.615811

Muller, C., Morales, P., & Reggio, P. H. (2019). Cannabinoid Ligands Targeting TRP Channels. Frontiers in molecular neuroscience, 11, 487. https://doi.org/10.3389/fnmol.2018.00487

Munro, S., Thomas, K. L., & Abu-Shaar, M. (1993). Molecular characterization of a peripheral receptor for cannabinoids. Nature, 365(6441), 61–65. https://doi.org/10.1038/365061a0

Myers, M. N., Zachut, M., Tam, J., & Contreras, G. A. (2021). A proposed modulatory role of the endocannabinoid system on adipose tissue metabolism and appetite in periparturient dairy cows. Journal of animal science and biotechnology, 12(1), 21. https://doi.org/10.1186/s40104-021-00549-3

Myers, M. J., Scott, M. L., Deaver, C. M., Farrell, D. E., & Yancy, H. F. (2010). Biomarkers of inflammation in cattle determining the effectiveness of anti-inflammatory drugs. Journal of veterinary pharmacology and therapeutics, 33(1), 1–8. https://doi.org/10.1111/j.1365-2885.2009.01096.x

Nakajima, Y., Mikami, O., Yoshioka, M., Motoi, Y., Ito, T., Ishikawa, Y., Fuse, M., Nakano, K., & Yasukawa, K. (1997). Elevated levels of tumor necrosis factor-alpha (TNF-alpha) and interleukin-6 (IL-6) activities in the sera and milk of cows with naturally occurring coliform mastitis. Research in veterinary science, 62(3), 297–298. https://doi.org/10.1016/s0034-5288(97)90209-5

Nakajima, Y., Furuichi, Y., Biswas, K. K., Hashiguchi, T., Kawahara, K., Yamaji, K., Uchimura, T., Izumi, Y., & Maruyama, I. (2006). Endocannabinoid, anandamide in gingival tissue regulates the periodontal inflammation through NF-kappaB pathway inhibition. FEBS letters, 580(2), 613–619. https://doi.org/10.1016/j.febslet.2005.12.079

National Animal Health Monitoring Service (NAHMS). (2014). Dairy 2014. Part. 1: Reference of Dairy Health and Management in the United States; USDA APHIS Veterinary Services: Fort Collins, CO, USA.

Nirodi, C. S., Crews, B. C., Kozak, K. R., Morrow, J. D., & Marnett, L. J. (2004). The glyceryl ester of prostaglandin E2 mobilizes calcium and activates signal transduction in RAW264.7 cells. Proceedings of the National Academy of Sciences of the United States of America, 101(7), 1840–1845. https://doi.org/10.1073/pnas.0303950101

Nogueras-Ortiz, C., Roman-Vendrell, C., Mateo-Semidey, G. E., Liao, Y. H., Kendall, D. A., & Yudowski, G. A. (2017). Retromer stops beta-arrestin 1-mediated signaling from internalized cannabinoid 2 receptors. Molecular biology of the cell, 28(24), 3554–3561. https://doi.org/10.1091/mbc.E17-03-0198

Nong, L., Newton, C., Friedman, H., & Klein, T. W. (2001). CB1 and CB2 receptor mRNA expression in human peripheral blood mononuclear cells (PBMC) from various donor types. Advances in experimental medicine and biology, 493, 229–233. https://doi.org/10.1007/0-306-47611-8_27

Ohtsuka, H., Kudo, K., Mori, K., Nagai, F., Hatsugaya, A., Tajima, M., Tamura, K., Hoshi, F., Koiwa, M., & Kawamura, S. (2001). Acute phase response in naturally occurring coliform mastitis. The Journal of veterinary medical science, 63(6), 675–678. https://doi.org/10.1292/jvms.63.675

Oishi, Y., & Manabe, I. (2018). Macrophages in inflammation, repair and regeneration. International immunology, 30(11), 511–528. https://doi.org/10.1093/intimm/dxy054

Oliveira, L., Hulland, C., & Ruegg, P. L. (2013). Characterization of clinical mastitis occurring in cows on 50 large dairy herds in Wisconsin. Journal of dairy science, 96(12), 7538–7549. https://doi.org/10.3168/jds.2012-6078

Osafo, N., Yeboah, O. K., & Antwi, A. O. (2021). Endocannabinoid system and its modulation of brain, gut, joint and skin inflammation. Molecular biology reports, 48(4), 3665–3680. https://doi.org/10.1007/s11033-021-06366-1

O'Sullivan S. E. (2016). An update on PPAR activation by cannabinoids. British journal of pharmacology, 173(12), 1899–1910. https://doi.org/10.1111/bph.13497

O'Sullivan, S. E., Kendall, D. A., & Randall, M. D. (2009). Time-dependent vascular effects of Endocannabinoids mediated by peroxisome proliferator-activated receptor gamma (PPARγ). PPAR research, 2009, 425289. https://doi.org/10.1155/2009/425289

Osycka-Salut, C. E., Martínez-León, E., Gervasi, M. G., Castellano, L., Davio, C., Chiarante, N., Franchi, A. M., Ribeiro, M. L., Díaz, E. S., & Perez-Martinez, S. (2020). Fibronectin induces capacitation-associated events through the endocannabinoid system in bull sperm. Theriogenology, 153, 91–101. https://doi.org/10.1016/j.theriogenology.2020.04.031

Pacher, P., & Mechoulam, R. (2011). Is lipid signaling through cannabinoid 2 receptors part of a protective system?. Progress in lipid research, 50(2), 193–211. https://doi.org/10.1016/j.plipres.2011.01.001

Pertwee R. G. (2006). The pharmacology of cannabinoid receptors and their ligands: an overview. International journal of obesity (2005), 30 Suppl 1, S13–S18. https://doi.org/10.1038/sj.ijo.0803272

Pertwee, R. G., Howlett, A. C., Abood, M. E., Alexander, S. P., Di Marzo, V., Elphick, M. R., Greasley, P. J., Hansen, H. S., Kunos, G., Mackie, K., Mechoulam, R., & Ross, R. A. (2010). International Union of Basic and Clinical Pharmacology. LXXIX. Cannabinoid receptors and their ligands: beyond CB_1 and CB_2. Pharmacological reviews, 62(4), 588–631. https://doi.org/10.1124/pr.110.003004

Pezeshki, A., Stordeur, P., Wallemacq, H., Schynts, F., Stevens, M., Boutet, P., Peelman, L. J., De Spiegeleer, B., Duchateau, L., Bureau, F., & Burvenich, C. (2011). Variation of inflammatory dynamics and mediators in primiparous cows after intramammary challenge with Escherichia coli. Veterinary research, 42(1), 15. https://doi.org/10.1186/1297-9716-42-15

Piomelli D. (2014). More surprises lying ahead. The endocannabinoids keep us guessing. Neuropharmacology, 76 Pt B, 228–234. https://doi.org/10.1016/j.neuropharm.2013.07.026

Poblete, I. M., Orliac, M. L., Briones, R., Adler-Graschinsky, E., & Huidobro-Toro, J. P. (2005). Anandamide elicits an acute release of nitric oxide through endothelial TRPV1 receptor activation in the rat arterial mesenteric bed. The Journal of physiology, 568(Pt 2), 539–551. https://doi.org/10.1113/jphysiol.2005.094292

Porcherie, A., Cunha, P., Trotereau, A., Roussel, P., Gilbert, F. B., Rainard, P., & Germon, P. (2012). Repertoire of Escherichia coli agonists sensed by innate immunity receptors of the bovine udder and mammary epithelial cells. Veterinary research, 43(1), 14. https://doi.org/10.1186/1297-9716-43-14

Price, M. R., Baillie, G. L., Thomas, A., Stevenson, L. A., Easson, M., Goodwin, R., McLean, A., McIntosh, L., Goodwin, G., Walker, G., Westwood, P., Marrs, J., Thomson, F., Cowley, P., Christopoulos, A., Pertwee, R. G., & Ross, R. A. (2005). Allosteric modulation of the cannabinoid CB1 receptor. Molecular pharmacology, 68(5), 1484–1495. https://doi.org/10.1124/mol.105.016162

Putman, A. K., Brown, J. L., Gandy, J. C., Wisnieski, L., & Sordillo, L. M. (2018). Changes in biomarkers of nutrient metabolism, inflammation, and oxidative stress in dairy cows during the transition into the early dry period. Journal of dairy science, 101(10), 9350–9359. https://doi.org/10.3168/jds.2018-14591

Rahaman, O., & Ganguly, D. (2021). Endocannabinoids in immune regulation and immunopathologies. Immunology, 164(2), 242–252. https://doi.org/10.1111/imm.13378

Rajesh, M., Mukhopadhyay, P., Haskó, G., Liaudet, L., Mackie, K., & Pacher, P. (2010). Cannabinoid-1 receptor activation induces reactive oxygen species-dependent and -independent mitogen-activated protein kinase activation and cell death in human coronary artery endothelial cells. British journal of pharmacology, 160(3), 688–700. https://doi.org/10.1111/j.1476-5381.2010.00712.x

Rajesh, M., Mukhopadhyay, P., Bátkai, S., Patel, V., Saito, K., Matsumoto, S., Kashiwaya, Y., Horváth, B., Mukhopadhyay, B., Becker, L., Haskó, G., Liaudet, L., Wink, D. A., Veves, A., Mechoulam, R., & Pacher, P. (2010). Cannabidiol attenuates cardiac dysfunction, oxidative stress, fibrosis, and inflammatory and cell death signaling pathways in diabetic cardiomyopathy. Journal of the American College of Cardiology, 56(25), 2115–2125. https://doi.org/10.1016/j.jacc.2010.07.033

Re, R., Pellegrini, N., Proteggente, A., Pannala, A., Yang, M., & Rice-Evans, C. (1999). Antioxidant activity applying an improved ABTS radical cation decolorization assay. Free radical biology & medicine, 26(9-10), 1231–1237. https://doi.org/10.1016/s0891-5849(98)00315-3

Redza-Dutordoir, M., & Averill-Bates, D. A. (2016). Activation of apoptosis signalling pathways by reactive oxygen species. Biochimica et biophysica acta, 1863(12), 2977–2992. https://doi.org/10.1016/j.bbamcr.2016.09.012

Ribeiro, A., Pontis, S., Mengatto, L., Armirotti, A., Chiurchiù, V., Capurro, V., Fiasella, A., Nuzzi, A., Romeo, E., Moreno-Sanz, G., Maccarrone, M., Reggiani, A., Tarzia, G., Mor, M., Bertozzi, F., Bandiera, T., & Piomelli, D. (2015). A Potent Systemically Active N-Acylethanolamine Acid Amidase Inhibitor that Suppresses Inflammation and Human Macrophage Activation. ACS chemical biology, 10(8), 1838–1846. https://doi.org/10.1021/acschembio.5b00114

Ribeiro, A., Ferraz-de-Paula, V., Pinheiro, M. L., Sakai, M., Costa-Pinto, F. A., & Palermo-Neto, J. (2010). Anandamide prior to sensitization increases cell-mediated immunity in mice. International immunopharmacology, 10(4), 431–439. https://doi.org/10.1016/j.intimp.2009.12.017

Rieck, S., Kilgus, S., Meyer, J. H., Huang, H., Zhao, L., Matthey, M., Wang, X., Schmitz-Valckenberg, S., Fleischmann, B. K., & Wenzel, D. (2021). Inhibition of Vascular Growth by Modulation of the Anandamide/Fatty Acid Amide Hydrolase Axis. Arteriosclerosis, thrombosis, and vascular biology, 41(12), 2974–2989. https://doi.org/10.1161/ATVBAHA.121.316973

Rittchen, S., Rohrer, K., Platzer, W., Knuplez, E., Bärnthaler, T., Marsh, L. M., Atallah, R., Sinn, K., Klepetko, W., Sharma, N., Nagaraj, C., & Heinemann, A. (2020). Prostaglandin D2 strengthens human endothelial barrier by activation of E-type receptor 4. Biochemical pharmacology, 182, 114277. https://doi.org/10.1016/j.bcp.2020.114277

Rockwell, C. E., & Kaminski, N. E. (2004). A cyclooxygenase metabolite of anandamide causes inhibition of interleukin-2 secretion in murine splenocytes. The Journal of pharmacology and experimental therapeutics, 311(2), 683–690. https://doi.org/10.1124/jpet.104.065524

Rockwell, C. E., Snider, N. T., Thompson, J. T., Vanden Heuvel, J. P., & Kaminski, N. E. (2006). Interleukin-2 suppression by 2-arachidonyl glycerol is mediated through peroxisome proliferator-activated receptor gamma independently of cannabinoid receptors 1 and 2. Molecular pharmacology, 70(1), 101–111. https://doi.org/10.1124/mol.105.019117

Roland, A. B., Ricobaraza, A., Carrel, D., Jordan, B. M., Rico, F., Simon, A., Humbert-Claude, M., Ferrier, J., McFadden, M. H., Scheuring, S., & Lenkei, Z. (2014). Cannabinoid-induced actomyosin contractility shapes neuronal morphology and growth. eLife, 3, e03159. https://doi.org/10.7554/eLife.03159

Rollin, E., Dhuyvetter, K. C., & Overton, M. W. (2015). The cost of clinical mastitis in the first 30 days of lactation: An economic modeling tool. Preventive veterinary medicine, 122(3), 257–264. https://doi.org/10.1016/j.prevetmed.2015.11.006

Roux, P. P., & Blenis, J. (2004). ERK and p38 MAPK-activated protein kinases: a family of protein kinases with diverse biological functions. Microbiology and molecular biology reviews : MMBR, 68(2), 320–344. https://doi.org/10.1128/MMBR.68.2.320-344.2004

Rouzer, C. A., & Marnett, L. J. (2011). Endocannabinoid oxygenation by cyclooxygenases, lipoxygenases, and cytochromes P450: cross-talk between the eicosanoid and endocannabinoid signaling pathways. Chemical reviews, 111(10), 5899–5921. https://doi.org/10.1021/cr2002799

Ryman, V. E., Packiriswamy, N., & Sordillo, L. M. (2016). Apoptosis of Endothelial Cells by 13-HPODE Contributes to Impairment of Endothelial Barrier Integrity. Mediators of inflammation, 2016, 9867138. https://doi.org/10.1155/2016/9867138

Ryman, V. E., Packiriswamy, N., & Sordillo, L. M. (2015). Role of endothelial cells in bovine mammary gland health and disease. Animal health research reviews, 16(2), 135–149. https://doi.org/10.1017/S1466252315000158

Sam, A. H., Salem, V., & Ghatei, M. A. (2011). Rimonabant: From RIO to Ban. Journal of obesity, 2011, 432607. https://doi.org/10.1155/2011/432607

Saroz, Y., Kho, D. T., Glass, M., Graham, E. S., & Grimsey, N. L. (2019). Cannabinoid Receptor 2 (CB2) Signals via G-alpha-s and Induces IL-6 and IL-10 Cytokine Secretion in Human Primary Leukocytes. ACS pharmacology & translational science, 2(6), 414–428. https://doi.org/10.1021/acsptsci.9b00049

Sawzdargo, M., Nguyen, T., Lee, D. K., Lynch, K. R., Cheng, R., Heng, H. H., George, S. R., & O'Dowd, B. F. (1999). Identification and cloning of three novel human G protein-coupled receptor genes GPR52, PsiGPR53 and GPR55: GPR55 is extensively expressed in human brain. Brain research. Molecular brain research, 64(2), 193–198. https://doi.org/10.1016/s0169-328x(98)00277-0

Schieber, M., & Chandel, N. S. (2014). ROS function in redox signaling and oxidative stress. Current biology: CB, 24(10), R453–R462. https://doi.org/10.1016/j.cub.2014.03.034

Serezani, C. H., Ballinger, M. N., Aronoff, D. M., & Peters-Golden, M. (2008). Cyclic AMP: master regulator of innate immune cell function. American journal of respiratory cell and molecular biology, 39(2), 127–132. https://doi.org/10.1165/rcmb.2008-0091TR

Siegmund, S. V., Qian, T., de Minicis, S., Harvey-White, J., Kunos, G., Vinod, K. Y., Hungund, B., & Schwabe, R. F. (2007). The endocannabinoid 2-arachidonoyl glycerol induces death of hepatic stellate cells via mitochondrial reactive oxygen species. FASEB journal : official publication of the Federation of American Societies for Experimental Biology, 21(11), 2798–2806. https://doi.org/10.1096/fj.06-7717com

Simon, G. M., & Cravatt, B. F. (2006). Endocannabinoid biosynthesis proceeding through glycerophospho-N-acyl ethanolamine and a role for alpha/beta-hydrolase 4 in this pathway. The Journal of biological chemistry, 281(36), 26465–26472. https://doi.org/10.1074/jbc.M604660200

Sintes, G. F., Bruckmaier, R. M., & Wellnitz, O. (2020). Nonsteroidal anti-inflammatory drugs affect the mammary epithelial barrier during inflammation. Journal of dairy science, 103(11), 10742–10753. https://doi.org/10.3168/jds.2020-18818

Smith, W. L., & Malkowski, M. G. (2019). Interactions of fatty acids, nonsteroidal anti-inflammatory drugs, and coxibs with the catalytic and allosteric subunits of cyclooxygenases-1 and -2. The Journal of biological chemistry, 294(5), 1697–1705. https://doi.org/10.1074/jbc.TM118.006295

Sordillo, L. M., Pighetti, G. M., & Davis, M. R. (1995). Enhanced production of bovine tumor necrosis factor-alpha during the periparturient period. Veterinary immunology and immunopathology, 49(3), 263–270. https://doi.org/10.1016/0165-2427(95)05465-0

Sordillo L. M. (2018). Mammary Gland Immunobiology and Resistance to Mastitis. The Veterinary clinics of North America. Food animal practice, 34(3), 507–523. https://doi.org/10.1016/j.cvfa.2018.07.005

Sordillo, L. M., & Aitken, S. L. (2009). Impact of oxidative stress on the health and immune function of dairy cattle. Veterinary immunology and immunopathology, 128(1-3), 104–109. https://doi.org/10.1016/j.vetimm.2008.10.305

Sordillo L. M., Mavangira V. (2014) The nexus between nutrient metabolism, oxidative stress and inflammation in transition cows. Animal Production Science, 54, 1204-1214.

Sordillo, L. M., & Peel, J. E. (1992). Effect of interferon-gamma on the production of tumor necrosis factor during acute Escherichia coli mastitis. Journal of dairy science, 75(8), 2119–2125. https://doi.org/10.3168/jds.S0022-0302(92)77971-5

Sordillo, L. M., Pighetti, G. M., & Davis, M. R. (1995). Enhanced production of bovine tumor necrosis factor-alpha during the periparturient period. Veterinary immunology and immunopathology, 49(3), 263–270. https://doi.org/10.1016/0165-2427(95)05465-0

Stančić, A., Jandl, K., Hasenöhrl, C., Reichmann, F., Marsche, G., Schuligoi, R., Heinemann, A., Storr, M., & Schicho, R. (2015). The GPR55 antagonist CID16020046 protects against intestinal inflammation. Neurogastroenterology and motility : the official journal of the European Gastrointestinal Motility Society, 27(10), 1432–1445. https://doi.org/10.1111/nmo.12639

Stanke-Labesque, F., Mallaret, M., Lefebvre, B., Hardy, G., Caron, F., & Bessard, G. (2004). 2-Arachidonoyl glycerol induces contraction of isolated rat aorta: role of cyclooxygenase-derived products. Cardiovascular research, 63(1), 155–160. https://doi.org/10.1016/j.cardiores.2004.03.024

Stanley, C. P., Hind, W. H., Tufarelli, C., & O'Sullivan, S. E. (2015). Cannabidiol causes endothelium-dependent vasorelaxation of human mesenteric arteries via CB1 activation. Cardiovascular research, 107(4), 568–578. https://doi.org/10.1093/cvr/cvv179

Stanley, C., & O'Sullivan, S. E. (2014). Vascular targets for cannabinoids: animal and human studies. British journal of pharmacology, 171(6), 1361–1378. https://doi.org/10.1111/bph.12560

Stanley, C. P., Hind, W. H., Tufarelli, C., & O'Sullivan, S. E. (2016). The endocannabinoid anandamide causes endothelium-dependent vasorelaxation in human mesenteric arteries. Pharmacological research, 113(Pt A), 356–363. https://doi.org/10.1016/j.phrs.2016.08.028

Staton, P. C., Hatcher, J. P., Walker, D. J., Morrison, A. D., Shapland, E. M., Hughes, J. P., Chong, E., Mander, P. K., Green, P. J., Billinton, A., Fulleylove, M., Lancaster, H. C., Smith, J. C., Bailey, L. T., Wise, A., Brown, A. J., Richardson, J. C., & Chessell, I. P. (2008). The putative cannabinoid receptor GPR55 plays a role in mechanical hyperalgesia associated with inflammatory and neuropathic pain. Pain, 139(1), 225–236. https://doi.org/10.1016/j.pain.2008.04.006

Steffens, S., & Pacher, P. (2012). Targeting cannabinoid receptor CB(2) in cardiovascular disorders: promises and controversies. British journal of pharmacology, 167(2), 313–323. https://doi.org/10.1111/j.1476-5381.2012.02042.x

Stella, N., Schweitzer, P., & Piomelli, D. (1997). A second endogenous cannabinoid that modulates long-term potentiation. Nature, 388(6644), 773–778. https://doi.org/10.1038/42015

Stock, M. L., & Coetzee, J. F. (2015). Clinical pharmacology of analgesic drugs in cattle. The Veterinary clinics of North America. Food animal practice, 31(1), 113–vii. https://doi.org/10.1016/j.cvfa.2014.11.002

Sugiura, T., & Waku, K. (2000). 2-Arachidonoylglycerol and the cannabinoid receptors. Chemistry and physics of lipids, 108(1-2), 89–106. https://doi.org/10.1016/s0009-3084(00)00189-4

Suofu, Y., Li, W., Jean-Alphonse, F. G., Jia, J., Khattar, N. K., Li, J., Baranov, S. V., Leronni, D., Mihalik, A. C., He, Y., Cecon, E., Wehbi, V. L., Kim, J., Heath, B. E., Baranova, O. V., Wang, X., Gable, M. J., Kretz, E. S., Di Benedetto, G., Lezon, T. R., … Friedlander, R. M. (2017). Dual role of mitochondria in producing melatonin and driving GPCR signaling to block cytochrome c release. Proceedings of the National Academy of Sciences of the United States of America, 114(38), E7997–E8006. https://doi.org/10.1073/pnas.1705768114

Takenouchi, R., Inoue, K., Kambe, Y., & Miyata, A. (2012). N-arachidonoyl glycine induces macrophage apoptosis via GPR18. Biochemical and biophysical research communications, 418(2), 366–371. https://doi.org/10.1016/j.bbrc.2012.01.027

Tanaka, T., Narazaki, M., & Kishimoto, T. (2014). IL-6 in inflammation, immunity, and disease. Cold Spring Harbor perspectives in biology, 6(10), a016295. https://doi.org/10.1101/cshperspect.a016295

Tanikawa, T., Kurohane, K., & Imai, Y. (2007). Induction of preferential chemotaxis of unstimulated B-lymphocytes by 2-arachidonoylglycerol in immunized mice. Microbiology and immunology, 51(10), 1013–1019. https://doi.org/10.1111/j.1348-0421.2007.tb03985.x

Tornqvist, H., & Belfrage, P. (1976). Purification and some properties of a monoacylglycerol-hydrolyzing enzyme of rat adipose tissue. The Journal of biological chemistry, 251(3), 813–819.

Turcotte, C., Chouinard, F., Lefebvre, J. S., & Flamand, N. (2015). Regulation of inflammation by cannabinoids, the endocannabinoids 2-arachidonoyl-glycerol and arachidonoyl-ethanolamide, and their metabolites. Journal of leukocyte biology, 97(6), 1049–1070. https://doi.org/10.1189/jlb.3RU0115-021R

Tsuboi, K., Uyama, T., Okamoto, Y., & Ueda, N. (2018). Endocannabinoids and related N-acylethanolamines: biological activities and metabolism. Inflammation and regeneration, 38, 28. https://doi.org/10.1186/s41232-018-0086-5

Urquhart, P., Nicolaou, A., & Woodward, D. F. (2015). Endocannabinoids and their oxygenation by cyclo-oxygenases, lipoxygenases and other oxygenases. Biochimica et biophysica acta, 1851(4), 366–376. https://doi.org/10.1016/j.bbalip.2014.12.015

US FDA (United States Food and Drug Administration). (1998). Implantation or Injectable Dosage Form New Animal Drugs; Flunixin Meglumine; US Federal Register, USA. Volume 63, pp. 38749–38750.

Usuda, D., & Kanda, T. (2014). Peroxisome proliferator-activated receptors for hypertension. World journal of cardiology, 6(8), 744–754. https://doi.org/10.4330/wjc.v6.i8.744

Van Der Stelt, M., Noordermeer, M. A., Kiss, T., Van Zadelhoff, G., Merghart, B., Veldink, G. A., & Vliegenthart, J. F. (2000). Formation of a new class of oxylipins from N-acyl(ethanol)amines by the lipoxygenase pathway. European journal of biochemistry, 267(7), 2000–2007. https://doi.org/10.1046/j.1432-1327.2000.01203.x

van der Stelt, M., Trevisani, M., Vellani, V., De Petrocellis, L., Schiano Moriello, A., Campi, B., McNaughton, P., Geppetti, P., & Di Marzo, V. (2005). Anandamide acts as an intracellular messenger amplifying Ca2+ influx via TRPV1 channels. The EMBO journal, 24(17), 3026–3037. https://doi.org/10.1038/sj.emboj.7600784

van 't Erve, T. J., Lih, F. B., Kadiiska, M. B., Deterding, L. J., Eling, T. E., & Mason, R. P. (2015). Reinterpreting the best biomarker of oxidative stress: The 8-iso-PGF(2α)/PGF(2α) ratio distinguishes chemical from enzymatic lipid peroxidation. Free radical biology & medicine, 83, 245–251. https://doi.org/10.1016/j.freeradbiomed.2015.03.004

Vane, J. R., & Botting, R. M. (1998). Anti-inflammatory drugs and their mechanism of action. Inflammation research: official journal of the European Histamine Research Society ... [et al.], 47 Suppl 2, S78–S87. https://doi.org/10.1007/s000110050284

Vivier, E., Tomasello, E., Baratin, M., Walzer, T., & Ugolini, S. (2008). Functions of natural killer cells. Nature immunology, 9(5), 503–510. https://doi.org/10.1038/ni1582

Walker, C., Brester, J. L., & Sordillo, L. M. (2021). Flunixin Meglumine Reduces Milk Isoprostane Concentrations in Holstein Dairy Cattle Suffering from Acute Coliform Mastitis. Antioxidants (Basel, Switzerland), 10(6), 834. https://doi.org/10.3390/antiox10060834

Williams, J., Wood, J., Pandarinathan, L., Karanian, D. A., Bahr, B. A., Vouros, P., & Makriyannis, A. (2007). Quantitative method for the profiling of the endocannabinoid metabolome by LC-atmospheric pressure chemical ionization-MS. Analytical chemistry, 79(15), 5582–5593. https://doi.org/10.1021/ac0624086

Wiltbank, M. C., Shiao, T. F., Bergfelt, D. R., & Ginther, O. J. (1995). Prostaglandin F2 alpha receptors in the early bovine corpus luteum. Biology of reproduction, 52(1), 74–78. https://doi.org/10.1095/biolreprod52.1.74

Witkamp R. (2016). Fatty acids, endocannabinoids and inflammation. European journal of pharmacology, 785, 96–107. https://doi.org/10.1016/j.ejphar.2015.08.051

Woodward, D. F., Krauss, A. H., Chen, J., Liang, Y., Li, C., Protzman, C. E., Bogardus, A., Chen, R., Kedzie, K. M., Krauss, H. A., Gil, D. W., Kharlamb, A., Wheeler, L. A., Babusis, D., Welty, D., Tang-Liu, D. D., Cherukury, M., Andrews, S. W., Burk, R. M., & Garst, M. E. (2003). Pharmacological characterization of a novel antiglaucoma agent, Bimatoprost (AGN 192024). The Journal of pharmacology and experimental therapeutics, 305(2), 772–785. https://doi.org/10.1124/jpet.102.047837

Woodward, D. F., Wang, J. W., & Poloso, N. J. (2013). Recent progress in prostaglandin F2α ethanolamide (prostamide F2α) research and therapeutics. Pharmacological reviews, 65(4), 1135–1147. https://doi.org/10.1124/pr.112.007088

Yang, Y., Bazhin, A. V., Werner, J., & Karakhanova, S. (2013). Reactive oxygen species in the immune system. International reviews of immunology, 32(3), 249–270. https://doi.org/10.3109/08830185.2012.755176

Ye, L., Cao, Z., Wang, W., & Zhou, N. (2019). New Insights in Cannabinoid Receptor Structure and Signaling. Current molecular pharmacology, 12(3), 239–248. https://doi.org/10.2174/1874467212666190215112036

Yeiser, E. E., Leslie, K. E., McGilliard, M. L., & Petersson-Wolfe, C. S. (2012). The effects of experimentally induced Escherichia coli mastitis and flunixin meglumine administration on activity measures, feed intake, and milk parameters. Journal of dairy science, 95(9), 4939–4949. https://doi.org/10.3168/jds.2011-5064

Yoshida, Y., Umeno, A., & Shichiri, M. (2013). Lipid peroxidation biomarkers for evaluating oxidative stress and assessing antioxidant capacity in vivo. Journal of clinical biochemistry and nutrition, 52(1), 9–16. https://doi.org/10.3164/jcbn.12-112

Zachut, M., Kra, G., Moallem, U., Livshitz, L., Levin, Y., Udi, S., Nemirovski, A., & Tam, J. (2018). Characterization of the endocannabinoid system in subcutaneous adipose tissue in periparturient dairy cows and its association to metabolic profiles. PloS one, 13(11), e0205996. https://doi.org/10.1371/journal.pone.0205996

Zentella de Piña, M., Vázquez-Meza, H., Agundis, C., Pereyra, M. A., Pardo, J. P., Villalobos-Molina, R., & Piña, E. (2007). Inhibition of cAMP-dependent protein kinase A: a novel cyclo-oxygenase-independent effect of non-steroidal anti-inflammatory drugs in adipocytes. Autonomic & autacoid pharmacology, 27(2), 85–92. https://doi.org/10.1111/j.1474-8673.2007.00392.x

Zhang, Y., Li, X., Zhang, H., Zhao, Z., Peng, Z., Wang, Z., Liu, G., & Li, X. (2018). Non-Esterified Fatty Acids Over-Activate the TLR2/4-NF-Kb Signaling Pathway to Increase Inflammatory Cytokine Synthesis in Neutrophils from Ketotic Cows. Cellular physiology and biochemistry : international journal of experimental cellular physiology, biochemistry, and pharmacology, 48(2), 827–837. https://doi.org/10.1159/000491913

Zoete, V., Grosdidier, A., & Michielin, O. (2007). Peroxisome proliferator-activated receptor structures: ligand specificity, molecular switch and interactions with regulators. Biochimica et biophysica acta, 1771(8), 915–925. https://doi.org/10.1016/j.bbalip.2007.01.007

Zoratti, C., Kipmen-Korgun, D., Osibow, K., Malli, R., & Graier, W. F. (2003). Anandamide initiates Ca(2+) signaling via CB2 receptor linked to phospholipase C in calf pulmonary endothelial cells. British journal of pharmacology, 140(8), 1351–1362. https://doi.org/10.1038/sj.bjp.0705529

Zou, H., Yuan, C., Dong, L., Sidhu, R. S., Hong, Y. H., Kuklev, D. V., & Smith, W. L. (2012). Human cyclooxygenase-1 activity and its responses to COX inhibitors are allosterically regulated by nonsubstrate fatty acids. Journal of lipid research, 53(7), 1336–1347. https://doi.org/10.1194/jlr.M026856

APPENDIX A: SUPPLEMENTAL MATERIALS

Table S1: Viability (ATP-production) of BAEC treated with AEA and AM251, with and without LPS (2, 8, 12, and 24 hours).

	2 hr		8 hr		12 hr		24 hr	
Treatment	Mean	SEM	Mean	SEM	Mean	SEM	Mean	SEM
Media	100.0000	0.0000	100.0000	0.0000	100.0000	0.0000	100.0000	0.0000
Vehicle	99.2731	1.7520	100.8842	1.5629	102.3911	1.4792	99.9362	1.7891
0.5 μM AEA	101.4192	2.9463	97.9030	3.1198	95.4717	3.8712	93.9856	4.0561
1 μM AEA	103.9571	2.8562	101.4820	2.5618	99.22815	4.7184	103.1779	5.2816
5 μM AEA	102.9129	3.0581	102.1354	3.9574	103.8136	4.0133	101.972	4.7945
25 ng/mL LPS	79.6392	2.0058	69.9947	2.5819	65.6811	3.1294	63.8732	4.6917
0.5 μM AEA + LPS	82.5801	3.5618	76.0937	3.6417	68.6592	3.5561	61.38756	3.3071
1 μM AEA + LPS	85.2789	3.8761	59.3472	4.0136	52.34523	2.5812	47.8163	4.0922
5 μM AEA + LPS	84.0966	2.9094	46.1829	3.7891	42.4897	3.5317	39.6493	4.1627
1 μM AM251 +LPS	75.0476	3.2372	73.9104	3.6801	74.22295	3.1093	75.0372	3.9761
0.5 μM AEA +1 μM AM251 + LPS	74.6107	4.5048	72.6192	4.0096	74.1389	3.6106	75.4436	4.7813
1 μM AEA + 1 μM AM251 + LPS	76.0154	3.6879	74.0816	3.6045	75.4617	4.0441	78.9467	5.1069
5 μM AEA + 1 μM AM251 + LPS	78.5881	3.0573	77.6545	2.6719	80.9516	3.5714	81.4812	4.7981

Table S2: Cytotoxicity of BAEC treated with AEA and AM251, with and without LPS (2, 8, 12, and 24 hours).

	2 hr		8 hr		12 hr		24 hr	
Treatment	Mean	SEM	Mean	SEM	Mean	SEM	Mean	SEM
Media	10.0000	0.0000	10.0000	0.0000	10.0000	0.0000	10.0000	0.0000
Vehicle	11.0031	0.8462	9.5476	1.0573	10.3319	0.9441	9.0047	1.0515
0.5 μM AEA	9.5619	1.9561	12.3452	2.0351	13.4256	2.4871	14.4762	1.9021
1 μM AEA	12.4816	2.4295	13.6493	2.4617	14.5941	2.5515	14.7769	3.6411
5 μM AEA	14.6944	2.0563	18.8313	3.0786	19.8093	3.0175	19.5257	4.3897
25 ng/mL LPS	51.5621	2.1537	57.3429	3.1638	59.6782	3.3246	55.2346	4.1792
0.5 μM AEA + LPS	49.7819	2.3691	59.5436	4.1837	58.5423	4.5859	57.2987	5.0700
1 μM AEA + LPS	53.1437	2.5015	62.9476	4.2916	63.5821	4.5343	59.0034	4.4578
5 μM AEA + LPS	56.9813	3.3022	65.8992	3.8919	68.4712	5.4287	69.4009	4.3413
1 μM AM251 +LPS	46.8604	2.7493	53.5717	4.3817	50.8719	4.9347	51.6981	5.2108
0.5 μM AEA +1 μM AM251 + LPS	48.3457	3.6172	51.9661	5.0943	51.7726	4.7791	52.7894	4.9072
1 μM AEA + 1 μM AM251 + LPS	47.2019	3.5881	50.4615	4.1637	48.9487	5.1043	51.0019	5.9666
5 μM AEA + 1 μM AM251 + LPS	49.5173	4.1306	53.9908	5.0038	50.9094	4.3468	48.9587	4.1937

Table S3: Cytochrome-C release of BAEC treated with AEA and AM251, with and without LPS (2, 8, 12, and 24 hours).

	2 hr		8 hr		12 hr		24 hr	
Treatment	Mean	SEM	Mean	SEM	Mean	SEM	Mean	SEM
Media	8.6476	0.0000	8.8154	1.3490	7.9961	0.4857	7.3492	1.4919
Vehicle	9.0192	0.5948	9.1491	0.7581	8.2043	1.5991	7.8495	2.8313
0.5 μM AEA	8.5096	1.2492	8.3243	1.9343	9.0305	2.1458	8.1391	2.5167
1 μM AEA	6.9291	0.9844	8.9181	0.9037	8.7183	1.4106	7.9466	2.0881
5 μM AEA	8.4048	2.7658	9.5933	2.1931	9.1048	3.1789	8.1097	3.1943
25 ng/mL LPS	13.3017	2.5681	16.5482	2.0384	19.9772	2.5691	17.5124	3.4407
0.5 μM AEA + LPS	17.5131	2.5953	19.3204	1.8875	19.3532	3.1044	18.5827	4.1656
1 μM AEA + LPS	18.2456	2.5617	20.1459	1.5903	20.4821	2.8173	19.5602	3.1039
5 μM AEA + LPS	21.7287	3.0583	26.3979	4.1738	21.0795	2.9104	19.8736	4.0571
1 μM AM251 +LPS	11.4802	2.9791	11.4286	3.1904	11.9139	3.5091	8.1761	3.8193
0.5 μM AEA +1 μM AM251 + LPS	11.0747	3.0065	12.8152	2.5678	11.7281	4.0082	10.1411	4.7615
1 μM AEA + 1 μM AM251 + LPS	14.5941	2.6344	15.1369	2.0538	14.7769	3.6179	13.4256	4.1203
5 μM AEA + 1 μM AM251 + LPS	17.6141	3.0471	16.4450	3.1294	16.0375	4.2076	15.1407	5.1997

Table S4: Caspase-3/7 activation of BAEC treated with AEA and AM251, with and without LPS (2, 8, 12, and 24 hours).

	2 hr		8 hr		12 hr		24 hr	
Treatment	Mean	SEM	Mean	SEM	Mean	SEM	Mean	SEM
Media	1.0000	0.0000	1.0000	0.0000	1.0000	0.0000	1.0000	0.0000
Vehicle	0.9021	0.2149	1.2019	0.3948	0.9923	0.3719	1.0318	0.3481
0.5 μM AEA	1.1036	0.3917	1.1949	0.4816	1.2018	0.6581	0.9836	0.3171
1 μM AEA	1.4005	0.5028	1.4257	0.5162	1.1409	0.7172	1.0381	0.5136
5 μM AEA	1.6542	0.9822	1.4981	0.4811	1.2647	0.7129	0.9934	0.7594
25 ng/mL LPS	4.3158	0.8536	4.4578	1.5417	4.7445	1.2481	5.0953	1.5361
0.5 μM AEA + LPS	4.2159	0.7553	5.2016	1.9938	5.1839	1.5618	4.7165	1.2491
1 μM AEA + LPS	5.0399	0.8059	7.2643	1.4172	7.1124	1.8739	6.8479	1.7282
5 μM AEA + LPS	6.4271	0.9387	9.1856	1.1099	8.7910	1.5251	8.8697	2.0124
1 μM AM251 +LPS	3.0567	0.9812	3.4066	0.8953	3.1838	0.9317	2.0840	0.8158
0.5 μM AEA +1 μM AM251 + LPS	2.9983	0.7484	3.3217	0.9182	2.9053	1.0381	2.7401	0.9416
1 μM AEA + 1 μM AM251 + LPS	4.1677	1.2943	5.8172	1.1381	4.1219	0.9471	2.9408	0.7244
5 μM AEA + 1 μM AM251 + LPS	3.9087	0.9541	5.1298	1.0461	4.6183	0.8492	3.0128	0.9881

Table S5: ROS production of BAEC treated with AEA and AM251, with and without LPS (2, 8, 12, and 24 hours).

	2 hr		8 hr		12 hr		24 hr	
Treatment	Mean	SEM	Mean	SEM	Mean	SEM	Mean	SEM
Media	1.0000	0.0000	1.0000	0.0000	1.0000	0.0000	1.0000	0.0000
Vehicle	0.9961	0.1034	0.9841	0.1385	1.0392	0.2859	0.9754	0.2498
0.5 μM AEA	7.5431	1.4701	10.5718	1.4026	13.4817	2.0577	8.9271	2.6783
1 μM AEA	11.7461	2.7566	14.1627	1.9715	14.9204	3.0121	15.0116	3.5886
5 μM AEA	12.5812	3.1045	17.4033	1.8561	17.5119	3.6055	16.0520	3.7221
25 ng/mL LPS	17.4092	2.7904	15.9004	2.2561	15.5938	3.7612	11.5702	3.6152
0.5 μM AEA + LPS	15.6206	4.8607	17.5923	4.6817	16.2458	4.4617	15.8162	4.5615
1 μM AEA + LPS	19.4721	3.6592	20.5371	4.0354	19.1232	3.8093	17.0589	3.4679
5 μM AEA + LPS	22.6903	4.0295	22.0662	5.9877	21.4144	4.1236	20.5980	4.0183
1 μM AM251 +LPS	15.8577	3.2886	13.8463	3.6163	13.0717	2.7709	15.2193	3.5592
0.5 μM AEA +1 μM AM251 + LPS	14.7079	2.2358	12.4917	4.4719	11.0375	3.9042	10.5131	3.6733
1 μM AEA + 1 μM AM251 + LPS	14.3129	3.1638	11.5812	4.3917	11.3656	3.4871	11.0654	4.0816
5 μM AEA + 1 μM AM251 + LPS	20.8312	4.3761	18.4311	3.0611	15.1369	4.5694	12.7287	3.5617

Table S6: IsoP production of BAEC treated with AEA and AM251, with and without LPS (2, 8, 12, and 24 hours).

	2 hr		8 hr		12 hr		24 hr	
Treatment	Mean	SEM	Mean	SEM	Mean	SEM	Mean	SEM
Media	0.0100	0.0000	0.0100	0.0000	0.0100	0.0000	0.0600	0.0021
Vehicle	0.0100	0.0000	0.0100	0.0000	0.0100	0.0000	0.1000	0.0274
0.5 μM AEA	5.9331	2.3172	55.3279	5.9022	32.5981	7.6617	14.0317	5.7726
1 μM AEA	6.0736	2.5489	79.5103	7.5340	64.5871	8.0214	67.5006	9.4129
5 μM AEA	19.0904	2.9567	115.6958	5.1320	97.0938	9.6052	82.9594	14.0298
25 ng/mL LPS	108.0581	7.4821	142.9510	8.0291	120.6091	11.5551	124.1405	16.4618
0.5 μM AEA + LPS	113.7992	5.9519	158.1267	9.9473	141.4352	10.5268	125.6018	20.3504
1 μM AEA + LPS	109.1833	6.4316	193.5319	11.5172	157.0238	13.8532	128.0155	19.8749
5 μM AEA + LPS	117.6012	6.0041	242.8511	14.5609	198.4019	15.1796	142.5972	27.3993
1 μM AM251 +LPS	84.6694	7.2356	129.5018	7.3461	106.1231	6.5061	102.3428	10.9238
0.5 μM AEA +1 μM AM251 + LPS	80.0281	6.7264	104.7691	13.6817	114.0923	11.8325	103.7906	14.4482
1 μM AEA + 1 μM AM251 + LPS	77.1957	7.3078	110.0823	11.5080	103.5012	9.1589	97.4311	17.9727
5 μM AEA + 1 μM AM251 + LPS	82.3281	11.0863	113.5428	9.0159	107.2481	10.4853	84.6914	14.4971

Table S7: ICAM-1 gene expression of BAEC treated with AEA and AM251, with and without LPS (2, 8, 12, and 24 hours).

	2 hr		8 hr		12 hr		24 hr	
Treatment	Mean	SEM	Mean	SEM	Mean	SEM	Mean	SEM
Media	1.0000	0.0000	1.0000	0.0000	1.0000	0.0000	1.0000	0.0000
Vehicle	1.1905	0.1392	0.9847	0.0941	1.1371	0.1812	1.2045	0.4918
0.5 μM AEA	1.2943	0.0848	1.1038	0.1043	1.0318	0.3148	2.4581	0.8918
1 μM AEA	0.8842	0.0910	0.9281	0.1197	0.9653	0.1263	1.9361	0.7863
5 μM AEA	0.7229	0.0746	0.9238	0.2381	0.9841	0.2598	2.0149	1.3902
25 ng/mL LPS	114.8774	13.5093	115.0459	11.5009	114.1448	10.5864	113.6220	13.5919
0.5 μM AEA + LPS	99.0206	11.0098	97.0924	8.5999	106.7432	11.0687	109.7372	12.5837
1 μM AEA + LPS	111.1432	14.1887	134.5883	14.4527	131.8584	13.0012	121.5713	15.4726
5 μM AEA + LPS	121.7838	12.6992	142.0624	12.5983	125.7202	14.1787	122.0364	11.0491
1 μM AM251 +LPS	89.5693	6.9091	84.2447	4.1662	85.4769	6.6528	88.8710	7.4193
0.5 μM AEA +1 μM AM251 + LPS	86.0039	8.1439	78.3191	7.5914	72.5018	5.1948	70.4174	8.1298
1 μM AEA + 1 μM AM251 + LPS	78.4559	9.0016	74.3734	6.2986	68.8882	9.5617	65.9318	11.8581
5 μM AEA + 1 μM AM251 + LPS	68.9391	12.3653	64.9913	8.1263	60.4918	10.4168	56.9371	13.0207

Table S8: VCAM-1 gene expression of BAEC treated with AEA and AM251, with and without LPS (2, 8, 12, and 24 hours).

	2 hr		8 hr		12 hr		24 hr	
Treatment	Mean	SEM	Mean	SEM	Mean	SEM	Mean	SEM
Media	1.0000	0.0000	1.0000	0.0000	1.0000	0.0000	1.0000	0.0000
Vehicle	1.0544	0.1354	0.9881	0.1239	1.0034	0.3918	0.9634	0.3027
0.5 μM AEA	0.8322	0.1450	0.8128	0.1048	1.1204	0.2907	0.9927	0.2205
1 μM AEA	0.9471	0.0832	0.8552	0.1218	1.0028	0.1946	1.1049	0.2487
5 μM AEA	0.8061	0.0906	0.7461	0.1049	0.9906	0.2381	1.2471	0.3812
25 ng/mL LPS	67.4719	5.6217	69.4236	5.0126	68.6522	6.9328	65.8127	7.5827
0.5 μM AEA + LPS	65.6108	5.0151	64.1948	5.1237	60.4953	5.8225	56.0018	7.1254
1 μM AEA + LPS	64.4009	5.9274	61.4017	4.9073	58.3918	5.2237	55.1376	6.3731
5 μM AEA + LPS	76.1482	4.9863	81.4781	5.1044	75.0217	5.6248	69.2636	6.6827
1 μM AM251 +LPS	71.4611	5.9823	68.0139	6.1782	65.1204	6.0260	62.9173	7.6213
0.5 μM AEA +1 μM AM251 + LPS	68.5901	8.5006	65.0471	8.9913	63.5955	9.4272	61.7496	11.4844
1 μM AEA + 1 μM AM251 + LPS	64.0105	6.4371	64.3627	7.1267	63.4172	8.8284	62.0564	9.5712
5 μM AEA + 1 μM AM251 + LPS	59.1298	5.9989	53.3453	6.0928	52.1687	8.8962	53.8947	9.0766

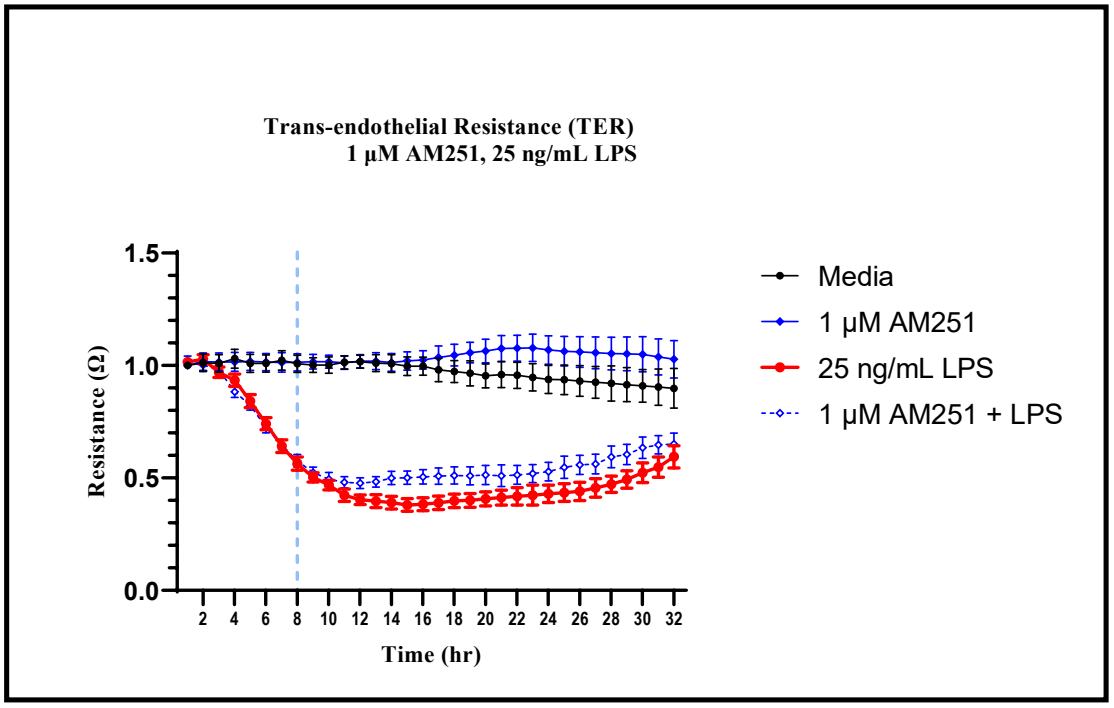

Figure S1: Trans-endothelial resistance of BAEC treated with 1µM AM251, with and without LPS.